EXTRACELLULAR SUPEROXIDE DISMUTASE AND MATRIX METALLOPROTEINASES IN PULMONARY FIBROSIS

by

Roderick Jason Tan

BS, Georgetown University, 1999

Submitted to the Graduate Faculty of

The School of Medicine in partial fulfillment

of the requirements for the degree of

Doctor of Philosophy

University of Pittsburgh

2005

UNIVERSITY OF PITTSBURGH

SCHOOL OF MEDICINE

This dissertation was presented

by

Roderick Jason Tan

It was defended on

September 6, 2005

and approved by

Dr. Charleen T. Chu, M.D., Ph.D.
Department of Pathology

Dr. Wendy M. Mars, Ph.D.
Department of Pathology

Dr. Prabir Ray, Ph.D.
Department of Medicine

Dr. Cary Wu, Ph.D.
Department of Pathology

Dr. Tim D. Oury, M.D., Ph.D.
Dissertation Director
Department of Pathology

COPYRIGHT

Copyright permission was granted for the use of parts from:

1. **Tan, R.J.** and Fattman, C.L., Watkins, S.C., and Oury, T.D. (2004). Redistribution of pulmonary EC-SOD after exposure to asbestos. *J Appl Physiol* 97(5): 2006-13.

2. Kinnula, V.L., Fattman, C.L., **Tan, R.J.**, and Oury, T.D. (2005). Oxidative stress in pulmonary fibrosis: a possible role for redox modulatory therapy. *Am J Respir Crit Care Med* 172(4): 417-22.

Documentation of permission letters are on file with Roderick J. Tan.

EXTRACELLULAR SUPEROXIDE DISMUTASE AND MATRIX METALLOPROTEINASES IN PULMONARY FIBROSIS

Roderick Jason Tan, PhD

University of Pittsburgh, 2005

ABSTRACT

Pulmonary fibrosis is the collective name for disorders characterized by excessive deposition of interstitial collagen in the lung. Although the molecular mechanisms underlying pulmonary fibrosis are poorly understood, current evidence implicates both oxidant/antioxidant and protease/antiprotease imbalances in disease development. **Extracellular superoxide dismutase (EC-SOD)** is an antioxidant enzyme protective against the development of pulmonary fibrosis in experimental models. EC-SOD localization in the lung is regulated by a heparin-binding domain conferring affinity for the extracellular matrix. This domain is susceptible to proteolytic removal, allowing EC-SOD to diffuse from the matrix. While the *in vivo* protease of EC-SOD has not been identified, it is known that members of the **matrix metalloproteinase (MMP)** family of proteases are upregulated in pulmonary fibrosis and could contribute to EC-SOD diffusion from the matrix. Furthermore, latent MMPs can be activated by oxidants, indicating that loss of EC-SOD from the matrix could lead to increased MMP activity.

It was hypothesized that the depletion of EC-SOD from the lung and interrelated increase in MMP activity contribute to pulmonary fibrosis development. To examine this hypothesis, a mouse model of pulmonary fibrosis initiated by asbestos fibers (asbestosis) was developed. This injury caused depletion of EC-SOD from the lung parenchyma. Simultaneously, EC-SOD

accumulated in the airspaces entirely due to release from airspace inflammatory cells. Depletion from lung matrices may be important since EC-SOD knockout mice develop worse inflammation and fibrosis after asbestos exposure.

The metalloproteinases, MMP-2 and MMP-9, were upregulated after asbestos exposure. MMPs appeared to be important in asbestosis development, as global pharmacologic inhibition of MMPs decreased disease severity. MMP inhibition also reduced airspace EC-SOD accumulation, indicating a role for MMPs in EC-SOD localization. EC-SOD knockout mice treated with asbestos did not have significantly different MMP-2 and -9 activity compared to wild type mice. However, in bleomycin injury, knockout mice had increased airspace MMP-9, indicating a role for EC-SOD in the regulation of this protease. In summary, our data provides strong evidence for contributory roles for both EC-SOD and MMPs in the development of pulmonary fibrosis and additionally provides novel insights into EC-SOD regulation in the lung.

TABLE OF CONTENTS

LIST OF TABLES

LIST OF FIGURES

ABBREVIATIONS

α1-PI	alpha-1-proteinase inhibitor
α2M	alpha-2-macroglobulin
Asb	asbestos
BAL	bronchoalveolar lavage
Bleo	bleomycin
CuZnSOD	copper/zinc superoxide dismutase
ECM	extracellular matrix
EC-SOD	extracellular superoxide dismutase
HBD	heparin-binding domain
HGF	hepatocyte growth factor
IL-1, -6, -8	interleukin-1, interleukin-6, interleukin-8
IPF	Idiopathic Pulmonary Fibrosis
KO	knockout
LPS	lipopolysaccharide
NAC	N-acetylcysteine
MnSOD	manganese superoxide dismutase
MMP	matrix metalloproteinase
PAI	plasminogen activator inhibitor
PDGF	platelet derived growth factor
PMN	polymorphonuclear leukocyte (PMN)
ROS	reactive oxygen species
RNS	reactive nitrogen species
SDS-PAGE	sodium dodecyl sulfate-polyacrylamide gel electrophoresis
Sal	saline
TGF	transforming growth factor
TiO2	titanium dioxide
TNF	tumor necrosis factor
tPA	tissue plasminogen activator
uPA	urokinase plasminogen activator
UIP	usual interstitial pneumonia
Veh	vehicle
WT	wild type

ACKNOWLEDGMENTS

I would like to thank my mentor, Tim Oury, for all of your advice and support during the course of this research. Through your enthusiasm for research and for training students, I feel that I have learned from you not only how to do good science (and what the mysterious "Cub Factor" is), but also how to foster a spirit of collaboration. In short, being in your lab has taught me so much, and I hope to be just as good a mentor to others in the future.

I would like to thank the members of my thesis committee for all of their insightful comments and suggestions that have shaped and focused the work that has become this thesis.

Thanks also to Cheryl Fattman, Lana Hanford, Lisa Schaefer, Toni Termin, Jake Tobolewski, Elisha Peterson, Fei Gao, Judd Englert, Pierre-Paul Lizotte, and Michelle Manni and everyone who has made working in the Oury lab so much fun. Your training, support, and all of your help have truly meant a lot to me.

Last but definitely not least, I am especially blessed to have wonderful family and friends that have been with me every step of the way. Mom and Dad, I can hardly believe that six years have passed since I joined the MD/PhD program. You have patiently listened, offered advice and reassurance, and helped me through it all. I wouldn't be here without you and all of your love and support. I'm also lucky to have the best brother (and biggest Steeler fan) in the world. Freddie, thanks for looking after your little brother and showing me the ropes more than just a few times. To the members of Pitt Med Class of 2003 and especially the would-be "Class of 2003" MD/PhD students: your friendship has been meant more than any of you can imagine. And finally, to Liz--who is a constant reminder that there is indeed a world outside of science and medicine--you have made life special and worthwhile in so many ways. I can think of no one else I would rather share this with than you.

1. INTRODUCTION

Pulmonary fibrosis is the collective name for a group of disorders characterized by deposition of excessive amounts of collagen in the lung. Pulmonary fibrosis can occur spontaneously without a known stimulus (idiopathic), in response to environmental and occupational exposures (asbestosis, silicosis), in response to drugs (bleomycin) and radiation, secondary to other diseases (scleroderma), and as a familial syndrome (1-6). These diseases are extremely debilitating, leading to severe restrictive pulmonary impairment, as well as intractable, as no therapies exist to adequately treat the majority of patients (1). Failure of current treatment regimens is largely owed to a general lack of understanding of the molecular mechanisms underlying pulmonary fibrosis. However, current evidence points to both oxidant/antioxidant and protease/antiprotease imbalances as having central roles in these diseases.

1.1. IDIOPATHIC PULMONARY FIBROSIS

Idiopathic pulmonary fibrosis (IPF) is the paradigm fibrotic lung disease. It is, by far, the most common of these diseases, accounting for 47-71% of all pulmonary fibrosis cases (7). Cryptogenic fibrosing alveolitis and idiopathic interstitial pneumonia are two other terms for IPF used outside of the United States (8). The estimated prevalence of IPF is 29 per 100,000 in the general population (9).

1.1.1. Pathophysiology

The primary function of the lung is to exchange gases between the bloodstream and the air we breathe. Specifically, oxygen is transferred to hemoglobin in the blood while carbon dioxide is released from the hemoglobin to the airspace for exhalation. Breathed air travels along a number of progressively narrowing conducting airways (trachea, bronchi, bronchioles) before reaching the respiratory bronchioles and alveoli where gas exchange actually occurs. Crucial to gas exchange is the cellular design of the lung with type I epithelial cells facing the airspace sharing a common basement membrane with vascular endothelial cells facing the blood. This barrier is exceedingly thin (as thin as 3.0 μm), allowing gas exchange to occur efficiently (10). Support cells include the type II epithelial cells, which are poised to regenerate damaged type I cells and serve as a stem cell for the lung epithelium, and the Clara cell, which together with type II cells produces much of the surfactant vital to normal alveoli function. Alveolar macrophages are also present and function in immunological defense (11).

The lung in IPF is markedly different. Interstitial collagen deposition leads to an inability of the lung to expand fully, thus decreasing total lung volume. This defect has led to the classification of IPF as a restrictive disease (1). In addition, thickening of alveolar septa increases the diffusion distance for gas exchange between the airspace and bloodstream. This twofold effect on the reduction of lung volume and increased diffusion distance severely impairs normal respiration.

The onset of IPF is usually insidious, with the first symptoms being nonproductive cough and shortness of breath (dyspnea) upon exertion. The disease generally progresses to dyspnea at rest and eventually to the hypoxemia and respiratory failure that is the cause of death in most

patients (12). IPF is a disease associated with aging as the peak incidence occurs after age fifty (1).

Cardiovascular complications also cause mortality in IPF, accounting for 27% of deaths. Pulmonary hypertension and subsequent cardiac hypertrophy can result from blockage or constriction of pulmonary blood vessels. The chronic hypoxemia in late stages of the disease is incapacitating and promotes stroke as well as heart ischemia and heart failure (12). Overall prognosis in IPF is dismal; mean survival after onset of symptoms is 2.8-3.6 years (7, 13).

1.1.2. Pathologic Findings

IPF is defined histologically by a pattern of usual interstitial pneumonia (UIP). The UIP pattern is that of patchy interstitial fibrosis appearing alongside normal lung. Fibrosis is often found in subpleural and basilar areas and is temporally heterogeneous, that is, in various stages of development at the same time. Fibroblastic foci composed of loose fibrosis populated by myofibroblasts (see Chapter 1.4.2) are scattered at the edges of this fibrosis. Moderate inflammation may be present and is comprised of lymphocytes, macrophages, neutrophils, mast cells, and eosinophils (14).

Grossly, the lungs from an IPF patient are small. The pleural surface has a "cobble-stoned" appearance due to scar retraction. Fibrosis is usually distributed in the lower lobes of the lung and in subpleural areas, with end-stage disease described as having honeycomb changes (14). Bronchoalveolar lavage shows increases in the same inflammatory cells noted above (1).

1.1.3. Treatment

Therapies for IPF are limited. Front-line treatment has relied on corticosteroids and have a limited success rate, leading to a response in only 10 to 30% of patients (7). Moreover, this treatment is limited by disabling side effects such as opportunistic infection, endocrine dysfunction, myopathy, and osteoporosis (1). Although additional immunosuppressive drugs are often added to this regimen, treatment with cyclophosphamide has shown little to no benefit (15) while azathioprine-treated patients had only modest improvement in lung function parameters and mortality (16). Unfortunately, antifibrotic medications such as colchicine and penicillamine have also shown little benefit (17).

Newer therapies have been attempted in the treatment of IPF. Interferon gamma-1b was recently tested in a large, multinational, placebo controlled trial. Unfortunately, in spite of promising preliminary data, interferon therapy did not significantly affect survival, lung function, or quality of life (18). Because of evidence indicating oxidative stress in IPF, therapies aimed at restoring oxidant/antioxidant imbalance are being tested (19). N-acetylcysteine, which stimulates the synthesis of the antioxidant glutathione, did not significantly affect survival but was found to improve pulmonary function tests in IPF patients (20).

Clearly, novel therapies are required to treat pulmonary fibrosis. Better understanding of the disease mechanisms is crucial in the development of these therapies.

1.2. ASBESTOSIS

Although IPF is the most common interstitial lung disease, fibrosis can also occur due to particle exposure. In short, asbestosis is pulmonary fibrosis due to the inhalation of asbestos fibers. Asbestosis is classified as a pneumoconiosis, that is, a pulmonary disease caused by exposure to

environmental dusts (21). While asbestosis is thought to occur through many of the same mechanisms as IPF, it is clear that asbestos fibers also have unique characteristics that contribute to pathogenesis and require separate study.

1.2.1. Asbestos and Lung Disease

Because of its unique physical properties, asbestos fibers have been utilized for thousands of years. High tensile strength and heat resistance has led to its use in concrete mixtures, brakes, shipbuilding, and insulation. Inexpensive and readily available, asbestos is extremely valuable for commercial and industrial applications (22).

Asbestos is composed of naturally occurring silica-containing mineral fibers. Fibers are divided into two groups: serpentine (curly fibers) and amphiboles (straight fibers) (23). Chrysotile asbestos is the only member of the serpentine group, and these fibers are curly and flexible. On the other hand, the amphiboles, including crocidolite (blue asbestos), amosite, tremolite, and others, are straight and are not pliable (22). In terms of health impact, amphiboles are thought to be more potent inducers of disease because of their greater tendency to accumulate in the lung, inefficient pulmonary clearance of these fibers, and better durability. Although controversial, this "amphibole hypothesis" may explain why a greater amount of chrysotile is required to cause disease compared to amphiboles (24). In fact, the true contribution of chrysotile asbestos to disease in humans is unclear as chrysotile is commonly contaminated with small amounts of tremolite asbestos (an amphibole) (2).

As would be expected, the largest number of cases of asbestos-related lung disease occurs in those with occupational exposure to the fibers. As such, miners and millers, cement workers, insulation workers, and shipyard workers have high risk of disease development (25). Diseases

caused by asbestos include asbestosis, pleural plaques, bronchogenic carcinoma, and mesothelioma (23).

1.2.2. Clinical and Pathologic Features of Asbestosis

Clinical manifestations of asbestosis are very similar to those described for IPF above but are generally less severe and slower in progression. As in IPF, patients experience shortness of breath and dry cough early in disease. These symptoms progress to respiratory failure and, eventually, death of the patient. Although both IPF and asbestosis are associated with lung cancer, asbestosis patients have much higher rates of lung cancer (21).

Asbestosis is also akin to IPF in pathologic features. Gross features are identical to that described for IPF, but additionally there may be pleural plaques. Histologic diagnosis requires observation of diffuse interstitial fibrosis *and* asbestos bodies in lung sections. In other words, asbestosis is essentially the patchy UIP pattern accompanied by asbestos bodies (21). Asbestos bodies are asbestos fibers that have become covered with iron, protein and polysaccharides and have a characteristic brown, dumbbell appearance microscopically. This process is not well understood but is thought to involve the action of macrophages (26).

1.3. EXPERIMENTAL MODELS OF PULMONARY FIBROSIS

Several *in vivo* animal models have been employed to examine the pathogenesis of pulmonary fibrosis. These models typically rely upon an initial injury stimulus that leads to abnormal repair and fibrosis in the lung. Two models that have been utilized extensively are the bleomycin and asbestos models.

1.3.1. Bleomycin Model

The bleomycin model is the most common experimental model of pulmonary fibrosis in use today. Bleomycin is a cancer therapeutic used in the treatment of lymphomas and solid tumors. Its use in cancer therapy is limited by significant skin toxicity and pulmonary fibrosis (27). These side effects are likely due to the absence in these tissues of bleomycin hydrolase, which inactivates bleomycin in other organs of the body (3).

Pulmonary fibrosis after bleomycin proceeds with an initial inflammatory phase followed by the actual development of fibrosis. The initial injury has been proposed to be oxidative in nature—bleomycin can bind both DNA and redox-active iron simultaneously. The iron can cause oxidative stress (see Chapter 1.4.5) that creates strand breaks in the DNA and presumably cellular dysfunction. Pulmonary inflammation comprised of neutrophils, macrophages, and lymphocytes develops during the first seven days and likely participates in pathogenesis, since therapies that reduce this inflammatory response are associated with reduced fibrosis (28, 29). Fibrosis can also begin to develop as early as day seven depending on the route of administration. This model has been successfully applied in mice, rats, hamsters, and rabbits (30-33).

1.3.2. Asbestos Model

The asbestos model involves the intratracheal instillation or inhalation of mineral fibers into the lung. Like the bleomycin model, asbestos induces an acute inflammatory response followed by fibrosis (34). Typically, the inflammation is dominated by neutrophils, although macrophages are present and may play a pivotal role in disease progression (35, 36). A number of asbestos fibers have been used, including crocidolite, amosite, and chrysotile (37-39). As in humans, the

type may be important, as amphiboles are retained in the lung longer than chrysotile (34, 40). Fiber length also is an important factor, as short fibers (<2.5 μm) were found to induce minimal fibrosis while longer fibers induced significant fibrosis (38, 41). Mice, rats, hamsters, and several other animals have been exposed to asbestos and developed fibrosis (35, 38, 42).

1.3.3. Pneumonia Model

While bacterial inhalation does not cause the development of pulmonary fibrosis, bacteria can be utilized to reproduce the airspace inflammation found in pulmonary fibrosis. While the actual development of pneumonia disease in response to bacteria varies due to genetic differences between mouse strains, the term pneumonia (as opposed to bacterial clearance) will be used for simplicity. Notably, both pulmonary fibrosis and pneumonia lead to the accumulation of large amounts of neutrophils in the airspaces (35, 43). The pneumonia is not complicated by interstitial fibrosis and extracellular matrix remodeling, nor does it lead to significant amounts of interstitial inflammation.

1.4. PATHOGENESIS OF PULMONARY FIBROSIS

The mechanisms underlying the development of IPF and asbestosis are still being elucidated. While the role of inflammation in the initiation or progression of the disease is unclear, current models view pulmonary fibrosis as a result of dysregulated repair processes. Key to this dysfunction is failure of reepithelialization, activation of fibroblasts and myofibroblasts, inflammation, matrix remodeling, and oxidative stress (44). These mechanisms likely apply to both IPF and asbestosis. For simplicity, the following review of pathogenesis will first describe

findings attributed to IPF and potentially all interstitial lung diseases. A more specialized description of asbestos-induced lung damage follows.

1.4.1. Alveolar Reepithelialization

Inability to regenerate pulmonary epithelium appears to play a major role in the development of pulmonary fibrosis. Damage to epithelia is thought to be an early step in disease. Fas-ligand pathway-induced apoptotic cell death in epithelium is increased, perhaps due to the actions of angiotensin II or transforming growth factor-beta1 (TGF-β1) (45-47). The epithelial mitogen and motogen, hepatocyte growth factor (HGF), is also upregulated in IPF, probably representing an attempt to restore the epithelial barrier (48). In fact, administration of HGF in animal models of pulmonary fibrosis reduces development of fibrosis (49). However, although type I cell hyperplasia has been observed in IPF, the stem-cell like type II cells display reduced proliferation and differentiation capacity (50).

The plasminogen system is also thought to be involved in restoration of the epithelial barrier. As plasma diffuses through damaged alveolar epithelium, fibrin clots are deposited in the lung (51). Optimal reepithelialization requires the clearance of fibrin. This process begins with conversion of plasminogen to plasmin by either urokinase plasminogen activator (uPA) or tissue plasminogen activator (tPA). Plasminogen activator inhibitors (PAIs) are capable of inhibiting both uPA and tPA (52).

Factors increasing overall plasmin activity reduce the severity of pulmonary fibrosis in experimental systems. In bleomycin models, plasminogen deficiency and PAI-1 overexpression led to increased fibrosis (51, 53). Deficiency of PAI-1 and overexpression of uPA prevented fibrosis (51, 54). This data is corroborated in human studies as IPF patients have suppressed

fibrinolytic capability (55). Interestingly, fibrinogen null mice were not protected from lung fibrosis, suggesting that plasmin has beneficial roles apart from degrading fibrin (56), perhaps through the activation of latent growth factors (57) or matrix metalloproteinases (58). In fact, the protection due to deficiency of PAI in mice is at least partly due to increased levels and availability of HGF in the lung (59).

Growth factors originating from epithelium likely contribute to pulmonary fibrosis. TGF-β1 is a profibrotic growth factor found to be upregulated in human IPF (60). Furthermore, induction of TGF-β1 by alveolar epithelial cells led to the development of pulmonary fibrosis in mice (61). TGF-β exerts its actions through signaling intermediates known as Smads. In bleomycin mouse models, the profibrotic Smads (Smads 2, 3, and 4) are increased in the lung while the antifibrotic Smad 7 is decreased (62). The profibrotic Smads have been linked to increased production of various collagen proteins as well as increased tissue inhibitor of metalloproteinase-1, which would lead to overall collagen deposition (63). One of the reasons behind the IFN-γ clinical trials in IPF patients is the fact that IFN-γ increased Smad 7 to inhibit TGF-β signaling and collagen synthesis (64, 65).

Other growth factors, cytokines, chemokines, and prostaglandins from epithelium have been implicated in pulmonary fibrosis. Overexpression of TGF-α from epithelium induced lung fibrosis in mice (66). Platelet-derived growth factor (PDGF) promotes fibroblast migration and growth and is increased in IPF epithelial cells (67). Tumor necrosis factor-alpha (TNF-α) expressed under the lung epithelial promoter induced inflammation that eventually led to fibrosis (68). On the other hand, prostaglandin E2, which has an inhibitory effect on fibroblasts, is downregulated in IPF (69).

1.4.2. Fibroblasts and Myofibroblasts

As the primary matrix-secreting cells in pulmonary fibrosis, fibroblasts and myofibroblasts play a key role in this disease. Although fibroblasts are normally recruited after injury, repair in pulmonary fibrosis is abnormal, leading to excessive fibroblast activity (44). Fibroblastic foci, composed of loose fibrosis populated with myofibroblasts, are a major focus of current research. These foci may represent the leading edge of fibrotic damage (70).

Proliferation of fibroblasts from IPF lungs can be either upregulated or downregulated, but downregulation is characteristic of advanced fibrosis and suggests more advanced differentiation (71). IPF fibroblasts also display anchorage independent growth *in vitro* (72) and lower apoptosis rates (73). Consistent with the disease process, IPF fibroblasts exhibit increased ECM production (74) and decreased capacity to degrade ECM due to increased tissue inhibitor of metalloproteinases (75, 76).

Fibroblasts can undergo conversion into myofibroblasts that possess an activated phenotype. The myofibroblast has features of both fibroblasts and smooth muscle cells, producing large amounts of ECM protein (77) and possessing a contractile phenotype (78). Myofibroblasts are also capable of producing growth factors (79), cytokines (80), chemokines (81), and reactive oxygen species (82, 83).

1.4.3. Inflammation

The role of inflammation in pulmonary fibrosis is controversial. A contributory role was previously assumed because of increases in leukocytes in BAL and histology sections in IPF. This inflammation is typically comprised of PMN, macrophages, eosinophils, mast cells, and lymphocytes (14). These cells are capable of releasing large amounts of oxidants, proteases,

growth factors, and cytokines that can damage or induce damage in the lung. The animal models of pulmonary fibrosis, including asbestos and bleomycin, support this concept, as fibrosis is generally preceded by inflammation (27, 35).

However, the causative nature of these changes has not been definitively proven in human disease. Corticosteroids are potent anti-inflammatory agents but their efficacy in improving survival and pulmonary function as front-line therapies in IPF is low. Levels of inflammation do not correlate with disease severity or outcome (84). Selman and colleagues point out that some renal and liver fibrotic diseases occur in the presence of very low levels of inflammation (7). In fact, one mouse model of IPF utilizing the overexpression of TGF-α demonstrated that development of fibrosis can occur in the absence of inflammation (66). Further, studies of epithelium and fibroblasts described above have demonstrated that these cells can produce the necessary factors to create a profibrotic environment and that inflammation may not be necessary. In light of this evidence, many investigators are beginning to view IPF as a disease of abnormal chronic wound repair instead of fibrosis due to unrelenting inflammation.

1.4.4. Matrix Turnover

Clearly, a disorder involving deposition of excess collagen must involve imbalances in matrix formation and degradation. In this regard, the matrix metalloproteinases and their inhibitors may play pivotal roles in the development of pulmonary fibrosis. Indeed, abnormal expression and activity of the metalloproteinases have been reported in IPF. These studies are discussed in more detail in Chapter 1.6.

1.4.5. Oxidative Stress

A number of studies are uncovering a role for oxidative stress in the development of pulmonary fibrosis. Oxidative stress refers to an imbalance in reactive oxygen species and antioxidants in which reactive oxygen species chemically modify biological molecules, potentially alterating their normal function. Lungs in IPF patients are exposed to a greater oxidative burden than lungs from normal individuals (19, 85), thus suggesting a role for oxidative stress in this disease.

1.4.5.1. Reactive Oxygen Species

Molecular oxygen is abundant in the atmosphere and vital to life. Oxygen is normally utilized as the terminal electron acceptor in the mitochondrial transport chain. In a reaction catalyzed by cytochrome c oxidase in the inner mitochondrial membrane, oxygen undergoes a four-electron reduction to water (86). However, oxygen can also undergo this reduction in an uncontrolled manner, leading to the production of potentially harmful chemical species.

Reactive oxygen species (ROS) are metabolites of oxygen that, in contrast to the parent molecule, have a propensity for participating in chemical reactions. When oxygen undergoes sequential one-electron reductions, superoxide ($O_2\bullet^-$), hydrogen peroxide (H_2O_2), and hydroxyl radical ($\bullet OH$) (which are all ROS) are formed before conversion to water (86):

$$O_2 \xrightarrow{e^-} O_2\bullet^- \xrightarrow[+\,2H^+]{e^-} H_2O_2 \xrightarrow[-\,OH^-]{e^-} \bullet OH \xrightarrow[+\,H^+]{e^-} H_20$$

Superoxide and hydroxyl radical are free radicals, while hydrogen peroxide is not. These metabolites can also lead to the production of other ROS. Peroxynitrite, a potent ROS, is produced by a reaction between superoxide and nitric oxide (see Chapter 1.4.5.2) (87) and a

reaction between hydrogen peroxide and nitrite (88). ROS can be formed in any cell that utilizes mitochondrial respiration or is exposed to oxygen, an idea confirmed by the ubiquitous presence of antioxidants. Most cells can also produce ROS in a concerted fashion through enzymes such as NADPH oxidases and xanthine oxidase (89, 90). Cells capable of especially high production of ROS include inflammatory cells and myofibroblasts.

ROS can cause chemical modifications in DNA (e.g. strand breaks, mutations), lipids (thromboxane formation, lipid peroxidation), proteins (altering function, often at sulfhydryl groups; protein fragmentation), and transcription factors (91, 92). Such modifications can seriously impair the biological functions of these molecules. In the chemical reactions, the ROS typically gain electrons and therefore act as oxidizing agents or oxidants. ROS are opposed by antioxidants, which remove ROS before they can cause damage to cells and tissues. Oxidative stress occurs when there is an imbalance favoring oxidants over antioxidants. Oxidative stress has been reported to play a role in cardiovascular disease (93, 94), neurodegeneration (95), cancer (96-98), and aging (99).

1.4.5.2. Superoxide

The superoxide radical anion ($O_2^{\bullet -}$) is the result of a one-electron reduction of molecular oxygen. Superoxide is always produced during the normal reduction of oxygen to water, but intracellularly, superoxide can also be formed in mitochondria by the reaction of oxygen with electrons leaked from the electron transport chain. Neutrophils, monocytes, and macrophages, among other cells, can also produce superoxide using NADPH oxidase (86). As part of host defense, neutrophils harness this superoxide to produce hypochlorous acid (HOCl, bleach)

through the myeloperoxidase enzyme. These reactions by inflammatory cells are known as the oxidative burst and can inflict major damage to invading pathogens as well as normal tissue (86).

Despite being a free radical, superoxide is relatively unreactive and is actually better at donating electrons (acting as a reductant) than accepting them (acting as an oxidant). Superoxide can nonetheless participate in reactions that produce potent oxidants (100). One such reaction is spontaneous dismutation in which superoxide acts as both an oxidizing and reducing agent in the same reaction. This leads to the production of hydrogen peroxide and oxygen:

$$2\ O_2\bullet^- \ + \ 2H^+ \ \rightarrow \ H_2O_2 \ + \ O_2$$

This reaction can also be catalyzed by antioxidant enzymes known as superoxide dismutases (see Chapter 1.5).

Superoxide can also participate in hydroxyl radical formation. Superoxide can react with nitric oxide (NO) at a rate of 10^9 to 10^{10} per mole per second to form the powerful oxidizer peroxynitrite ($ONOO^-$) (101). Peroxynitrite can mediate major modifications of biological molecules, such as the formation of nitrotyrosine modifications at tyrosine residues in proteins (87). Peroxynitrite also decomposes at physiological pH to form hydroxyl radical and nitrogen dioxide:

$$O_2\bullet^- \ + \ NO\bullet \ \rightarrow \ ONOO^-$$

$$ONOO^- \ + \ H^+ \ \rightarrow \ ONOOH$$

$$ONOOH \ \rightarrow \ \bullet OH \ + \ NO_2\bullet$$

Peroxynitrite, the hydroxyl radical, and nitrogen dioxide are all potent oxidants thought to be important in a number of diseases, including pulmonary fibrosis (102, 103). Since there is

increased nitric oxide production in pulmonary fibrosis (103, 104), this pathway may be of particular importance in this disease.

Superoxide can also produce hydroxyl radical though the Haber-Weiss reaction, in which ferric iron (Fe^{3+}) is reduced to ferrous iron (Fe^{2+}) by superoxide (105). Ferrous iron then reacts with hydrogen peroxide to form the hydroxyl radical:

$$O_2\bullet^- + Fe^{3+} \rightarrow Fe^{2+} + O_2$$

$$H_2O_2 + Fe^{2+} \rightarrow \bullet OH + OH^- + Fe^{3+}$$

Therefore, iron undergoes oxidation/reduction (redox) as a catalyst for this reaction. The second reaction by itself is also known as the Fenton reaction. Since availability of free ferric and ferrous iron is limited in the body, the physiological importance of this reaction may be limited to cases in which exogenous iron is present. Notably, the ability of asbestos fibers to bind metal ions could provide a source of redox-available iron for this reaction (see Chapter 1.4.6).

1.4.5.3. Nitrosative Stress

Nitric oxide ($NO\bullet$) is capable of forming powerful oxidants, and these species can modify and alter the functions of proteins. Nitrosative stress occurs in disease states in which excess reactive nitrogen species (RNS) leads to undesirable modifications of biological molecules. Nitric oxide is produced by nitric oxide synthases (NOS) from L-arginine and oxygen. Two NOS enzymes are constitutively expressed and produce nitric oxide at low levels under normal conditions. The inducible form of these enzymes (iNOS), can produce up to 20 times more nitric oxide and is upregulated in response to stimuli such as lipopolysaccharide (87).

As noted above, peroxynitrite is produced by the rapid reaction between superoxide and nitric oxide. Production of this powerful oxidant is probably a defense against microorganisms, as evidenced by the fact that salmonella have evolved peroxynitrite reductase enzymes to cope with its release (106). Peroxynitrite can oxidize thiols and modify tyrosines on proteins. Such modifications can seriously alter protein function, which has been described in Alzheimer's Disease and ulcerative colitis of the gut, among other diseases (107, 108). Nitric oxide also has a potential role in cell signaling, as it inhibits the phosphorylation of the inhibitor of NF-κB (109).

1.4.5.4. The Lung's Antioxidant Defenses

The lung may be especially vulnerable to ROS as it is exposed to higher oxygen tensions than other vital organs. Furthermore, cigarette smoke and other environmental pollutants represent additional oxidant burdens for the lung. These exposures necessitate strong antioxidant defenses to prevent excessive damage to the lung (110).

Various antioxidants with specialized functions are present in the lung to scavenge the different ROS. Glutathione may be the most important bulk scavenger of hydrogen peroxide in the lung and is 140 times more abundant in lung epithelial lining fluid compared to blood (111). Reduced gluatathione (GSH) is utilized by glutathione peroxidase enzymes to reduce hydrogen peroxide to water. Hydrogen peroxide is also removed by catalase, which enzymatically catalyzes its reduction to water (86). The superoxide dismutases (see Chapter 1.5) are a major group of three antioxidants that collectively scavenge superoxide intracellularly and extracellularly (112). Vitamins, mucins, metal-binding proteins, and albumin also have potential antioxidant functions in the lung (19, 86).

1.4.5.5. Oxidative Stress in IPF

Current evidence indicates that IPF lungs are exposed to especially high oxidant burdens. Bronchoalveolar lavage (BAL) fluid from IPF patients possessed increased oxidative stress markers including lipid peroxidation (85) and 8-isoprostane (113). IPF lungs contain more myeloperoxidase (114), while inflammatory cells from IPF patients release more superoxide and hydrogen peroxide than normal (115, 116).

Abnormal nitric oxide regulation has also been observed in IPF. Saleh and colleagues found increased nitrotyrosine in IPF lungs, indicating peroxynitrite-mediated modifications (103). This study and others also found increases in iNOS in early to intermediate stage IPF localizing to macrophages, neutrophils, and alveolar epithelium (117). However, iNOS expression was significantly decreased in end-stage samples, suggesting a role only in early and intermediate disease (103).

Numerous studies in human IPF lung samples have described abnormal antioxidant levels. A number of investigations have observed decreased reduced (protective) glutathione in both alveolar lining fluid (85) and intracellularly (118). Although catalase exhibited no major changes, manganese superoxide dismutase (MnSOD) is markedly upregulated in UIP lungs compared to normal lung. While this may represent a compensatory response against increased oxidants, MnSOD levels were found to be low in mature fibrosis, suggesting a deficiency in antioxidant protection late in IPF (119).

While the above studies in human IPF are invaluable, ROS and RNS have also been implicated in experimental models of pulmonary fibrosis. In bleomycin-induced pulmonary fibrosis in mice, superoxide dismutase activity was protective against disease development (discussed in more detail in Chapter 1.5.5). Experimental therapies with agents possessing

antioxidant capability reduced fibrosis development (120-124). Reduction in mortality, inflammation, and lipid peroxidation were noted. NOS inhibition also reduced fibrosis without affecting inflammation in one study, (125). However, inflammation was increased in iNOS null mice in a conflicting study (126).

The potential targets of increased oxidative stress in IPF are numerous. It has been proposed that ROS can interact with proteases and their inhibitors to alter their function in the lung (127). The matrix metalloproteinases (see Chapter 1.6) represent an entire family of proteolytic enzymes that can be activated by ROS through oxidative modification of the cysteine switch (128). In addition, protease inhibitors such as tissue inhibitors of metalloproteinases (129), alpha-2-macroglobulin (130), and secretory leukocyte protease inhibitor (131) can be inactivated by oxidative stress. The inactivation of alpha-1-proteinase inhibitor (α1-PI) by cigarette smoke ROS is pathogenic in the development of emphysema (132, 133). Notably, α1-PI deficiency was described in familial IPF (134). Smokers have higher rates of IPF, which may be explained through inactivation of α1-PI by ROS (135).

TGF-β is a potent profibrotic growth factor and can be modulated by ROS. ROS can release this growth factor from lung epithelium (136) and cause its activation through dissociation from latency associated peptide (137). Active TGF-β can in turn induce myofibroblasts to produce more ROS in a positive feedback loop (83).

Transcription factors are sensitive to oxidative stress. The Nrf2 transcription factor is redox sensitive and is responsible for the upregulation of a number of antioxidants, including glutathione peroxidase (138). NF-κB is also sensitive to redox modulation, and its activity is abrogated in NAC-treated animal models (139).

Based on the evidence above, antioxidant therapies were designed to treat patients with IPF. Trials involving N-acetylcysteine (NAC) have been encouraging. NAC is a source of cysteine, the precursor for glutathione synthesis. NAC therapy increased both intracellular glutathione in BAL fluid cells and extracellular glutathione in the BAL fluid itself (20, 118, 140). IPF patients on this therapy exhibited improved pulmonary function tests and blood oxygen saturation compared to pre-therapy (20). A large European trial is confirming these results with NAC (141).

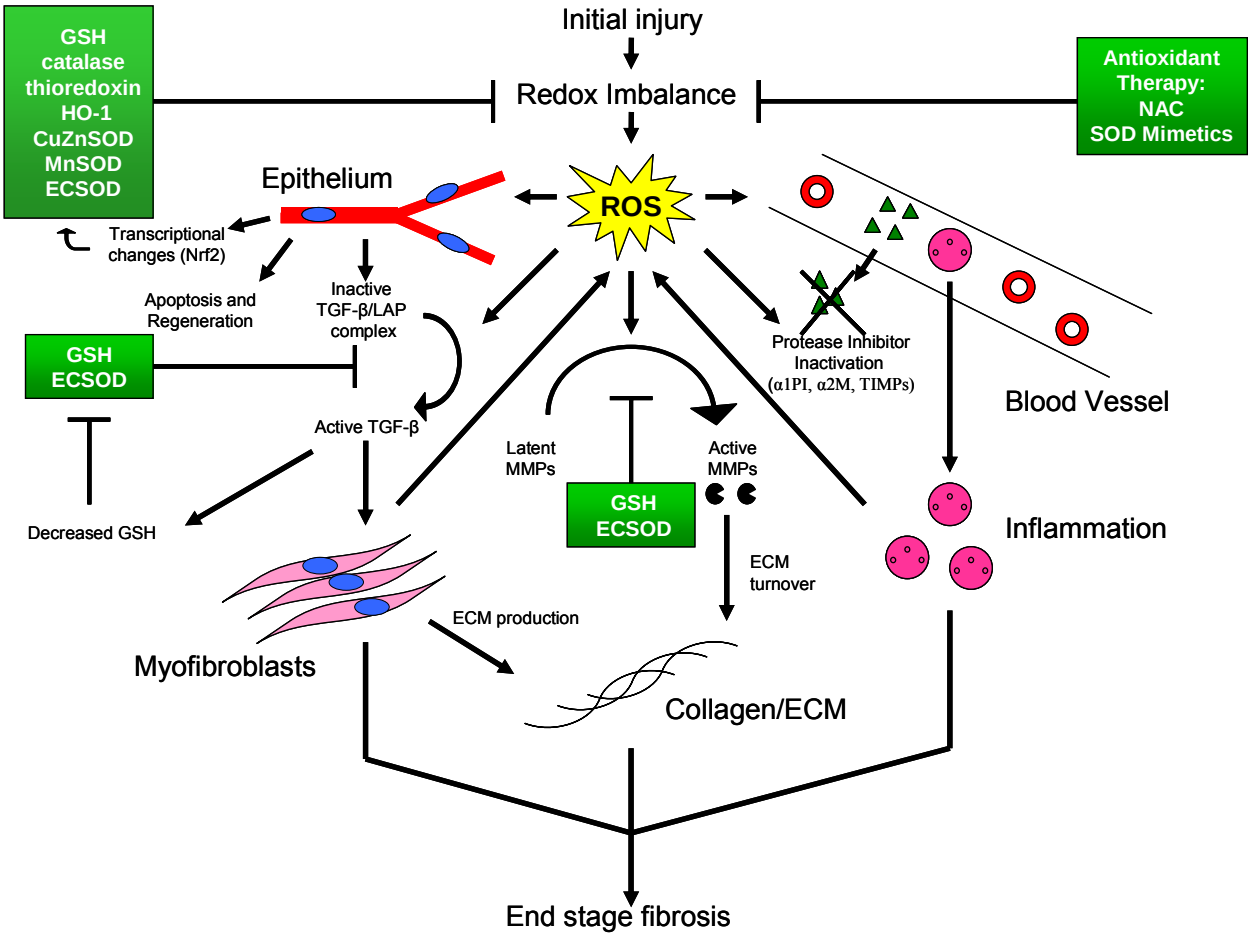

Figure 1. Overview of the role of oxidative stress in pulmonary fibrosis.

Exogenous and endogenous irritants in IPF create a redox imbalance resulting in the production of reactive oxygen species (ROS). Widespread effects on epithelium, myofibroblasts, growth factors (e.g. TGF-β), inflammatory cells, proteases (e.g. MMPs), protease inhibitors, and the extracellular matrix (ECM) may ultimately contribute to the development of end stage fibrosis. Shown also are endogenous antioxidants (green boxes) and the steps at which they can protect the lungs from the effects of ROS. Processes outside the cell, such as the activation of TGF-β and MMPs, would be primarily affected by the major extracellular antioxidants including GSH, EC-SOD, and small molecules such as vitamins. Exogenous antioxidants such as N-acetylcysteine (NAC) and superoxide dismutase (SOD) mimetics can augment antioxidant defenses and thus serve as potential therapies for IPF. *Definition of abbreviations:* GSH = glutathione; GPx = glutathione peroxidase; eGPx = extracellular glutathione peroxidase; HO-1 = heme oxygenase-1; CuZnSOD = copper/zinc superoxide dismutase; MnSOD = manganese superoxide dismutase; ECSOD = extracellular superoxide dismutase; α1PI = alpha-1-proteinase inhibitionr; α2M = alpha-2-macroglobulin; TIMP = tissue inhibitior of metalloproteinases.

1.4.6. Pathogenesis of asbestosis

The pathogenesis of asbestosis is thought to involve many of the same mechanisms described above for IPF, which is not surprising considering the similarities between the diseases clinically and pathologically. Growth factors, cytokines, inflammation, oxidative stress, apoptosis, and signaling are all thought to contribute to asbestosis pathogenesis.

Various growth factors and cytokines are increased in asbestos-mediated injury. A number of studies have noted an upregulation of the profibrotic TGF-β after asbestos exposure (142-144). Asbestos-induced increases in fibroblast growth factor (145), and in PDGF (146) and its receptor (147) have also been described.

Inflammation appears to play a more definite pathogenic role in the development of asbestosis than in IPF. In humans with asbestosis and in animal models of this disease, BAL fluid contains increased macrophages and neutrophils (38, 148, 149). Asbestos-exposed endothelial cell cultures upregulate ICAM-1 which increases neutrophil adherence, an important step in diapedesis into lung tissue (150). The chemoattractants, macrophage inflammatory protein (MIP) and interleukin-8, and proinflammatory cytokines, TNF-α and IL-1, were all upregulated in response to asbestos (151-154). As phagocytic inflammatory cells unsuccessfully attempt to engulf asbestos, a process that has been termed "frustrated phagocytosis," these cells produce ROS (155, 156).

1.4.6.1. Role of oxidative and nitrosative stress.

Perhaps even more than in IPF pathogenesis, ROS and RNS are hypothesized to play a major role in the development of asbestos-related diseases. The reason for this emphasis is twofold. First, the iron present on asbestos fibers can, at least theoretically, catalyze the Haber-Weiss

reaction to produce potent oxidants such as the hydroxyl radical. Thus, many studies focus on iron-loading or iron chelation of asbestos fibers as a method by which to modulate ROS production in model systems. Second, the inflammatory cells that populate the lung in asbestosis are potent producers of oxidants and can add significantly to the oxidant burden in the lung.

A large body of literature provides support for the free radical hypothesis of asbestos injury. Investigators have detected the *in vivo* formation of both lipid peroxidation products and hydroxyl radicals after intratracheal administration of asbestos in rats (157, 158). The source of this ROS may be inflammation, as exposure of macrophages to asbestos leads to increased production of hydrogen peroxide, superoxide, and both inducible NOS and nitric oxide (35, 156, 159, 160). Lungs from rats treated with asbestos increase production of CuZnSOD, MnSOD, catalase, and glutathione peroxidase, likely as a compensatory increase in response to elevated oxidative stress (161).

Experimental evidence has also shed light on some of the targets of ROS in asbestosis. Through an iron-dependent mechanism, asbestos was shown to increase expression of PDGF-A, TGF-β1, and procollagen in rat tracheal explants. The growth factor effects were dependent upon the extracellular signal-regulated protein kinase (ERK) pathway, while procollagen was governed by NF-κB (146), both of which are redox sensitive (162). Asbestos also causes DNA strand breaks, an event associated with ROS and which in this study correlated with hydroxyl radical formation, also in an iron-dependent manner (163). Nitric oxide was found to be involved in the oxidation of DNA in human epithelium, as measured by levels of 8-hydroxy-2-deoxyguanosine (164). In alveolar epithelial cultures, asbestos induced mitochondrial dysfunction (37) and caspase-3 activation leading to apoptosis that was attenuated by iron chelation and hydroxyl radical scavengers (165).

Experimental studies have described conflicting results regarding superoxide dismutase involvement in the disease. MnSOD overexpression protected epithelium from asbestos-mediated cytotoxicity (166). Macrophages were also protected from cytotoxicity by superoxide dismutase and catalase *in vitro* (160). However, one investigation found no effect from osmotic pump treatment in rats with superoxide dismutase conjugated to polyethylene glycol to increase half-life. This study did find a protective effect with similarly conjugated catalase (149). These differences may be due, at least in part, to the localization of the SOD that is being added to the system. MnSOD is intracellular while conjugated SOD is extracellular. Furthermore, the conjugation to polyethylene glycol may prevent SOD from getting to the cell surface. The role of SOD in asbestosis remains to be further elucidated.

1.5. EXTRACELLULAR SUPEROXIDE DISMUTASE

Extracellular superoxide dismutase (EC-SOD) is the third mammalian enzyme discovered that catalyzes the dismutation of the superoxide anion to hydrogen peroxide and oxygen. Particularly abundant in the lung, a number of functions in the pulmonary architecture have been attributed to EC-SOD. In particular, current evidence suggests that loss of EC-SOD plays a role in the development of interstitial lung disease.

1.5.1. Historical Background

The first discovery of superoxide dismutases (SODs) took place in 1969, when Joe McCord and Irwin Fridovich demonstrated superoxide dismutase activity for a previously described protein, erythrocuprein. This protein came to be known as copper/zinc SOD (CuZnSOD, also known as SOD1) because of its metal content (167). The authors noted that the existence of the enzyme

indicated a vital role in protection against the superoxide radical. Manganese SOD (MnSOD, or SOD2) was discovered four years later by Weisiger and Fridovich in mitochondria, and unlike CuZnSOD was insensitive to cyanide (168). It was not until 1982, thirteen years after the first discovery of SODs, that the third mammalian isozyme was purified from human lung by Stefan Marklund (169).

Extracellular superoxide dismutase (EC-SOD, or SOD3) had a much higher molecular weight than the other two SODs. It was partially purified utilizing concanavalin A-sepharose, indicating the presence of N-linked carbohydrate moieties. The enzyme eluted from a heparin-sepharose column in three fractions, denoting varying affinity for heparin. Like CuZnSOD, EC-SOD was sensitive to cyanide (169).

1.5.2. Biochemistry of EC-SOD

EC-SOD (EC 1.15.1.1) is a 135kD, homotetrameric enzyme capable of catalyzing the dismutation of superoxide free radicals. The complete enzyme is formed by two disulfide linked dimers (Figure 2). The intersubunit disulfide bridges connect cysteines at the C-terminal end of each subunit (170). Noncovalent interactions at the N-termini hold together the four subunits of the complete enzyme. While both mouse and human EC-SOD share this overall structure, rat EC-SOD exists only as a dimer (171). N-linked glycosylation at Asn89 (numbering according to the human protein) explains the affinity of EC-SOD to concanavalin A (172). Each subunit contains one copper and one zinc atom (169).

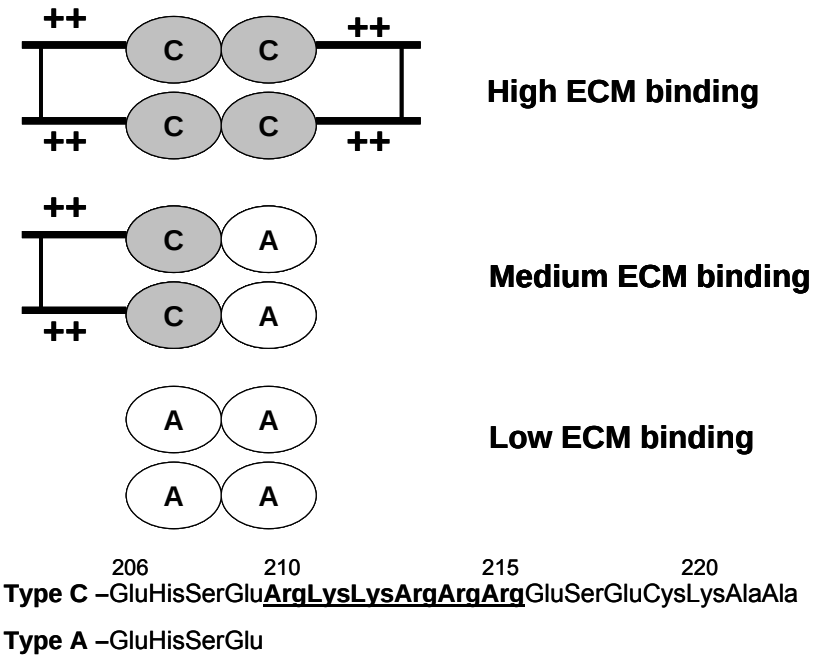

Figure 2. The EC-SOD homotetramer can have varying affinities for heparin.

EC-SOD in mice and humans is composed of four identical subunits. Two of the subunits form a disulfide-linked dimer at the C-terminus while noncovalent interactions at the N-terminus hold the complete tetramer together. Each subunit is synthesized with a heparin-binding domain near the C-terminus with the underlined sequence shown at the bottom of the figure (a Type C subunit). The four heparin-binding domains can be sequentially cleaved by proteases (forming Type A subunits) after protein synthesis, leading to high, medium, and low affinity for heparin.

The C-terminal domain of EC-SOD is unique among SOD enzymes and plays a role in regulating tissue distribution. Positions 210-215 in the enzyme are composed of six positively charged amino acids with the sequence Arg-Lys-Lys-Arg-Arg-Arg in both humans and mice. This sequence provides affinity for heparin and the extracellular matrix (173, 174). A mutation in this sequence converting arginine at position 213 to glycine has been described in humans. This mutation significantly reduces the heparin affinity of EC-SOD, leading to a 10-fold increase in plasma EC-SOD and confirming the importance of this heparin-binding domain in EC-SOD's matrix localization (175). This mutation may play a role in cardiovascular health (see Section 1.5.4).

The heparin-binding domain (HBD) can be posttranslationally cleaved from the enzyme, leading to a loss of heparin affinity. The truncated EC-SOD has a sequence ending at Glu209 and retains full enzymatic activity (172). Since each subunit of EC-SOD has its own HBD, the tetrameric enzyme could have zero to four total HBDs, leading to EC-SOD with affinity for heparin that varies from none to strong. Indeed, during heparin-sepharose purification of EC-SOD, the enzyme was recovered in three fractions: type A (no affinity), type B (moderate affinity), and type C (strong affinity) (169, 173). A number of proteases, including trypsin and plasmin, have been shown to cleave this domain *in vitro* (176). Although furin has also been demonstrated to cleave this domain intracellularly in cell cultures (177, 178), the *in vivo* protease responsible for this cleavage in lung tissue, particularly in disease states, is currently unknown.

Recently, a second structure of EC-SOD was described with a different pattern of intrachain disulfide bridges. The newly discovered tertiary structure creates a more constrained structure that is enzymatically inactive. This inactive EC-SOD is present in low abundance in humans but has not been found in any other species including the mouse. The importance of this form of EC-SOD is currently being examined (179).

The EC-SOD gene is approximately 5900 bp long, located on human chromosome 4 (180, 181). The promoter contains antioxidant and xenobiotic response elements, and AP-1 binding sites (181). Interferon-γ increases EC-SOD expression while TNF-α and TGF-β suppress it (182).

1.5.3. Distribution of EC-SOD

EC-SOD is present in many tissues and extracellular fluids. The enzyme exists in particularly high concentrations in arteries and in pulmonary airways (183). EC-SOD is also abundant in

lung alveoli of humans and mice where it is produced by type II epithelial cells, bronchial epithelial cells, macrophages, and neutrophils (184-186). EC-SOD is also present in plasma, kidney, heart, brain, and the uterus (173, 175, 186, 187).

1.5.4. Function of EC-SOD in tissues

EC-SOD catalyzes the dismutation reaction of superoxide at a rate constant of 1×10^9 per mole per second, which is almost diffusion limited (169). The enzyme thus produces oxygen and hydrogen peroxide, the latter detoxified through the action of catalase and peroxidases in cells and tissues. More importantly, SOD removes superoxide from the system, eliminating a potential source of potent oxidants (see Chapter 1.4.5.2).

EC-SOD has multiple roles in normal homeostasis. Since superoxide can react with nitric oxide at diffusion limited rates, EC-SOD can preserve nitric oxide to allow vasorelaxation and other functions (172). Scavenging of superoxide also prevents the formation of peroxynitrite and hydroxyl radical and decreases oxidant-mediated damage to tissues (112). Since neutrophils produce large amounts of superoxide, EC-SOD may act to balance the large pro-oxidant activities of these inflammatory cells (184). EC-SOD is also known to bind type I collagen and protect it from oxidative fragmentation, indicating an important role in protecting ECM components from oxidative stress (174).

EC-SOD has been implicated in a number of diseases in a number of different organ systems in the body. Atherosclerosis is thought to involve ROS, and patients with coronary artery disease have significantly reduced EC-SOD levels (188). Even more impressive is an association found between persons with the Arg213Gly mutation of EC-SOD and ischemic heart disease. In a large prospective study, Juul and colleagues found that persons with the mutation,

which leads to accelerated loss of EC-SOD from arterial walls, carry 1.5 times the risk of ischemic heart disease (189). Experimentally, diabetic arteries contained less EC-SOD than nondiabetic controls (112), and EC-SOD protects against focal cerebral ischemia (190, 191). Ischemia/reperfusion injury was also reduced in experiments using recombinant EC-SOD (192). EC-SOD knockout mice have impaired learning and memory (193). Controversy exists over the role of EC-SOD in rheumatoid arthritis, but its abundance in synovial fluids suggests that it could be protective (194).

The presence of EC-SOD in alveoli, the primary site of damage in pulmonary fibrosis, implies a function in protecting the lung from oxidants (195). Utilizing knockout and transgenic mice, EC-SOD was found to be protective in various animal models of lung disease, including hyperoxia in adult (196, 197) and newborn mice (198), lung damage from oil fly ash (199), hemorrhage-induced lung injury (200), and LPS-induced neutrophilic inflammation (201). EC-SOD is effectively able to inhibit the pulmonary inflammation common to these diseases. This effect may be related to decreases in NF-κB activity (200) and to blocking ROS-mediated upregulation of vascular selectins and proinflammatory cytokines (MIP-2, TNF-α) important for neutrophil diapedesis and chemotaxis (201).

1.5.5. EC-SOD in pulmonary fibrosis

An increasing body of evidence supports a role for EC-SOD in the pathogenesis of pulmonary fibrosis. In a bleomycin mouse model of pulmonary fibrosis, EC-SOD has been shown to have a protective effect. Transgenic mice that express increased levels of EC-SOD are protected from development of pulmonary fibrosis (202). Similarly, treating mice with exogenous SOD or SOD mimetics leads to decreased severity of bleomycin-induced disease (120, 203). On the other

hand, EC-SOD knockouts develop more severe fibrosis after bleomycin. In the knockout mice, this fibrosis is accompanied by increases in inflammation and an increase in oxidative fragmentation of collagen (204) which may propagate the inflammatory response as collagen fragments are known chemoattractants and activators of neutrophils (205, 206). These studies indicate that EC-SOD plays a protective role against inflammation and pulmonary fibrosis.

Notably, EC-SOD is depleted from the lung parenchyma of mice treated with bleomycin (207) or hyperoxia (208). This depletion appeared to be due to the proteolytic cleavage of the heparin-binding domain of EC-SOD and was associated with accumulation of proteolyzed EC-SOD in the airspaces presumed to originate from the lung parenchyma. This study suggested increased susceptibility of the lung to oxidative stress in pulmonary fibrosis and hyperoxic interstitial lung injury through proteolytic removal of EC-SOD from lung parenchyma. The *in vivo* protease responsible for this redistribution is currently unknown, but a number of proteases including the MMP family are known to be upregulated in IPF and hyperoxia which may contribute to this redistribution of EC-SOD.

Collectively, the studies described above indicate important functions for EC-SOD in pulmonary fibrosis. No studies of EC-SOD in human IPF have been reported in the literature. Importantly, EC-SOD has also never been examined in the context of pneumoconiosis diseases.

1.6. MATRIX METALLOPROTEINASES

The matrix metalloproteinases (MMPs) are a family of proteolytic enzymes with the capability of degrading a wide variety of extracellular proteins. The first discovery of these enzymes came in 1962, when Gross and Lapiere described collagenase activity in metamorphosing tadpoles

(209). At least 25 MMPs are now known to exist and are attributed diverse roles described in normal tissue and disease (210).

1.6.1. Biochemistry of Matrix Metalloproteinases

The basic structure of MMPs involves a number of building blocks common to all members of this family. These building blocks include a signal peptide, prodomain/propeptide, catalytic domain, and C-terminal hemopexin-like domain. The signal peptide governs secretion from the cell, while the C-terminal domain plays a role in substrate specificity. The catalytic domain is highly conserved among the MMPs, consisting of the sequence **H**EXG**H**XXGXX**H**S/T, in which the three histidines coordinate with an active site zinc atom. The propeptide consists of a conserved cysteine in the sequence PR**C**XXPD that coordinates with the active site zinc and renders the enzyme inactive at time of synthesis. Some MMPs possess unique domains in addition to those described above, such as GPI-linked transmembrane domains and fibronectin-like repeats. At the other extreme is MMP-7 (matrilysin), a "minimal" MMP that possesses only the signal domain, prodomain, and catalytic domains and lacks the hemopexin-like domain.

MMPs have been grouped by their *in vitro* substrate specificity, although much debate surrounds their *in vivo* substrates. A partial list of the MMPs and their substrates is shown in Table 1. The collagenases are capable of cleaving collagen types I and II (211). The gelatinases (MMP-2 and -9, also known as gelatinase A and B) are known for their ability to degrade not only gelatin (denatured collagen) but also native type IV collagen, the critical component to basement membranes. However, diverse roles for the MMPs are being described, and structural ECM components are no longer the only recognized substrates for these enzymes.

Table 1. Partial list of metalloproteinases implicated in pulmonary fibrosis and their substrates.

MMP	Other name	Substrates	Expressed in
MMP-1 **MMP-8** **MMP-13**	Interstitial collagenase Neutrophil collagenase Rat collagenase	Type I and II fibrillar collagens (209, 211)	Fibroblasts (212), inflammatory cells (213)
MMP-2 **MMP-9**	Gelatinase A Gelatinase B	Native type IV collagen (214), gelatins (215), α1-proteinase inhibitor (MMP-9 only) (216)	Fibroblasts (214), inflammatory cells (213, 217), epithelium (218, 219)
MMP-7	Matrilysin	Syndecans (29), e-cadherin (220), FAS ligand (221), pro-alpha-defensins (222), a1-proteinase inhibitor (223)	Epithelium (224)

As noted above, MMPs share a common mode of activation termed the "cysteine switch" whereby disruption of the active site cysteine-zinc bond leads to autocatalytic cleavage of the prodomain and activation of the latent enzyme. However, this disruption can occur in a number of ways. Proteolysis of the prodomain has been demonstrated by furin (225), plasmin (226), and other metalloproteinases (227) leading to activation of MMPs. A well-described mode for MMP cross-activation is the cell surface activation of MMP-2 by the membrane anchored MT-MMP1 through a mechanism requiring the MMP inhibitor, TIMP-2 (228).

Modification of the cysteine switch by ROS or RNS can also activate MMPs. Hypochlorous acid oxidizes and activates MMP-7 (229). Hydrogen peroxide, peroxynitrite, and oxidants produced by the xanthine/xanthine oxidase system can activate both MMP-2 and MMP-9 (230, 231). The cysteine switch of MMP-9 can also be activated by nitric oxide through S-nitrosylation of the thiol group (232)(29). In addition, ROS have been shown to directly induce MMP transcription (233). Importantly, ROS do not always activate proteases, but can inactivate

them as well. Hypochlorous acid can inactivate gelatinases (234) and even MMP-7 (235), which it previously was shown to activate, at high concentrations. Therefore, it is likely that local concentrations of ROS/RNS will determine whether MMPs are activated or inactivated. It has been suggested that the rapid activation and subsequent inactivation of MMPs by oxidative mechanisms could regulate powerful "quantum bursts" of proteolytic activity (210).

Endogenous inhibitors serve to inactivate MMPs after prodomain cleavage. Four tissue inhibitors of metalloproteinases (TIMPs) have been described. TIMPs can bind MMPs with 1:1 stoichiometry to inhibit their activity. There is some specificity, as certain TIMPs preferentially bind some MMPs (236). However, as described above, some TIMPs can play a role in activating MMPs (228). Another general inhibitor of MMPs is alpha-2-macroglobulin (a2M). This large inhibitor traps proteases and governs their removal from tissues and the circulation (237).

Among the members of the MMP family, much research has focused on the roles of MMP-2, MMP-9, and MMP-7 in the development of IPF. Increases in all three of these MMPs have been demonstrated in human IPF and in experimental models. The exact function of these proteases *in vivo* in the lung requires further study.

1.6.2. MMP-2 and MMP-9: the Gelatinases

MMP-2, also known as gelatinase A or 72-kDa gelatinase, can be produced by both fibroblasts (212) and epithelium (218) in the lung. MMP-2 possesses a fibronectin-like domain that likely mediates binding to gelatins (238). MMP-2 proteolytically cleaves gelatin (239), type IV collagen (240), and elastin (241). TGF-β is capable of upregulating MMP-2 in fibroblasts (212). The enzyme can be activated by MT-MMP-1 (228), urokinase, and plasmin (242). ROS can also activate MMP-2 as described above.

MMP-9, also known as gelatinase B or 92-kDa gelatinase, is produced by neutrophils (243, 244), macrophages (245), T cells (246), and some fibroblasts (247). While normal lung does not produce much MMP-9, the following cells can be induced to produce it: bronchial epithelial cells (248), alveolar type II cells (218, 249), and fibroblasts (250). Like MMP-2, MMP-9 has a fibronectin-like repeat allowing for binding to gelatin (251). MMP-9 can cleave gelatins (252), type IV collagen (214), elastin (241), alpha-1-antitrypsin (216), and TGF-β1 (253), among other substrates. MMP-9 is upregulated by TGF-β, epidermal growth factor, and TNF-α (247).

Several studies have implicated MMP-2 and MMP-9 in human and experimental interstitial lung disease. The gelatinases' substrate specificity for type IV collagen indicates a role in the degradation of basement membranes (254), and an early event in pulmonary fibrosis is the disruption of these basement membranes (255). Loss of this barrier has been proposed to be important for inflammatory cell and fibroblast migration in the lung (256).

In investigations in humans, levels of MMP-2 and MMP-9 were elevated in lungs and BAL fluid of patients with IPF (76, 257). The upregulation of MMP-2 and -9 may be an important discovery since basement membranes are degraded during the course of pulmonary fibrosis and since these two MMPs can degrade type IV collagen in basement membranes. The above studies also found an increase in TIMP-2 in IPF (76, 257), which apart from its inhibitory capabilities can actually activate MMP-2 through a cell-surface mechanism (258). These same MMPs and TIMPs were also found to be upregulated in myofibroblasts and epithelium of IPF patients (75).

Experimental models of fibrosis have shown similar results. First, a role for MMPs in general in experimental pulmonary fibrosis was definitively shown because the

metalloproteinase inhibitor, batimastat, was able to inhibit the development of bleomycin-induced pulmonary fibrosis (28). Bleomycin-induced fibrosis in rabbits exhibited an early increase in MMP-9 followed by a more chronic expression of MMP-1 and MMP-2 as well as TIMP-1 and TIMP-2 (33). Asbestos exposure to PMNs *in vitro* caused release of proteases with increased "collagenase" activity, but the exact proteases were not identified (259). The only *in vivo* study examining asbestos and MMPs utilized the less fibrogenic chrysotile fibers and revealed increased mRNA for MMP-1 but not MMP-2 or TIMP-1 in response to chrysotile alone, and increased mRNA for MMP-2 and TIMP-1 when combined with cigarette smoke (260). MMP-9 and protein levels were not tested. Experimental lung silicosis also displayed an increase in MMP-2 and MMP-9 with reductions in TIMP-1 and TIMP-2 (261). Another study in silica-exposed mice revealed that Clara cell depletion leads to MMP-2 and MMP-9 upregulation, suggesting that Clara cells inhibit gelatinase production (262). Increased gelatinase activity was also associated with LPS-induced lung fibrosis (263), paraquat and hyperoxia-induced fibrosis (264), and in hyperoxic lung injury (218, 249, 265). These studies show that the two gelatinases may play a role in many lung diseases.

There is controversy surrounding the data presented above as well as the actual role of these MMPs in the lung. Unlike the other studies, one bleomycin study found increases in MMP-2 but not in MMP-9 (266). Studies in mice null for MMP-9 revealed similar levels of pulmonary inflammation after LPS exposure (217, 267). Furthermore, when these knockout mice were instead exposed to bleomycin to induce pulmonary fibrosis, there was no change in development of fibrosis at 21 days by histology, collagen content, or elastin content (219). The one phenotype observed was the absence of alveolar bronchiolization in the knockout mice. Alveolar bronchiolization describes the migration of bronchial epithelial cells such as Clara and

ciliated cells into areas of damaged alveoli, possibly as a repair mechanism. The loss of this in knockout mice indicated that MMP-9 does play a role in bronchial cell migration in the lung, irrespective of a negative effect on total fibrosis.

1.6.3. Matrix Metalloproteinase-7

MMP-7 (matrilysin) has the smallest molecular weight of any of the known MMPs. It possesses only the minimal structure of signal, propeptide, and catalytic domains. MMP-7 is induced by LPS (268), TNF-α, IL-1 (269), and IL-6 (270), while IFN-gamma downregulates it in macrophages (271). MMP-7 can cleave MMP-2 and MMP-9 as well as ADAM28, converting them to their active forms (224). MMP-7 is known to activate the alpha-defensins, an important part of the innate immune system (222).

MMP-7 was found to have a surprising role in the pathogenesis of pulmonary fibrosis. Initial gene microarray analysis performed on lungs from IPF patients and controls revealed that the gene most drastically altered was MMP-7, which exhibited increased expression in IPF over controls. When matrilysin knockout mice were given bleomycin, pulmonary fibrosis was markedly attenuated compared to wild type mice (244). It was later discovered that MMP-7 cleaves syndecans, upon which the mouse KC chemokine is bound. KC is analogous to the IL-8 neutrophil chemoattractant in humans. Without MMP-7, neutrophils could extravasate into the lung interstitium from the vasculature, but did not advance into the airspaces. This attenuation of airspace inflammation is thought to explain part of the protection of the MMP-7 knockouts from the effects of pulmonary fibrosis (29).

In spite of these described roles for MMPs in IPF and bleomycin-induced pulmonary fibrosis, the MMPs have not been examined for either their distribution or function in asbestosis.

MMPs have also not been evaluated for a role in the regulation of EC-SOD in any disease including pulmonary fibrosis.

1.7. CONCLUSIONS

Idiopathic pulmonary fibrosis and asbestosis are debilitating diseases that currently lack an effective treatment or cure. While many aspects of the development of these diseases are still being elucidated, an increasing body of evidence indicates an important role for both oxidant/antioxidant and protease/antiprotease imbalances and interactions. The antioxidant EC-SOD is expressed at high levels in normal lung but is depleted from lung parenchyma in bleomycin-induced pulmonary fibrosis. This depletion appears to be due to the proteolytic cleavage of its heparin-binding domain. Simultaneous with this depletion is an accumulation of EC-SOD in the BAL fluid. The mechanism underlying this change in EC-SOD is unknown but may involve the action of MMPs that are upregulated in pulmonary fibrosis. In turn, EC-SOD may also regulate MMPs through the prevention of oxidative activation of these enzymes. **It is therefore hypothesized that depletion of EC-SOD from the lung and interrelated increases in MMP enzymes contribute to disease development in pulmonary fibrosis.** To test this hypothesis, both EC-SOD and MMPs were examined in a mouse model of asbestosis due to amphibole fibers. Neither EC-SOD nor MMPs have been studied in the context of asbestos-related fibrotic lung disease. It is hoped that this research can identify novel mechanisms underlying pulmonary fibrosis that can be utilized in future treatments for the disease.

2. RATIONALE AND HYPOTHESIS

Studies in idiopathic pulmonary fibrosis have indicated a role for oxidant/antioxidant imbalance in the pathogenesis of the disease. IPF patients have increased markers of oxidative and nitrosative stress (85, 103), and their inflammatory cells are primed to release more ROS than normal (115). Meanwhile, endogenous antioxidant levels are altered in IPF lungs compared to normal controls, as glutathione levels are markedly decreased in the lung (118). Therapy with N-acetylcysteine, aimed at restoring this balance by increasing glutathione, has led to improved lung function in IPF patients (20).

Extracellular superoxide dismutase is an antioxidant enzyme abundant in the lung and protective in a variety of experimental lung disease models, including exposure to hyperoxia, LPS, and oil fly ash (197, 199, 201). EC-SOD also protects against the development of bleomycin-induced pulmonary fibrosis (202, 204). Importantly, in the bleomycin model, EC-SOD is removed from the extracellular matrix of the lung and accumulates in the airspaces (207). The mechanism of this depletion is likely the proteolysis of the heparin-binding domain of EC-SOD, which confers affinity for the matrix. Loss of this antioxidant from the lung parenchyma would increase susceptibility to oxidative stress and possibly enhance progression of the disease.

Potential targets of increased oxidative stress in the lung include the matrix metalloproteinase family of enzymes. Members of this family, including MMP-1, MMP-2, MMP-7, and MMP-9, have been demonstrated to be upregulated in pulmonary fibrosis (33, 76, 244). Possible roles for these MMPs in pulmonary fibrosis include enhancement of cell migration through degradation of basement membranes and establishment of chemotactic gradients for inflammatory cells (29, 256). The MMPs are secreted as latent enzymes, requiring activation to cleave substrate (128). Current evidence indicates that ROS can activate these MMPs, suggesting a method by which EC-SOD depletion from lung parenchyma could exert

pathogenic effects (229). There is the possibility of positive feedback as well, as MMPs could cleave the heparin-binding domain of EC-SOD, leading to further removal from the lung matrix.

In light of this data, it is hypothesized that depletion of EC-SOD from the lung and interrelated increases in MMPs contribute to disease development in pulmonary fibrosis. To study the regulation of EC-SOD and MMPs in this disease, a mouse model of pulmonary fibrosis involving the intratracheal instillation of asbestos fibers was utilized. I also examined the potential relationships between EC-SOD and MMPs in an attempt to better understand how antioxidants and proteases could contribute through converging pathways to the development of pulmonary fibrosis.

3. MATERIALS AND METHODS

3.1. ANIMAL MANIPULATIONS

3.1.1. Mice

8-10 week old **C57BL/6 wild type mice** were obtained from Taconic (Germantown, NY). **EC-SOD knockout mice** were originally derived by Dr. Stefan Marklund and acquired for breeding in our animal facility (196). These mice were produced on the C57BL/6 background through the targeted disruption of the mouse ec-sod gene with a gene encoding neomycin resistance. **EC-SOD transgenic overexpressing mice** were described previously (197). The entire gene encoding human EC-SOD was ligated into a vector containing the surfactant protein C promoter which targets expression to type II epithelium and distal bronchial epithelial cells. Offspring resulting from injection of this construct into fertilized eggs were backcrossed into the B6C3 mouse strain for greater than six generations. **MMP-9 knockout mice** and **FVB/NJ wild type** controls were obtained from Jackson Laboratories (Bar Harbor, ME).

3.1.2. Intratracheal instillation of asbestos and bleomycin

Asbestos and bleomycin animal exposures were reviewed and approved by the University of Pittsburgh Institutional Animal Care and Use Committee. 8-10 week old age and sex-matched C57BL/6 mice or EC-SOD knockout mice (Taconic, Germantown, NY) were used in experiments. In the case of EC-SOD transgenic overexpressors, nontransgenic littermates were utilized as controls. Males and females did not have significantly different responses in any of our experiments.

Mice were anesthetized with brief exposure to isoflurane (Abbot Laboratories, Chicago, IL) and then intratracheally instilled with 0.1 mg of asbestos, 0.1 mg titanium dioxide (Sigma, St. Louis, MO), or 0.9% saline vehicle. Crocidolite asbestos fibers (>10 μm in length) were used in these experiments and were a kind gift of Dr. Andy Ghio at the National Institute of Environmental Health Sciences. In bleomycin experiments, mice were intratracheally instilled with 0.06 units of bleomycin sulfate (Bedford Laboratories, Bedford, OH) or saline vehicle. Mice were euthanized with an injection of 5 mg pentobarbital (Sigma) at 1, 3, 7, 14, or 28 days, as indicated in the results.

Bronchoalveolar lavage (BAL) fluid was obtained by the intratracheal instillation and recovery of 0.8 ml 0.9% saline. Lungs were removed and flash frozen in liquid nitrogen. BAL and lung samples were stored at -80°C until used for biochemical analyses. Lungs from some mice were inflation fixed with 10% buffered formalin (Fisher Scientific, Pittsburgh, PA) for at least 2 hours before overnight incubation in 70% ethanol. Lungs were paraffin embedded by Research Histology Services at the University of Pittsburgh.

3.1.3. MMP inhibition

In vivo MMP inhibition was performed with the broad spectrum metalloproteinase inhibitor, GM6001 (also known as galardin) (EMD Biosciences/Calbiochem, La Jolla, CA). GM6001 was dissolved in dimethyl sulfoxide (Sigma) and aliquots stored at -20°C. On days of injection, these aliquots were thawed and mixed with saline to make a final solution of 1.0 mg/ml in 0.9% saline. Mice being treated with GM6001 or vehicle were intraperitoneally injected (0.2 mg per mouse) every day for 14 days beginning on day -1. On day 0, mice were intratracheally instilled with 0.1 mg asbestos or titanium dioxide. These mice were euthanized at day 13.

3.1.4. Bacterial Pneumonia studies

Pneumonia studies were performed in collaboration with Drs. Janet Lee and Thomas Martin at the University of Washington. C57BL/6 breeders were originally obtained from the Jackson Laboratory (Bar Harbor, ME) and bred in the vivarium of the VA Puget Sound Health Care Systems Research facility. Age and sex matched animals were used in all experiments. Animals were maintained in specific pathogen free cages. Bacterial inhalation experiments were conducted in accordance with the Institutional Animal Care and Use Committee at the VA Puget Sound Health Care Systems and the University of Washington.

3.1.4.1. Bacteria.

E. coli, serotype K-1, was a clinical isolate obtained from the blood of a patient with biliary sepsis. To establish virulence in animals, these bacteria were inoculated into the lungs of a specific pathogen free New Zealand White rabbit. After 24 hours, the blood and spleen homogenates were diluted and added to LB agar using the pour plate method and colonies allowed to form. These bacteria were frozen at -70°C. Before an experiment an aliquot of frozen bacteria was thawed and inoculated into 50 mL of Luria broth (Gibco-BRL Laboratories, Gaithersburg, MD) which was incubated for 6 h at 37°C shaking at 225 rpm. For the aerosol experiments, this culture was inoculated into 1 L of Luria broth and incubated for another 14 h under the same conditions. The broth was centrifuged at 9,000 rpm, and the bacterial pellet was washed twice with sterile 0.9% NaCl. The washed bacterial pellet was resuspended in 22 mL 0.9% NaCl, and divided equally into two nebulizers. Quantitative cultures were performed on the bacterial slurry.

3.1.4.2. Bacterial inhalation exposures.

Mice were placed in wire-mesh cages placed inside a closed aerosolization chamber. The bacterial suspension was placed in twin 10-mL nebulizers and applied as an aerosol at 15 lb/in^2 for 30 minutes. Following bacterial delivery, the mice were either euthanatized immediately in order to establish the initial bacterial inoculum, or euthanized at 24 h for measurements of bacterial burden. Mice were euthanatized with 120 mg/kg pentobarbital and exsanguinated by direct cardiac puncture. The thoracic cavity was opened by midline incision. The trachea was exposed and cannulated with a 20 gauge catheter, which was secured with a 2-0 silk suture. The left mainstem bronchus was identified, divided at the hilum, and the entire left lung was placed in 1 mL sterile H_2O for subsequent homogenization. Bronchoalveolar lavage (BAL) was performed on the right lung using 0.9% NaCl containing 0.6 mM EDTA instilled in one aliquot of 0.6 ml, followed by 3 aliquots of 0.5 ml. The right lung was subsequently fixed with 4% paraformaldehyde at an inflation pressure of 15 cm H_20. Quantitative cultures of bacterial burden were performed on the lung homogenates obtained from each animal at 0, 6, and 24 hours by spreading serial 10-fold dilutions of the lung homogenates in warm LB agar using the pour plate method.

3.2. HUMAN IPF STUDIES

Frozen unfixed lung samples were provided by the University of Pittsburgh Tissue Bank. Four pulmonary fibrosis lung samples were obtained from patients with pathologically-identified Usual Interstitial Pneumonia. Lung samples were embedded in OCT medium and 5 μm sections cut from the blocks using a cryostat. These slides were stained with hematoxylin and eosin as described above. Regions of histologically normal alveolar parenchyma and areas of fibrotic

lung were identified histologically and used to guide the excision of these regions of tissue from the frozen blocks. Care was taken to avoid bronchi and bronchioles as well as large blood vessels since these structures contain large amounts of EC-SOD. The tissue was homogenized and sonicated in 10 volumes buffer as described in 3.3.2. After centrifugation, the supernatant was isolated and protein concentrations measured with the Coomassie Plus Protein Assay Reagent (Pierce). Samples were subjected to reducing SDS-PAGE as described in Chapter 3.3.4.

3.3. BIOCHEMICAL AND CELLULAR ANALYSES

3.3.1. Bronchoalveolar lavage fluid analysis.

For the asbestos and bleomycin experiments, total protein was determined using the Coomassie Plus Protein Assay Reagent (Pierce, Rockford, IL). Total white blood cell counts were obtained using a Beckman Z1 Coulter Particle Counter (Beckman Coulter, Fullerton, CA) set to count particles greater than 6 μm in diameter. The cell concentrations obtained were multiplied by the total BAL volume recovered from the mouse to determine total (absolute) cell counts. To obtain a differential count, 100 μL of BAL fluid (diluted 1:2 for asbestos samples) were adhered to glass slides with a cytospin and stained with Diff Quik reagents (Dade Behring Inc., Newark DE). Numbers of macrophages, neutrophils, lymphocytes, and eosinophils were counted under a microscope until a total of 400 cells were counted for each mouse. The percentages derived from this count were multiplied by the total cell count obtained on the Coulter counter to obtain total numbers of each type of leukocyte.

For the pneumonia experiments, total cell counts in the BAL fluid were performed using a Neubauer chamber. Cell differentials were performed by counting 200 consecutive cells from

cytospin preparations stained with Diff Quik. The remainder of the BAL fluid was spun at 200 x *g*, and supernatants were stored at –70°C.

3.3.2. Lung homogenization.

Lungs from asbestos and bleomycin studies were homogenized and sonicated in 50 mM potassium phosphate (pH 7.4) with 0.3 M potassium bromide and containing 3 mM diethylenetriaminepentacetic acid and 0.5 mM phenylmethylsulfonylfluoride. Homogenates were centrifuged at 20,000 x g for 20 minutes. The supernatant was recovered and the insoluble pellet subjected to detergent re-extraction using a 50mM Tris-HCl, 150mM NaCl, 10mM CHAPS detergent buffer, pH 7.4, containing 100 μM dichloroisocoumarin (serine protease inhibitor) and 10 μM E-64 (cysteine protease inhibitor). CHAPS detergent aids in the extraction of MMPs (272). Total protein concentration determinations were made using the Coomassie Plus Protein Assay reagent (Pierce). All homogenates were stored at –70°C.

For the pneumonia experiments, the left lung homogenates were separated into aliquots for quantitative cultures, western blot analysis, and myeloperoxidase determinations. For the western blots, the lung homogenate was added to a buffer containing 0.5% Triton-X-100, 150 mM NaCl, 15 mM Tris, 1 mM $CaCl_2$ and 1 mM $MgCl_2$ (pH 7.4), incubated on ice for 30 minutes, and spun at 10,000 x *g* for 20 minutes. The supernatants were stored at –70°C. For the MPO measurements, the lung homogenate was added to a buffer containing 50 mM potassium phosphate (pH 6.0), 5 mM EDTA, and 5% w/v hexadecyltrimethyl ammonium bromide. The mixture was sonicated, spun at 12,000 x *g* for 30 minutes, and the supernatants were stored at –70°C.

3.3.3. EC-SOD Activity Assay

After an aliquot was removed from lung homogenate supernatants (obtained before CHAPS detergent extraction) for western blotting, the remaining homogenate was passed over a concanavalin A Sepharose (Sigma) in a polystyrene mini-column (Pierce) equilibrated with 50 mM HEPES (pH 7.0), 0.25 M NaCl. This column binds EC-SOD but not other SODs (207). After elution from the column with 0.5 M α-methylmannoside, the separated EC-SOD was concentrated with Centriprep-30 concentrators (Millipore, Bedford, MA).

EC-SOD activity was measured by inhibition of the reduction of partially acetylated cytochrome c (Sigma) by superoxide at pH 10. Xanthine (50 mM) (Sigma) and xanthine oxidase (Boehringer Mannheim, Germany) were utilized to generate superoxide. The xanthine oxidase was titrated until change in absorbance per minute of cytochrome c equaled 0.025. Samples (lung homogenates or BAL fluid) were added to the cytochrome c/xanthine/xanthine oxidase and titrated until 1 SOD unit was achieved and then measurements repeated 3 times. SOD units were calculated as: [(rate without sample / rate with sample) – 1]. The average was divided by the sample volume required to achieve the SOD unit to express as SOD units per mL. These values were normalized to gram weight of lung for lung homogenate samples. In the case of BAL fluid, measurements were normalized to BAL volume.

3.3.4. Western blot analysis.

BAL fluid or lung homogenates samples were boiled for 10 minutes in the presence of 50 mM DTT and 1% SDS and subjected to SDS-PAGE using a Mini-slab gel system (Idea Scientific, Minneapolis, MN) and blotted onto PVDF membranes (Millipore, Bedford, MA) at 500 mA using a Hoefer TE series transfer unit (Hoefer, San Francisco, CA). Equal protein loading was used for all western blots. Typically, 5 to 10 μg of protein were loaded onto a gel. Blots were blocked overnight in 5% milk in phosphate buffered saline with 0.3% Tween-20 (PBST) before application of primary antibodies.

Antibodies were all diluted in PBST. Antibody to detect mouse EC-SOD on blots (1:10,000 dilution) was generated against the whole protein and was previously described (207). The same antibody detects human EC-SOD in SPC EC-SOD transgenic mice at the same dilution. In human UIP studies, EC-SOD was detected with an antibody specifically directed against human EC-SOD (1:5,000 dilution). TIMP-1 was detected with antibody at a 1:1,000 dilution (Triple Point Biologics, Forest Grove, OR). TIMP-2 was detected with antibody at 1:200 dilution (Chemicon, Temecula, CA). Secondary antibodies conjugated to horseradish peroxidase were added to blots for detection. Donkey anti-rabbit IgG antibodies (Amerhsam Biosciences/GE Healthcare Piscataway, NJ) were used at a 1:5,000 dilution while sheep anti-mouse IgG antibodies (Amersham/GE) were used at a 1:10,000 dilution. All of the primary antibodies were made in rabbits except the TIMP-2 antibody, which was made in mouse. ECL detection reagents (Amersham/GE) were utilized to visualize bands. Blots were stripped and reprobed with antibody against β-actin at a 1:5,000 dilution (Sigma) as a loading control. Densitometry was performed to quantify band intensity and standardized to β-actin using Kodak 1D software (Rochester, NY).

3.3.5. Gelatin Zymography.

To quantify protein levels of MMP-2 and MMP-9, BAL fluid or lung homogenates were subjected to gelatin zymography. Equal protein samples of BAL fluid (5 μg) or the CHAPS detergent extractions (15 μg) of lung homogenates were applied to 10% SDS/PAGE gels containing gelatin (Invitrogen, Carlsbad, CA). After completion of electrophoresis, the gel was washed in Triton X-100 (Fisher, Pittsburgh, PA) and incubated for 22-24 hours at 37°C in pH 7.4 buffer containing 5 mM calcium and 1 μM zinc. After staining of the gel with Coomassie Staining Solution (40% methanol, 13.3% glacial acetic acid, 0.1% Coomassie Brilliant Blue (Fisher)), areas of MMP activity appeared as clear bands. Purified mouse MMP-2 (Calbiochem, Temecula, CA) and MMP-9 (EMD Biosciences, San Diego, CA) and MMP-2 and MMP-9 samples purified from liver homogenates using gelatin-sepharose (Amersham/GE) were used to identify the bands as MMP-2 and MMP-9. Densitometry was performed with Kodak 1D software as described in the western blotting methods above.

3.3.6. Hydroxyproline Assay.

Whole lungs were dried and acid hydrolyzed in sealed, oxygen-purged glass ampoules containing 2 ml of 6 N HCl for 24 hours at 110ºC. Samples were again dried and then resuspended in 1.5 ml phosphate buffered saline followed by incubation at 60ºC for 1 hour. Samples were centrifuged at 13,000 rpm for 10 minutes and the supernatant taken for hydroxyproline analysis.

Hydroxyproline was measured by the addition of 2 mL of diluted sample (typically 1:40) to a 1 mL solution of 50 mM chloramine T (Sigma), 30% methyl cellusolve (ethylene glycol monomethyl ether) (Sigma), and buffer (0.12 M citric acid, 0.45 M sodium acetate, 0.425 M

sodium hydroxide, 0.6% glacial acetic acid, pH 6). After a 20 minute incubation at room temperature, 1 mL of 3.15 M perchloric acid was added and incubated for 5 minutes. 1 mL of 1.34 M p-dimethylaminobenzaldehyde was added and incubated at 60ºC for 20 minutes. Samples were read in 96 well plates in triplicate at 557 nm. Concentration values were multiplied by dilution factor and divided by two to achieve μg/lung units.

3.3.7. MPO activity assay.

The Amplex Red peroxidase assay kit (Molecular Probes, Eugene, OR, USA) was used to determine MPO activity in the lung homogenates. Lung tissue homogenates were prepared as above, and then mixed with reaction buffer, H_2O_2, and Amplex Red reagent according to the manufacturer's instructions. The Amplex Red reagent reacts with H_2O_2 in the presence of peroxidase to produce the fluorescent molecule resorufin. The fluorescence of each sample was measured using a cytofluorometer set at excitation wavelength 530 nm and emission wavelength 590 nm (CytoFluor II, PerSeptive Biosystems, Foster City, CA, USA). The MPO activity was obtained by calculating resorufin units for each unknown lung homogenate sample using a resorufin standard curve.

3.3.8. RNA isolation.

Lungs to be used for RNA isolation were recovered from mice and immediately flash frozen with liquid nitrogen. RNA was isolated using the RNeasy Maxi Kit (Qiagen, Valencia, CA) as per the manufacturer's instructions. Whole frozen lungs were homogenized in buffer RLT containing 0.143 M beta-mercaptoethanol. After centrifugation (3000 g x 5 minutes), supernatant was recovered and mixed with 70% ethanol. This mixture was added to an RNeasy

Maxi column and centrifuged again. After several washes of the column, RNase free DNase (Qiagen) was added to the filter membrane for 15 minutes to remove contaminating DNA. Additional washes were followed by recovery of RNA from the filter with two elutions using 0.8 mL water each time.

3.3.9. Quantitative reverse transcriptase polymerase chain reaction.

Isolated RNA was examined for EC-SOD mRNA message using Taqman Gene Expression Assays (Applied Biosystems, Foster City, CA). RNA (1 μg) was first subjected to a reverse transcriptase reaction using 2 μL 10X PCR buffer II, 4 μL 25mM $MgCl_2$, 2 μL dNTP mix (10mM stock of each nucleotide), 1 μL random hexamer primers (3 μg), 1 μL RNasin (1 U) and 1 μL MuLV reverse transcriptase (2.5 U)(all from Applied Biosystems) per 20 μL reaction to create cDNA. The following program was used on a thermocycler for reverse transcription: 40 min at 42°C, 5 min at 99°, 5 min at 5°. After the run, water was added to bring the final volume of each sample to 50 μL. Each 50 μL reaction received 9 μL of the cDNA, 25 μL 2X Universal PCR buffer, and 2.5 μL 20X expression assay buffer (Applied Biosystems) for either mouse EC-SOD as the target or mouse GAPDH as endogenous control. Reactions were done in triplicate wells of a 96-well PCR plate (USA Scientific, Ocala, FL) with GAPDH as an endogenous control used in duplicate. Quantitative analysis was then performed on an ABI SDS7000 (Applied Biosystems). Crossing thresholds for EC-SOD were obtained and divided by the crossing threshold for GAPDH. The results were averaged for each group.

3.4. HISTOLOGICAL ANALYSES

3.4.1. Hematoxylin and eosin histology staining.

5 μm sections were cut from paraffin embedded blocks using a microtome and floated in a 37ºC water bath before adherence to positively charged glass slides (Fisher). Slides were baked at 60ºC overnight before staining procedures were performed. Slides were deparaffinized by dips in xylene, followed by graded swishes in ethanol (100% to 95% to 70%) and water before 1 minute incubation in Gill's hematoxylin (Vector Laboratories, Burlingame, CA) and 5 seconds in 0.1% eosin Y, 0.01% phloxine B, 85% EtOH, 5% glacial acetic acid solution. Slides were then dipped in graded ethanol (70% to 95% to 100%) and xylene and coverslipped.

3.4.2. Histological Scoring.

Hematoxylin and eosin stained slides were scored by a pathologist (Tim Oury) blinded to sample groups. Individual fields were examined with a light microscope at high power (400X) magnification. Every other field was scored in a spiraling pattern beginning peripherally in the lung and ending more centrally until twenty fields were counted for each slide. In order to be counted, each field had to contain alveolar tissue in greater than 50% of the field. Scoring in each field was based on the percentage of alveolar tissue with interstitial fibrosis according to the following scale: 0 = no fibrosis, 1 = up to 25%, 2 = 25-50%, 3 = 50-75%, 4 = 75-100%.

3.4.3. Immunohistochemistry.

Immunohistochemistry for EC-SOD was performed on 5 μm sections from paraffin-embedded mouse lungs using an automated slide staining system (Dako, Carpinteria, CA). Slides were

deparaffinized by overnight baking at 60ºC and by three 20 minute incubations in Clear Rite (Richard Allen Scientific, Kalamazoo, MI). Slides were then dipped in 100% ethanol followed by 95% ethanol and incubated in 6% hydrogen peroxide in methanol (30 minutes) to inactivate endogenous peroxidases. This was followed by a incubation in 0.1% pepsin in 0.01 N HCl (10 minutes) for antigen retrieval. After blocking with Maxitags Protein Blocking Agent (Thermo Electron, Pittsburgh, PA) (30 minutes), slides were incubated with the same antibody against mouse EC-SOD (1:500) used in western blotting or with normal rabbit sera as a control for 60 min. A 30 min incubation in biotinylated secondary antibody (1:1000) was followed by incubation in ABC reagent (Vector Laboratories) for 30 min. Slides were developed with the Nova Red staining kit (Vector). All slides were stained on the same day and developed for the same amount of time. Slides were not counterstained. Photos of ten random fields from each slide taken at 400X magnification were analyzed for EC-SOD staining intensity using Metamorph software (Molecular Devices, Sunnyvale, CA). We have previously shown that quantification of EC-SOD staining in immunoperoxidase-stained slides using this method produces similar results compared with immunofluorescence staining (208).

To examine MMP-2 levels, goat antibody directed against this MMP (R&D Systems, Minneapolis, MN) was utilized in the same protocol listed above for EC-SOD except that slides were counterstained in Gill's Hematoxylin (Vector Laboratories) for 1 minute following Nova Red staining. Anti-MMP-2 antibody was used at a 1:25 concentration and secondary biotinylated anti-goat antibody (ICN, Costa Mesa, CA) was utilized at a 1:500 dilution. Similarly goat anti-MMP-9 antibody (R&D Systems) was used at a 1:50 concentration with secondary biotinylated anti-goat at 1:500 dilution (ICN). As a negative control, normal goat IgG (R&D Systems) was utilized at the same concentration as the primary antibody.

3.5. STATISTICAL ANALYSES

Data are provided as means +/- standard error of measurement (SEM). All comparisons between two groups were made using a Student's t test. All comparisons between more than two groups were made by one way ANOVA with Tukey's post test. The Graphpad Prism 4 statistical software package (Graphpad, San Diego, CA) was used for all statistical testing. A P value of less than or equal to 0.05 was considered statistically significant.

4. ASBESTOS INDUCES PULMONARY INFLAMMATION AND FIBROSIS

In order to examine the role of EC-SOD and MMPs in pulmonary fibrosis, we first designed and characterized a model of pulmonary fibrosis after intratracheal instillation of asbestos fibers. Although bleomycin is still the most commonly used agent to experimentally induce fibrosis in the lung, bleomycin does not recapitulate many of the findings of human IPF, including the development of fibroblastic foci (3). Also, in the mouse, bleomycin fibrotic lesions are self-limiting and mice will not progress to respiratory failure (273). Bleomycin is also metabolized within 24 hours of exposure (273). Asbestos, on the other hand, would not be metabolized, and pathogenesis may be more indicative of the human disease. Furthermore, asbestos is clearly a better model to study asbestosis.

4.1. ASBESTOS EXPOSURE CAUSES NEUTROPHILIC INFLAMMATION AND EPITHELIAL/ENDOTHELIAL BARRIER BREAKDOWN

C57BL/6 wild type mice were intratracheally instilled with 0.1 mg of crocidolite asbestos to determine their effects on the lung. Control mice were instead treated with vehicle (0.9% sterile saline) or with an inert particulate control, titanium dioxide (TiO2). To assess the acute effects of asbestos exposure, mice were euthanized at 24 hours and bronchoalveolar lavage (BAL) fluid was collected. Lungs were recovered for either histology or homogenization.

In Figure 3, histology of asbestos-exposed lungs shows a dramatic change compared to control lungs. Asbestos fibers can be found in bronchioles and alveolar regions, and are usually accompanied by inflammatory aggregates and interstitial thickening and edema. The majority of the inflammatory cells possessed segmented nuclei typical of polymorphonuclear neutrophils (PMNs). As expected, there were no signs of fibrosis at this early timepoint.

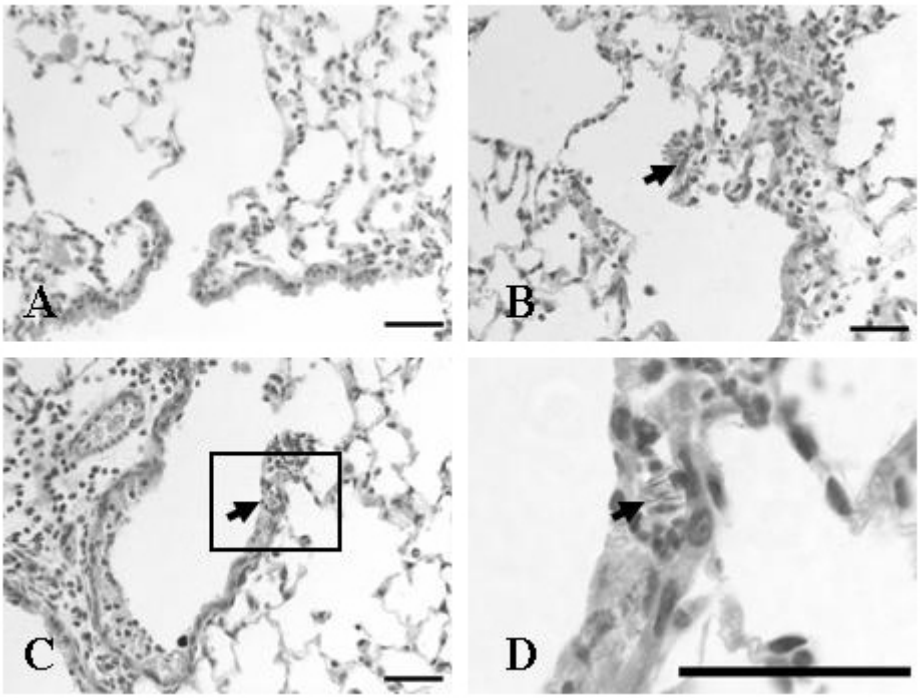

Figure 3. Asbestos induces pulmonary inflammation and edema 24 hours after exposure.

C57BL/6 mice were intratrachaelly instilled with saline or 0.1 mg crocidolite asbestos. Mice were euthanized at 24 hours and the lungs inflation-fixed in formalin. Hematoxylin and eosin staining was performed on lung sections from mice exposed to saline (A) or asbestos (B, C). Mice exposed to titanium dioxide (not shown) looked identical to saline-treated mice in panel A. Asbestos fibers are shown with an arrow. Boxed area (in C) is shown at greater magnification (in D) to show fibers in detail. Bar equals 25 µm.

BAL fluid analyses, as a sampling of airspace protein and cell content, also indicated significant inflammation and damage. BAL fluid protein was markedly elevated in the asbestos mice when compared to either saline or TiO2 controls (Figure 4). This protein accumulation indicates increased permeability between the vascular and alveolar airspaces. The total number of white blood cells were also counted and revealed intense inflammation in the lung (Figure 5). When BAL fluid differentials were counted, the majority of these cells were determined to be neutrophils (Figure 6 and Figure 7). Macrophages could also be found and in some cases were observed unsuccessfully phagocytosing asbestos fibers. This represents "frustrated" phagocytosis, which is discussed in the introduction (see Chapter 1.4.6).

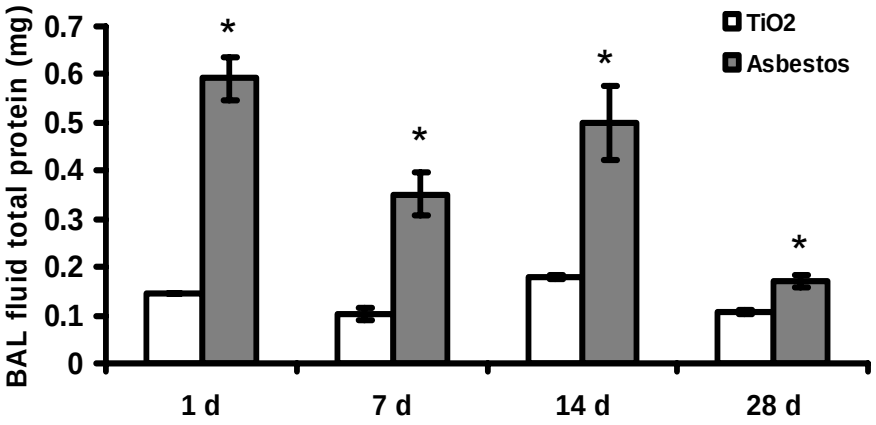

Figure 4. Asbestos increases total protein in the bronchoalveolar lavage (BAL) fluid.

BAL fluid was recovered by instillation and recovery of 0.8 mL saline at the indicated timepoints after instillation of titanium dioxide (TiO2) or asbestos. Total protein was determined using the Coomassie Plus protein reagent assay. Higher protein levels indicate endothelial-epithelial layer permeability, an indicator of lung damage. *p < 0.05, Student's t test.

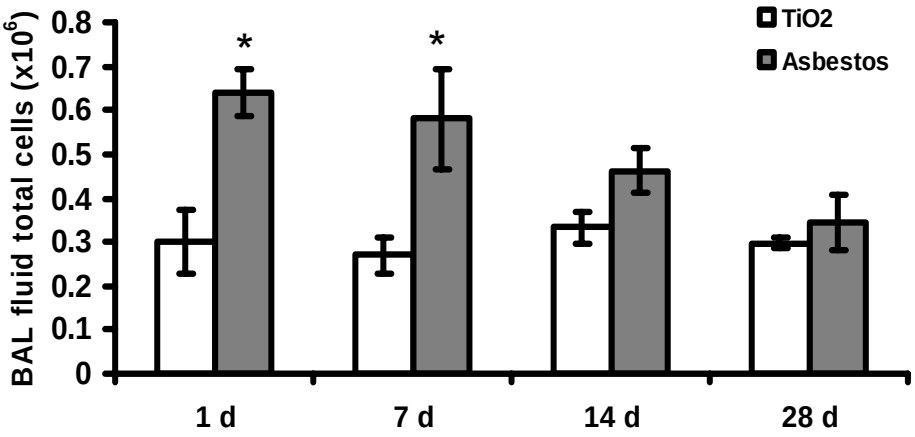

Figure 5. Asbestos exposure causes airspace inflammation.

White blood cell concentrations (cells/ml) in BAL fluid were counted on a Coulter particle counter at the indicated timepoints post-asbestos or titanium dioxide (TiO2) exposure. Total BAL fluid cells were calculated as concentrations times total volume of BAL fluid recovered. *p < 0.05, Student's t test.

Mice were also euthanized at longer timepoints post-asbestos instillation in order to determine whether fibrosis developed in response to asbestos. The BAL fluid parameters showed some attenuation at the later timepoints. The BAL fluid protein levels remained significantly elevated (Figure 4), while total inflammation subsided by 14 days (Figure 5). However, there was still a significant increase in neutrophils in the BAL fluid at 7, 14, and 28 days (Figure 7).

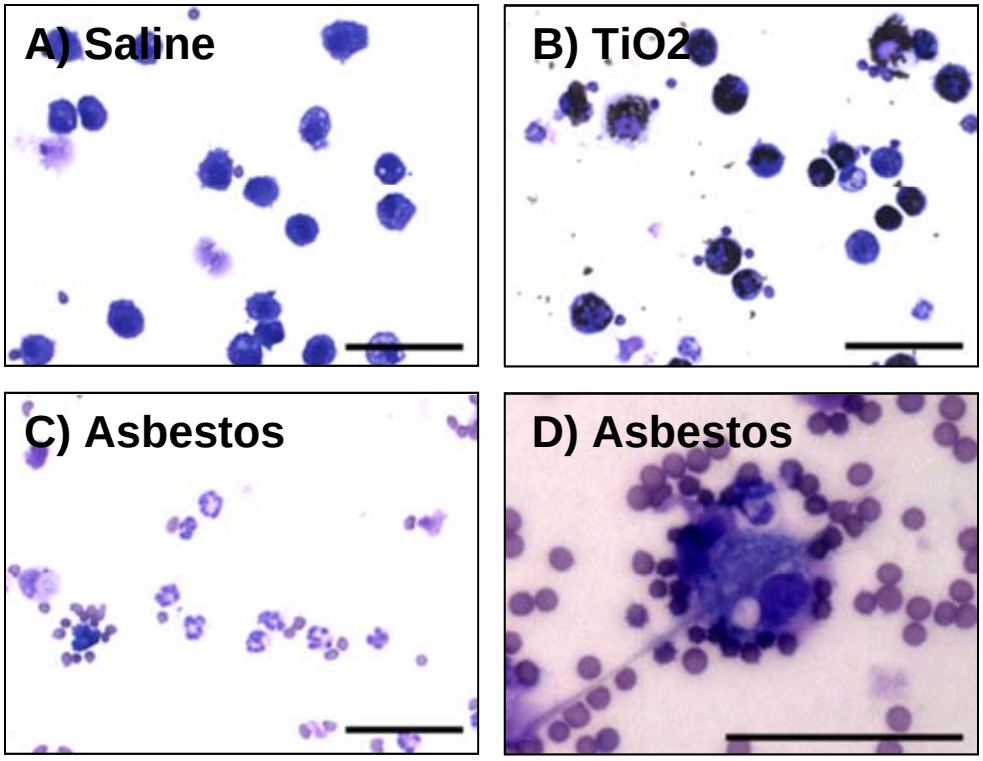

Figure 6. Asbestos expsoure increases airspace PMN at 24 hours post-instillation.

24 hours after intratracheal instillation with saline, TiO2, or asbestos, BAL fluid was recovered and spun onto slides and subjected to Diff Quik staining for leukocytes. A) BAL cells from saline-treated mice are shown as a reference and contain normal alveolar macrophages. B) TiO2-treated mice show macrophages engulfing black titanium particles and a few scattered PMN. C) Asbestos-exposed mice have a large increase in PMN content. D) A macrophage attempting (frustrated) phagocytosis of an asbestos fiber. The relative quantities of cells on each slide carries no significance as the BAL fluid was diluted to different amounts in each slide. Bar equals 50 μm.

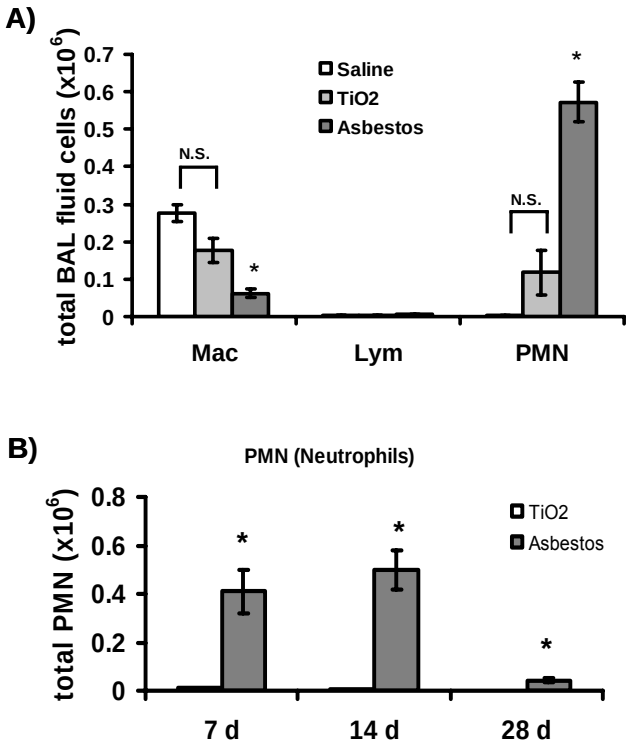

Figure 7. PMN are increased after asbestos exposure.

Wild type mice were intratracheally instilled with saline, titanium dioxide (TiO2), or asbestos. BAL fluid was recovered at 1, 7, 14, and 28 days. Differential counts were performed on cytospins. Asbestos-exposed mice had fewer macrophages at 24 hours (A). These mice also had greater amounts of neutrophils at all timepoints (B). Saline and TiO2 controls were not significantly different from each other at 24 hours.

*** p < 0.05, one way ANOVA and Tukey's post test in top figure, or Student's t test in bottom figure, comparing control(s) and asbestos at each timepoint.**

4.2. ASBESTOS EXPOSURE CAUSES PULMONARY FIBROSIS

The major change observed at later timepoints was the development of fibrosis. At 7 days in asbestos-exposed mice, inflammation and a small amount of fibrosis was observed by histology (Figure 8). Fibrosis surrounded the bronchioles, in agreement with what is found early in human asbestosis (21). Lungs from mice sacrificed 14 and 28 days after asbestos revealed progressively more fibrosis and a greater involvement of alveolar septa. Some evidence was also found for the development of fibroblastic foci, described as loose fibrosis populated by

myofibroblasts scattered at the edges of this fibrosis (14). This is evidence that our asbestos model is more akin, at least histopathologically, to IPF than the bleomycin model.

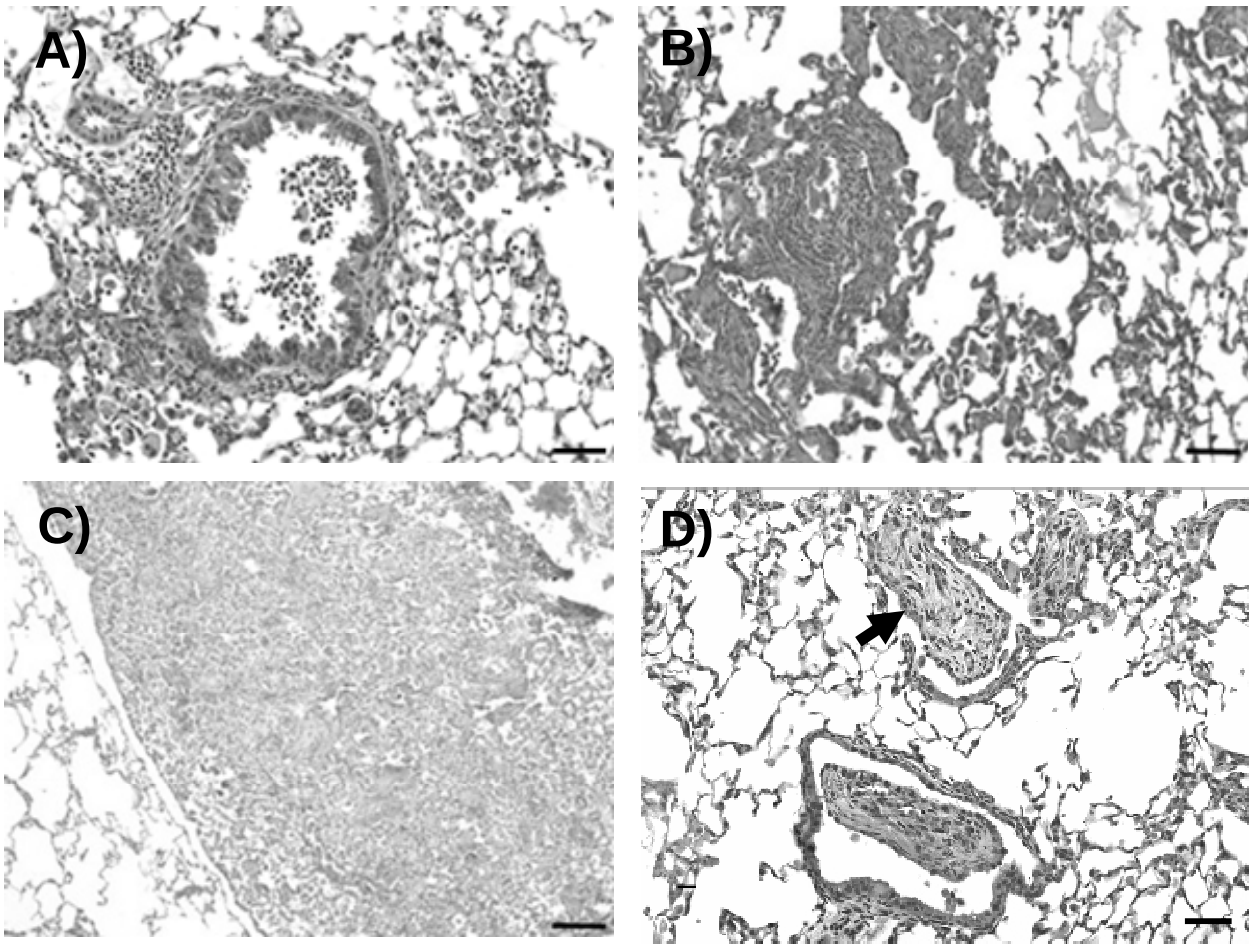

Figure 8. Fibrosis in mouse lungs 7-28 days after asbestos exposure.

Mice were sacrificed at 7, 14, and 28 days post asbestos exposure. Standard hematoxylin and eosin staining was performed on 5 μm lung sections. A) 7 day lungs possessed inflammation and minimal fibrosis, localizing to the areas around the bronchioles. Compare with normal lung section in Figure 3A. B) 14 day lungs possess increased fibrosis, extending into alveolar walls. C) 28 day lung with extensive fibrosis in one lobe next to a normal lobe. D) 28 day lung displaying a structure resembling a fibroblastic focus (arrow) with myofibroblasts in loose connective tissue). Bar equals 50 μm.

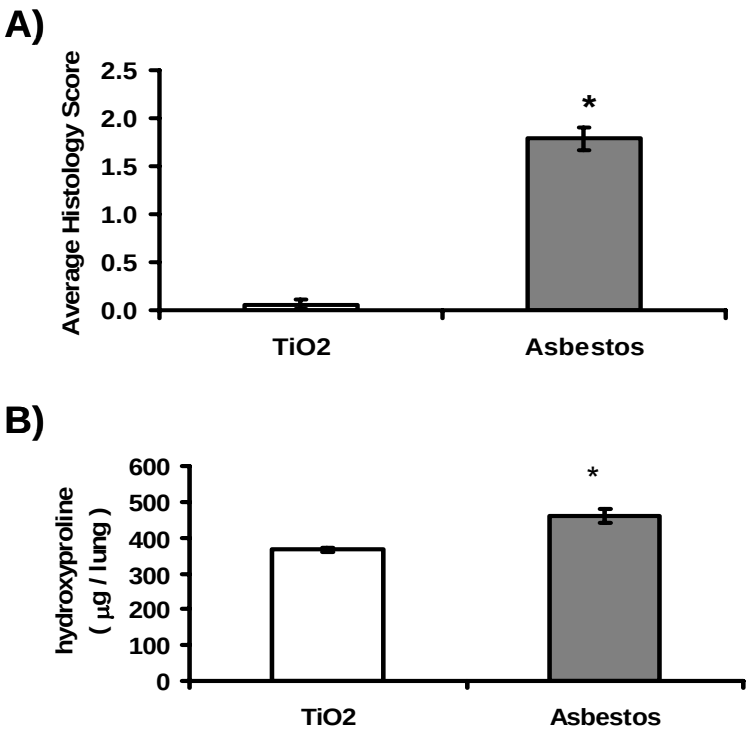

Figure 9. Fibrosis is increased 14 days after asbetos exposure.

Fibrosis was measured in wild type C57BL/6 mice 14 days after exposure to asbestos. A) Average histology score was determined by a blinded pathologist (T.D.O.) for TiO2- and asbestos-treated mice. Scoring system was as follows: 0=no fibrosis, 1=0-25% fibrosis, 2=25-50%, 3=50-75%, 4=75-100%. B) Hydroxyproline levels were determined as an indicator of fibrosis. * $p < 0.05$, Student's t test.

4.3. CONCLUSIONS

Intratracheal instillation of asbestos in mice is associated with a significant inflammatory response at 24 hours predominated by PMNs. PMNs remain elevated until at least 28 days post-exposure. The lungs enter a fibrotic phase of excess collagen deposition affecting bronciholes as early as day 7 and progressing into alveolar regions at 14 and 28 days. These results indicate that our asbestos model closely approximates the changes observed in human asbestosis. The rapid progression of pathologic lesions, leading to significant levels of fibrosis at 14 days (Figure 9), facilitates study of the molecular mechanisms of this disease throughout its development. Importantly, neither EC-SOD nor MMPs have been examined in the current literature of

asbestosis. Furthermore, because of the presence of fibroblastic foci, our model may more closely approximate human IPF than the bleomycin model (which lacks these lesions) since these foci are hallmarks of IPF.

5. ASBESTOS EXPOSURE ALTERS EC-SOD LOCALIZATION IN THE LUNG

Because of previous studies describing a redistribution of EC-SOD in pulmonary disease (207, 208), it was hypothesized that our asbestos model would also reveal changes in EC-SOD localization. To test this hypothesis, I examined BAL fluid and lung homogenates from mice treated with asbestos. A change in antioxidant status in the lung could play a role in the pathogenesis of disease, particularly in light of the oxidative stress attributed to asbestos fibers (158).

5.1. ACUTE ASBESTOS EXPOSURE DEPLETES EC-SOD FROM LUNG PARENCHYMA

Wild type mice were intratracheally instilled with asbestos and euthanized at 24 hours. Lungs were homogenized, and EC-SOD was isolated from the other SOD enzymes using a concanavalin A column. Using a well-established method to measure SOD activity using cytochrome c (207, 208), the amount of EC-SOD activity in the lung was determined. As shown in Figure 10, total lung EC-SOD activity was decreased in asbestos-treated mice compared to controls.

Western blots were performed to verify our activity assay, and to determine whether loss in activity is due to loss of protein or to protein inactivation. Lung homogenates from mice were subjected to reducing SDS-PAGE to dissociate EC-SOD into its component monomers. EC-SOD monomers migrate as doublets on electrophoresis because of the presence or absence of the heparin binding domain, leading to two different molecular weights. Western blots revealed a decrease in EC-SOD in the lung at 24 hours (Figure 11).

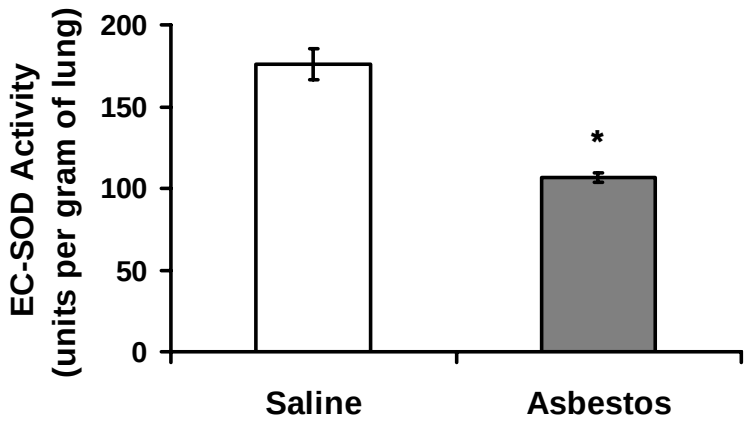

Figure 10. EC-SOD activity decreases after exposure to asbestos.

EC-SOD was isolated and concentrated from lung homogenates of mice treated 24 hours previously with saline or asbestos (N=9). Activity was assessed via the inhibition of cytochrome c at pH 10. * $p < 0.05$, Student's t test.

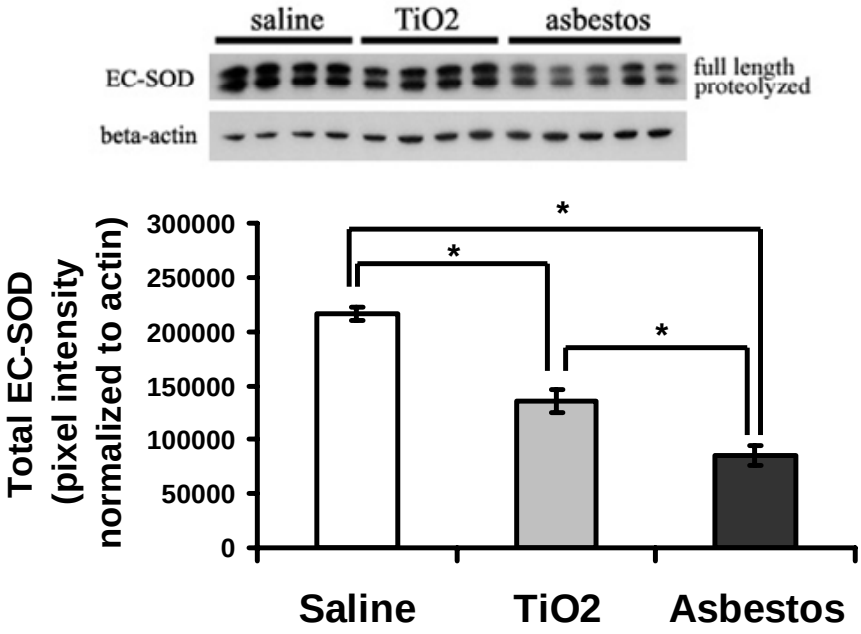

Figure 11. EC-SOD protein is depleted from the lung 24 hours after asbestos.

Lung homogenates (10 μg) from mice treated with saline, TiO2, and asbestos (0.1 mg) were subjected to reducing SDS-PAGE. Western blotting was performed and blots probed with antibody against mouse EC-SOD (1:10,000 dilution). Blots were stripped and reprobed with antibody against beta-actin (1:5,000) as a loading control. * $p < 0.05$ one way ANOVA and Tukey's post test.

To determine whether EC-SOD depletion is due to a loss from the lung parenchyma, quantitative immunohistochemistry was performed. Five micron, paraffin-embedded sections were stained with antibody directed against mouse EC-SOD. After staining with a chromogenic substrate, slides were subjected to morphometric analysis for staining intensity using Metamorph software. In normal lungs from mice that did not receive asbestos, EC-SOD was found lining the alveolar septa with intense staining (Figure 12). EC-SOD was also localized to pulmonary vasculature and bronchiolar epithelium. In asbestos-treated mice sacrificed at 24 hours, EC-SOD staining in alveolar septa was dramatically reduced. This indicated that the observed depletion of EC-SOD was due to loss from the parenchyma. This depletion from the lung is significant, as this could lead to greater oxidative stress in this area of the lung and progression of the disease. While the depletion of EC-SOD from lung parenchyma is more dramatic on immunohistochemistry than on western blots, it must be noted that western blots are performed on total lung homogenates. As intratracheal instillation of asbestos leads to heterogeneous injury throughout the lung, the normal areas of lung still have normal levels of EC-SOD. This would dilute the effect in total lung homogenates followed by western blotting.

EC-SOD expression at the mRNA level was determined through the use of quantitative reverse transcriptase polymerase chain reaction (Figure 13). Using this technique, we found that expression of EC-SOD in total lung RNA isolates was markedly decreased after asbestos treatment. This may in part explain the decrease in EC-SOD in the lung.

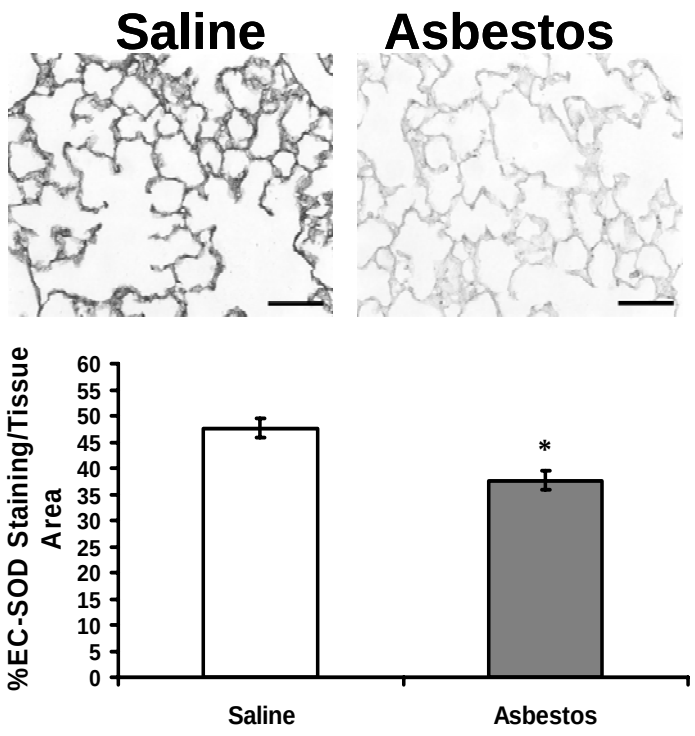

Figure 12. Asbestos leads to depletion of EC-SOD from lung parenchyma 24 hours post-instillation.

Immunohistochemistry was performed on paraffin embedded slides from saline-treated (A) and asbestos-treated (B) mice 24 hours after asbestos exposure. The same EC-SOD antibody used in western blotting (1:500 dilution) was used for slide staining. All slides were developed on the same day for the same amount of time. Ten random fields from each slide (N=4-5 for each group) were photographed and subjected to Metamorph software analysis to quantify staining intensity. * $p < 0.05$, Student's t test

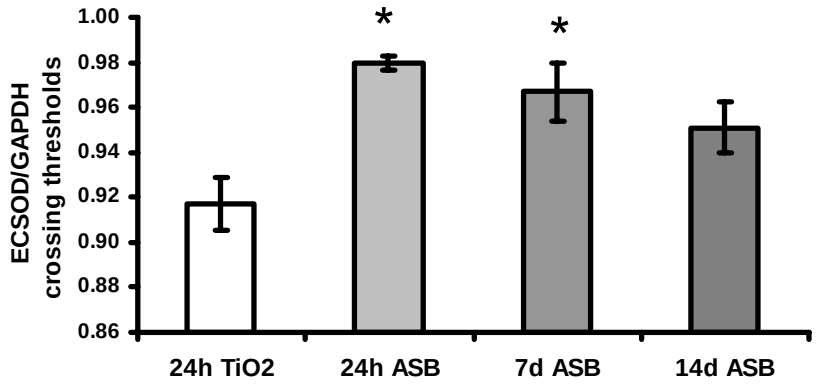

Figure 13. Lung EC-SOD expression decreases after asbestos exposure.

Quantitative reverse transcriptase polymerase chain reaction was performed on 1 μg total RNA extracted from the lungs of mice treated with 0.1 mg crocidolite asbestos. N=3 for each timepoint. Crossing thresholds were determined and averaged for each group. Higher thresholds denote less EC-SOD expression. * $p < 0.05$ compared to TiO2, one way ANOVA and Tukey's post test.

5.2. EC-SOD ACCUMULATES IN AIRSPACES AFTER ACUTE ASBESTOS

Although we demonstrated the depletion of EC-SOD from lungs due to the inhalation of asbestos, the fate of the parenchymal EC-SOD was unknown. Based on the presence of the heparin-binding domain of EC-SOD, and the propensity for this binding domain to be proteolytically cleaved from the enzyme (176), we hypothesized that EC-SOD was being cleared from lung parenchyma due to the action of proteases. Cleaved EC-SOD would have reduced affinity for extracellular matrices. In theory, this cleaved EC-SOD could diffuse into the airspaces of the lung or the plasma. The breakdown of endothelial and epithelial barriers, as indicated by the presence of protein and inflammation in the bronchoalveolar lavage (BAL) fluid, would facilitate this diffusion. We therefore examined BAL fluid for the presence of EC-SOD by western blotting.

Figure 14 shows the western blot for BAL fluid recovered from mice euthanized 24 hours post-asbestos treatment. Compared to control mice, asbestos-exposed mice had significantly greater accumulation of EC-SOD in the BAL fluid. This accumulation is unlikely to originate from plasma leakage into the lung since EC-SOD levels in the plasma are normally undetectable. Plasma leakage due to endothelial/epithelial breakdown is therefore more likely to dilute lung EC-SOD than contribute to its levels, causing underestimation of the BAL fluid EC-SOD.

Furthermore, the majority of this EC-SOD was the proteolyzed form lacking the heparin-binding domain. This indicated that the airspace EC-SOD could arise from full length EC-SOD in the lung parenchyma that was proteolyzed and released from the matrix. This truncated EC-SOD would then diffuse in the airspace, where it accumulates. However, inflammatory cells such as neutrophils and macrophages produce EC-SOD (184, 207). Thus, the intense inflammation seen in asbestos-mediated lung disease could also be a source of airspace EC-SOD.

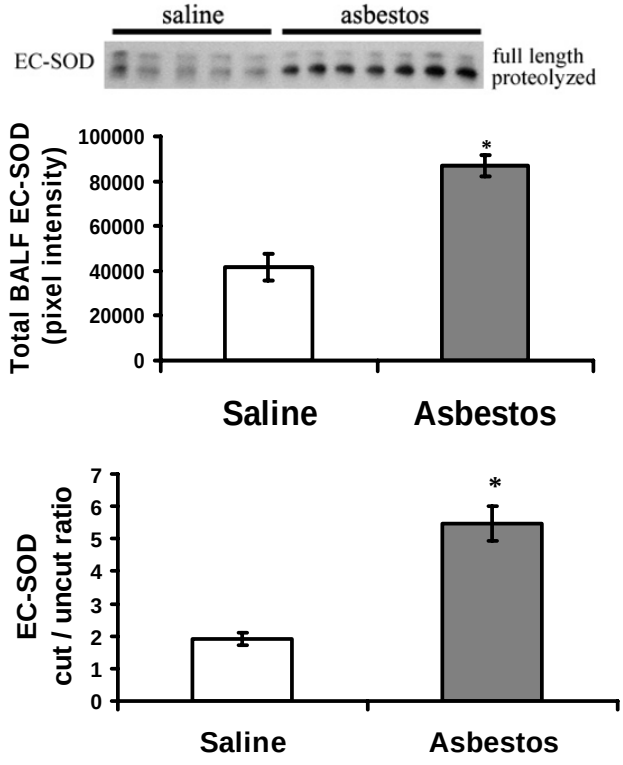

Figure 14. Acute asbestos exposure leads to accumulation of proteolyzed EC-SOD in the airspace.

Western blotting was performed on BAL fluid (equal protein loaded, 10 μg) from mice sacrificed 24 hours after intratracheal administration of 0.1 mg crocidolite asbestos. Densitometry was performed and total EC-SOD and cut/uncut ratio (i.e. proteolyzed/full length) EC-SOD was determined. * $p<0.05$ Student's t test.

5.3. EC-SOD CHANGES PERSIST AT LATER TIMEPOINTS

To examine whether the localization changes in EC-SOD are a result of processes occurring only early after asbestos damage or whether the change is more permanent, we determined EC-SOD levels in the BAL fluid and lung at 7, 14, and 28 days. As shown in Figure 15, depletion of EC-SOD from lung homogenates persists at later timepoints. Similarly, the BAL fluid reveals that airspace levels of EC-SOD are increased after asbestos treatment, even at 7, 14, and 28 days (Figure 16). EC-SOD expression is also decreased at 7 days but appears to recover by 14 days (Figure 13). This data shows that the localization changes in EC-SOD are long lived and that the

loss of EC-SOD from lung parenchyma is chronic. This suggests that the lungs possess less antioxidant protection at all timepoints during the course of asbestos-mediated lung disease.

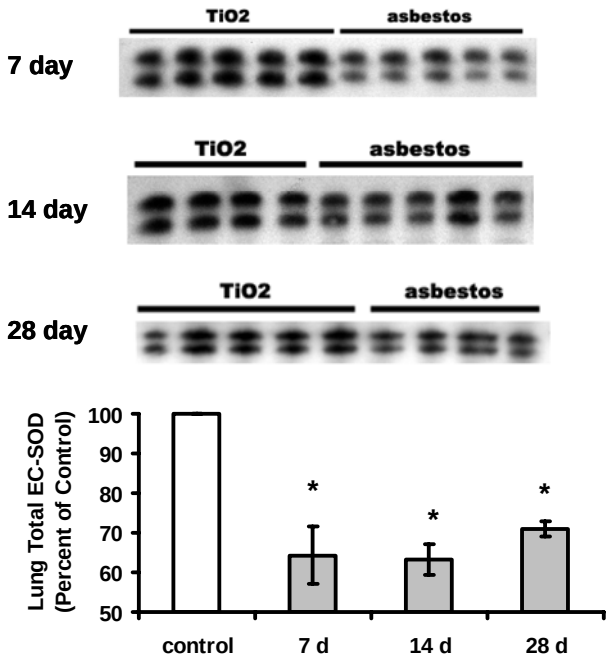

Figure 15. EC-SOD is depleted from lung 7, 14, and 28 days after asbestos exposure.

Western blotting was performed on equal protein amounts of lung homogenates (10 μg) from mice treated with asbestos and sacrificed at the times indicated. Densitometry was performed and normalized to β-actin as a loading control. Densitometry values were expressed as percent of control at that timepoint. Results indicated a loss of EC-SOD in lung homogenates of asbestos mice at all timepoints.

5.4. CONCLUSIONS

An oxidant/antioxidant imbalance is theorized to underlie the pathogenesis of asbestos-mediated lung disease. Asbestos exposure *in vitro* and *in vivo* leads to ROS formation detectable through markers of oxidative stress (156, 158). Asbestos also upregulates antioxidants such as manganese superoxide dismutase and glutathione peroxidase, signifying a compensatory response to oxidative stress (161).

EC-SOD has been previously implicated in acute and chronic lung injuries. In two models of lung injury, a decrease in EC-SOD protein levels in lung extracellular matrix was reported by our laboratory (207, 208). This is associated with an increase in the proteolyzed form of EC-SOD lacking the heparin-binding domain in both the lung and bronchoalveolar lavage fluid (BALF) (207). These results suggest that increased proteolysis of EC-SOD leads to its removal from the lung parenchyma, perhaps leading to increased oxidative stress in the ECM. The results also implicate decreases in EC-SOD expression as mRNA levels of EC-SOD decrease after asbestos exposure compared to controls. In support of a protective role for EC-SOD against lung injury, transgenic overexpression of EC-SOD or treatment with SOD mimetics protects against bleomycin-induced pulmonary fibrosis (120, 202), while EC-SOD knockouts are more susceptible (204).

EC-SOD is depleted from lung parenchyma as early as 1 day and as late as 28 days after exposure to asbestos. This depletion of EC-SOD from the parenchyma could lead to increased oxidative stress in the lung which could stimulate progression of the disease and was associated with both inflammation (1 day) and fibrosis (7-28 days). The functional role of this depletion is examined directly in Chapter 7 with EC-SOD knockout mice.

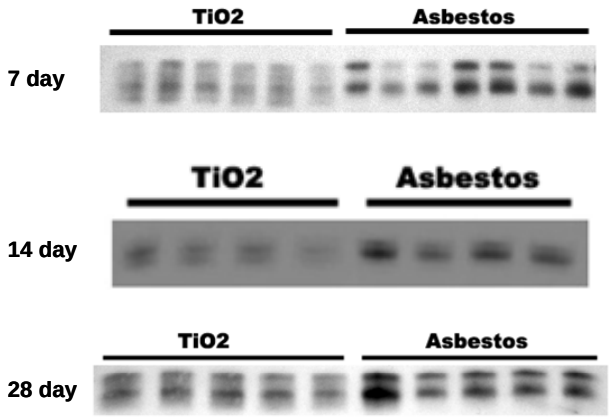

Figure 16. EC-SOD accumulation in the airspaces persists to 28 days.

Western blotting was performed on equal protein amounts of BAL fluid (5 μg) from the same mice in Figure 15. EC-SOD is found at higher levels in BAL fluid of mice treated with asbestos at all timepoints tested.

This depletion contrasts with the timecourse of EC-SOD removal in lung parenchyma of mice treated with bleomycin. In the bleomycin model, EC-SOD is initially depleted from the parenchyma at 7 days but returns to normal levels at 14 days (204), and it is known that fibrosis regresses in this model if bleomycin is not continuously supplied (266). Persistence of depletion of EC-SOD from the lung in asbestosis indicates that the asbestos model produces more chronic lesions than bleomycin. Since EC-SOD is depleted from fibrotic areas of long-standing human IPF (see Chapter 8), asbestos may be a better model for IPF.

The depletion of EC-SOD from lung parenchyma coincides with the accumulation of proteolyzed EC-SOD in the bronchoalveolar lavage fluid. While this suggests that lung parenchyma EC-SOD is being cleaved and released into the BAL fluid, the possibility exists that inflammatory cells in the airspaces release this antioxidant. Loss of lung parenchymal EC-SOD may simply be due to degradation or clearance into the circulation, or through decreased expression. The source of the airspace EC-SOD is examined in greater detail in Chapter 6.

6. AIRSPACE INFLAMMATION AND EC-SOD

The studies described in Chapter 5 reveal a depletion of EC-SOD from the lung parenchyma and an accumulation of EC-SOD in the airspaces in an asbestos-induced model of pulmonary fibrosis. However, the mechanisms governing these changes in EC-SOD localization are unknown. Specifically, the relative contributions of the airspace inflammation and of the interstitial inflammation and interstitial extracellular matrix remodeling to EC-SOD distribution have not yet been examined. It was hypothesized that the depletion of EC-SOD from the lung parenchyma required interstitial processes that occurred in pulmonary fibrosis. It was also hypothesized that the clearance of EC-SOD from the lung parenchyma led to the observed accumulation of this protein in the airspaces. In order to test these hypotheses, EC-SOD was examined in a model of pulmonary airspace inflammation induced by the inhalation of bacteria. Airspace inflammation without accompanying interstitial processes would provide valuable insight into EC-SOD regulation in pulmonary fibrosis in which multiple airspace and interstitial processes are taking place.

6.1. BACTERIAL INHALATION LEADS TO AIRSPACE INFLAMMATION

K1 serotype *E. coli* bacteria were isolated and propagated from a patient with sepsis as described in Materials and Methods (see Chapter 3.1.4.1). Wild type C57BL/6 mice were then exposed to the bacteria through the inhalational mode of inoculation. These mice were euthanized at 0, 6, and 24 hours after exposure and parameters of lung inflammation were examined.

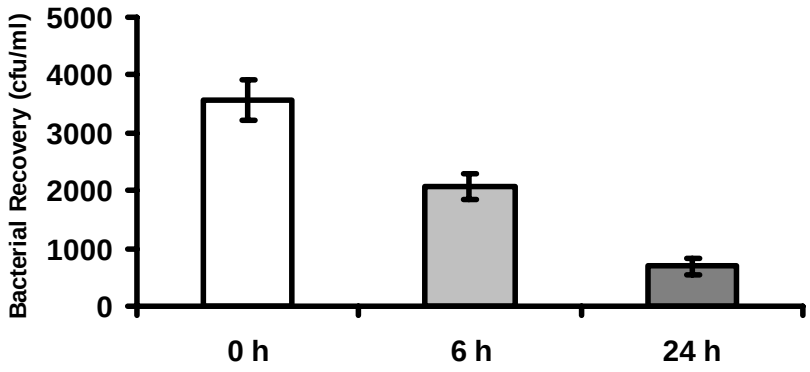

Figure 17. Bacterial recovery from lungs of mice that have inhaled E.coli.

C57BL/6 mice were exposed to *E. coli* bacteria through inhalation. Left lungs were isolated from mice euthanized at three timepoints to determine initial bacterial load (0 hour), or the bacterial burden as the lung clears the infection (6 and 24 hours). Data is expressed as colony forming units (cfu) formed per mL of lung homogenate.

Bacterial recovery from the lungs of these mice was used as an indicator of initial bacterial load as well as to track the clearance of bacteria from the lung. This clearance is a normal part of the immunological defense against such organisms. To determine bacterial load, the left lungs were isolated from mice and homogenized followed by plating of the homogenate on LB agar and counting of colonies after incubation. At time 0, there is a large amount of bacteria in the lungs, leading to approximately 3,567 colony forming units per mL (Figure 17). This number decreased at 6 and 24 hours, with 700 cfu/mL at the latter timepoint.

Histology of the lungs at 0 hours revealed normal lungs with only a few macrophages in the airspaces (Figure 18). At 24 hours, the airspaces have increased numbers of inflammatory cells. At greater magnification, the majority of the cells were determined to be PMN. In spite of this airspace inflammation, the lung parenchyma was spared from inflammation and any apparent histologic changes or damage.

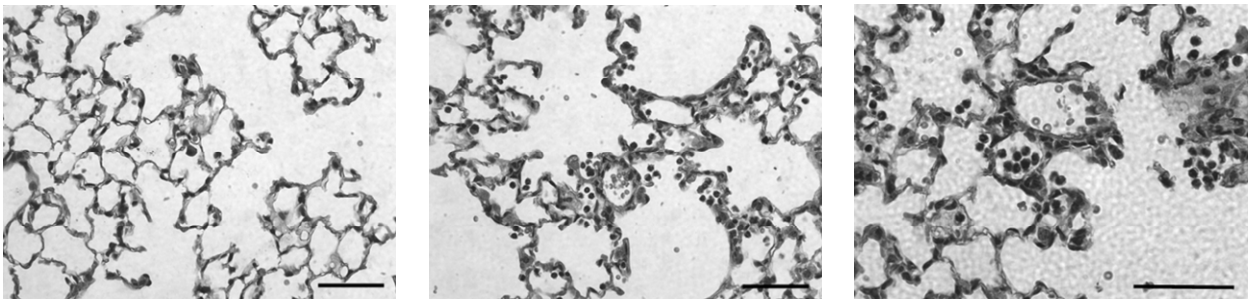

Figure 18. Mice exposed to bacteria have increased inflammatory cells in the airspaces.

Hematoxylin and eosin staining was performed on lung sections from mice exposed to bacteria. While lungs are normal at 0 hours (left panel), airspace inflammation typical of pneumonia appears at 24 hours (middle panel), and is dominated by PMN (right panel). Note that the lung parenchyma (alveolar septa, bronchioles) is normal in spite of this airspace inflammation.

To quantify the influx of these PMNs, total cell counts, myeloperoxidase, and MMP-9 measurements were performed. Myeloperoxidase and MMP-9 are both enzymes produced by neutrophils and therefore can be used as surrogate markers for this cell (200, 274). Total cell counts of PMNs in the BAL fluid revealed a significant increase at 6 and 24 hours compared to time 0 (Figure 19). Further, myeloperoxidase levels showed a trend to increase at 6 and 24 hours, and MMP-9 was significantly upregulated at 24 hours.

Collectively, this data characterizes the airspace inflammation that results after mice are exposed to bacteria. This pneumonia model shares a number of notable characteristics with the asbestosis/pulmonary fibrosis model described in Chapter 4, including airspace inflammation that is predominated by PMNs. However, this model also differs from pulmonary fibrosis in that it lacks interstitial processes such as inflammation and extracellular matrix remodeling in the lung interstitium. By dissociating the airspace and interstitial processes, the pneumonia model should provide evidence for the relative roles of these processes in the redistribution of EC-SOD that occurs in response to inflammatory and fibrotic injuries in the lung.

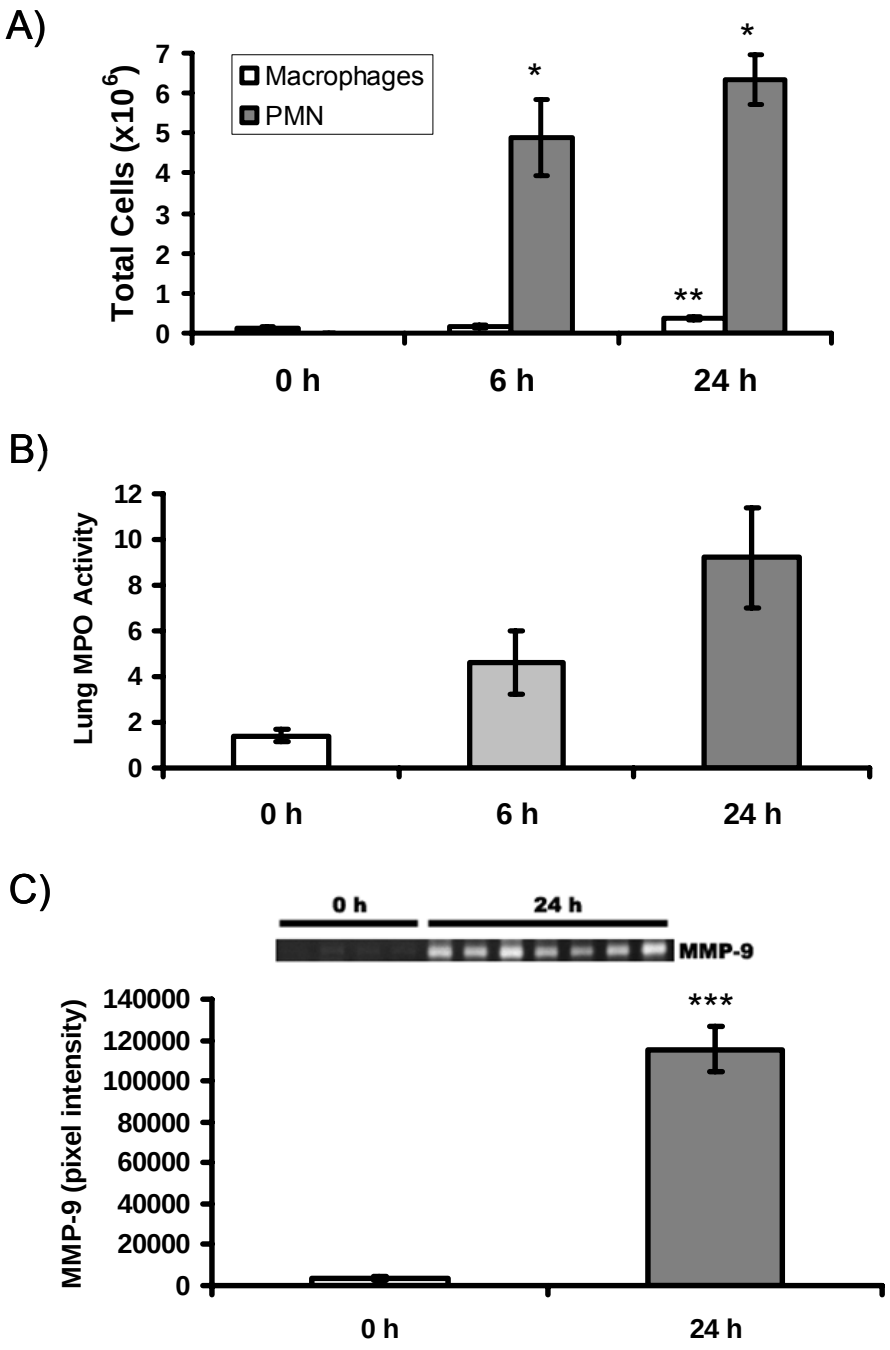

Figure 19. PMN and macrophages are increased after bacterial exposure.

PMNs and macrophages were quantitatively analyzed through direct cell counts in BAL fluid (A). Myeloperoxidase activity from lung homogenates (B), and gelatin zymography for MMP-9 in BAL fluid (1 μg) (C) were assessed as surrogate markers for PMN. Overall, these figures show an increase in inflammation at 6 and 24 hours after bacterial inhalation in mice. * $p < 0.05$ compared to 0 h, one way ANOVA and Tukey's post test. ** $p < 0.05$ compared to both 0 h and 6 h, one way ANOVA and Tukey's post test, *** $p < 0.05$, Student's t test.

6.2. INFLAMMATION LEADS TO EC-SOD ACCUMULATION IN AIRSPACES

EC-SOD levels were determined in BAL fluid of mice exposed to *E. coli* bacteria. Although there was no significant accumulation of EC-SOD in BAL fluid at 6 hours compared to 0 hours (Figure 20), there was a significant increase at 24 hours (Figure 21). The ratio of cut to uncut EC-SOD was also increased at 24 hours compared to time 0. EC-SOD assay results confirmed our findings, as no detectable levels of EC-SOD were found for four out of five samples at 0 and at 6 hours, but EC-SOD activity was observed at 24 hours (Figure 22).

6.3. AIRSPACE INFLAMMATION DOES NOT ALTER PARENCHYMAL EC-SOD

Although the BAL fluid showed a similar increase in EC-SOD levels in pneumonia and in pulmonary fibrosis, the lung parenchymal levels were unknown. The abundance of EC-SOD in the lung parenchyma was measured using western blotting. Western blots revealed no significant change in lung parenchymal EC-SOD at 0, 6, or 24 hours (Figure 23). Immunohistochemistry was also performed to verify these results. Lung sections at time 0 revealed strong alveolar staining for EC-SOD (Figure 24). Sections from mouse lungs harvested at 24 hours possessed a similar intensity of staining for EC-SOD.

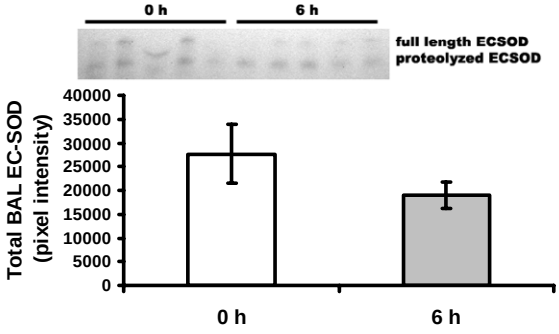

Figure 20. EC-SOD in BAL fluid is not significantly altered 0 and 6 hours after bacterial exposure.

EC-SOD levels in BAL fluid (5 μg of each sample loaded) were determined by western blotting followed by densitometry. There was no significant difference between 0 hour and 6 hour timepoints.

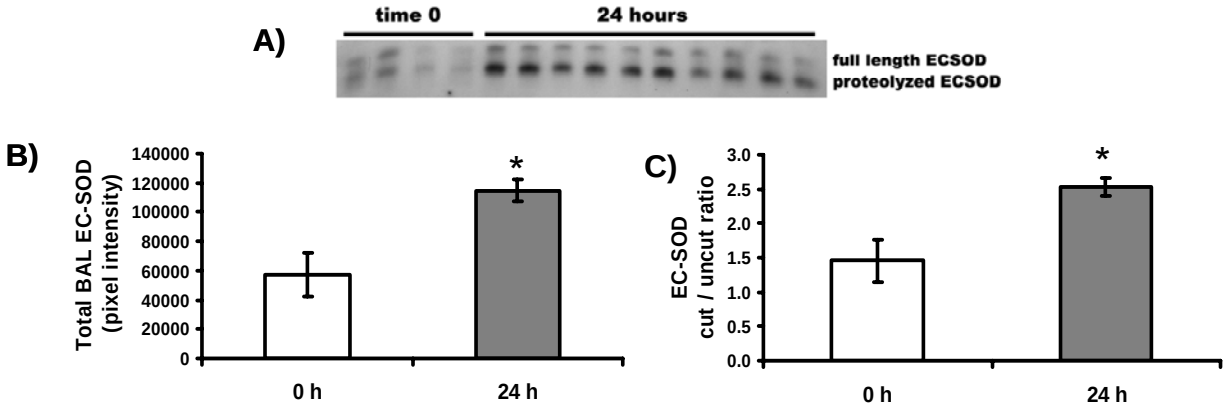

Figure 21. EC-SOD accumulates in the BAL fluid at 24 hours post-bacterial inhalation.

EC-SOD levels in BAL fluid (3 μg) 24 hours after inhalation of bacteria was measured by western blotting (A). Densitometry showed increased EC-SOD at 24 hours compared to 0 hours (B). The EC-SOD at 24 hours also had an increase in cut to uncut ratio (C). * $p < 0.05$, Student's t test.

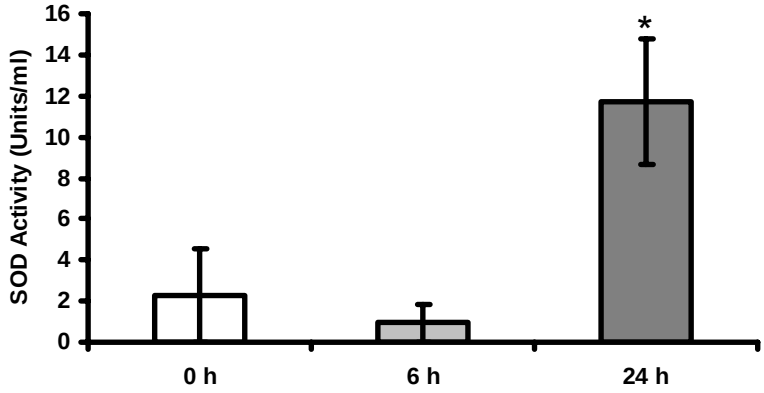

Figure 22. EC-SOD Activity in BAL fluid increases 24 hours after bacteria exposure.

EC-SOD activity was determined in BAL fluid (N=5 at each timepoint) recovered at the indicated timepoints after bacterial inhalation in mice. Activity was determined through inhibition of the reduction of cytochrome c by the xanthine/xanthine oxidase superoxide-generating system. At 0 and 6 hours, four out of five samples were below detectable levels of EC-SOD activity. * $p < 0.05$, one way ANOVA and Tukey's post test.

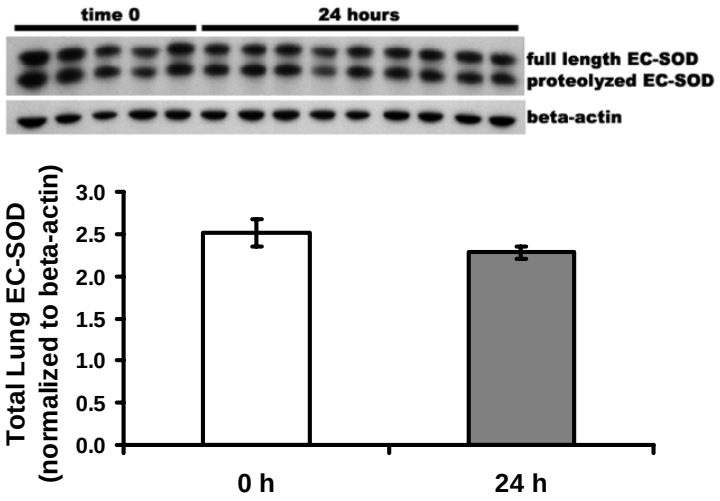

Figure 23. EC-SOD is not depleted from the lung after bacterial exposure.

Western blotting was performed on equivalent protein amounts of lung homogenates (8 μg) from mice exposed to bacteria. Densitometry was normalized to β-actin as a loading control. In contrast to pulmonary fibrosis models, total EC-SOD is unchanged in lung homogenates 24 hours after inoculation. p = 0.15, Student's t test.

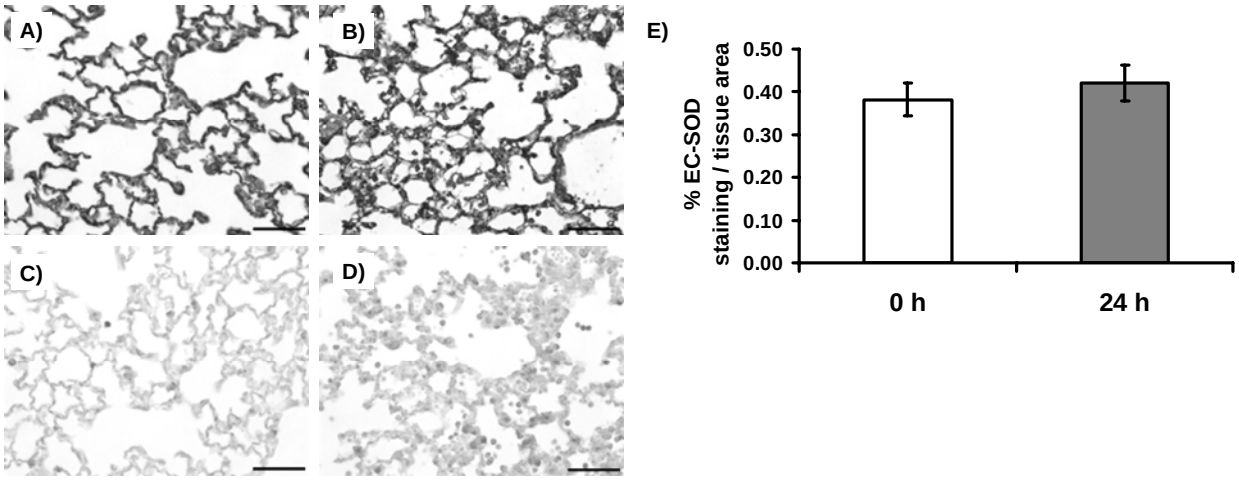

Figure 24. EC-SOD is not removed from lung parenchyma during airspace inflammation.

5 μm thick paraffin embedded lung sections from mice sacrificed at 0 hours (A and C) or at 24 hours (B and D) after *E. coli* bacterial inhalation were stained with antibody against EC-SOD (1:500 dilution, A and B) or with normal rabbit serum (1:500, C and D). EC-SOD labeling intensity (E) is unchanged 24 h after inoculation (p = 0.54, Student's t test). Bar equals 50 μm.

These results indicated that, although there was accumulation of EC-SOD in the BAL fluid during airspace inflammation, there was no depletion of EC-SOD from the lung parenchyma. In contrast, pulmonary fibrosis models lead to depletion from lung parenchyma as well as accumulation in the airspace. This indicated that the removal of EC-SOD from the interstitium is unique to pulmonary fibrosis, due to processes unique to that disease, and cannot be recapitulated with airspace inflammation alone.

6.4. AIRSPACE EC-SOD ORIGINATES FROM INFLAMMATORY CELLS

As the pneumonia experiments suggested that the EC-SOD accumulating in the airspace/BAL fluid does not arise from the lung parenchyma, it was hypothesized that there must be another source of this protein in the airspaces. The most obvious source appeared to be the macrophages and neutrophils, which are known to produce EC-SOD (184). It was hypothesized that these inflammatory cells release EC-SOD into the airspaces.

Immunohistochemical staining provided evidence of an inflammatory cell origin of EC-SOD. When staining sections with anti-EC-SOD antibody, staining localized to neutrophils and macrophages in addition to alveolar epithelium (Figure 25). However, localization of EC-SOD to inflammatory cells still does not prove that the antioxidant is solely arising from these cells.

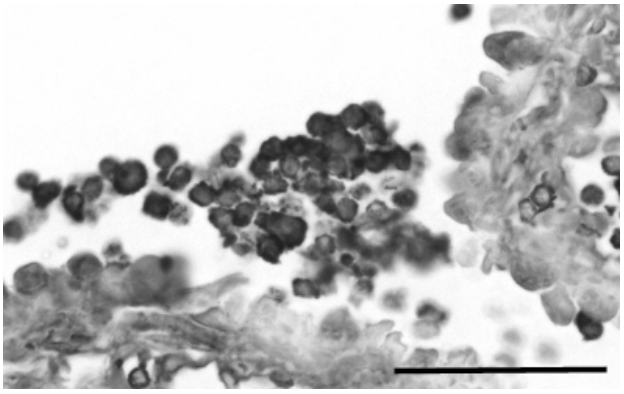

Figure 25. EC-SOD localized to PMN and macrophages in bacterial pneumonia.

Immunohistochemical staining was performed with anti-mouse EC-SOD antibody as in Figure 24. PMN and macrophages both stained strongly for EC-SOD. Bar equals 50 μm.

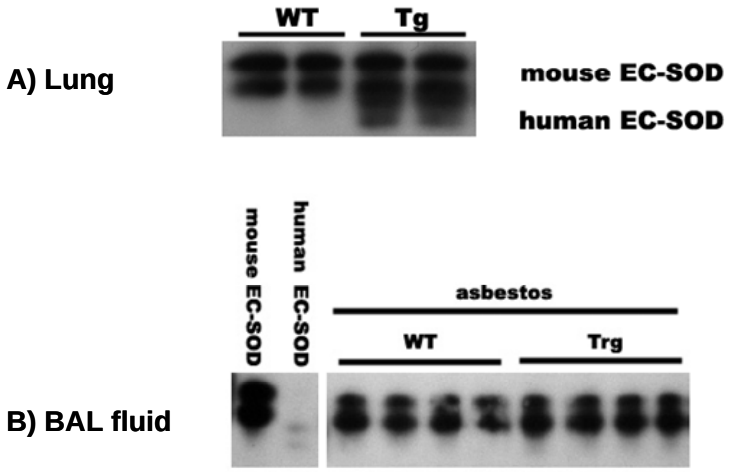

Figure 26. Airspace EC-SOD originates from outside the lung in asbestosis.

Western blots for EC-SOD were performed on equal protein loaded lung homogenates (A) and BAL fluid (10 μg) (B) from SPC EC-SOD transgenic (Tg) and wild type (WT) mice. A) Tg mice produce both the human and mouse forms of EC-SOD (distinguishable on reducing SDS-PAGE) in the lung while inflammatory cells express only mouse EC-SOD. B) 14 days after exposure to an inflammatory stimulus (asbestos), there is BAL fluid accumulation of only mouse EC-SOD in the Tg mice, suggesting an extrapulmonary source of EC-SOD (i.e. infiltrating inflammatory cells).

To further examine the role of inflammatory cells in airspace EC-SOD accumulation, experiments were performed with a strain of transgenic mice possessing lung-specific expression of human EC-SOD. These mice possess the gene for human EC-SOD under the lung-specific surfactant protein C (SPC) promoter and have been described previously (197). Inflammatory cells and all other tissues produce only mouse EC-SOD, and the human and mouse EC-SOD can be distinguished on reducing SDS-PAGE by size.

Transgenic mice and wild type littermates were exposed to saline or to asbestos fibers by intratracheal instillation and sacrificed at 14 days. This is a timepoint at which it is known that EC-SOD is depleted from the lung and accumulates in the BAL fluid after asbestos exposure (see Figure 15). Western blotting for human and mouse EC-SOD was performed with an antibody that detects both human and mouse forms. In the lung homogenates from saline-treated mice, both human and mouse EC-SOD are detected in the transgenic mice, while only the mouse form is present in wild types (Figure 26).

In the BAL fluid of mice treated with asbestos, only the mouse form of EC-SOD is observed (Figure 26). This indicated that lung EC-SOD is not released into the airspaces in pulmonary fibrosis. Instead, the airspace accumulation of this antioxidant is most likely due to release from cells originating outside of the lung. In this case, these cells are macrophages and PMNs. In this experiment, however, we cannot rule out the possibility that only mouse EC-SOD from the lung, but not human EC-SOD from the lung, is being redistributed to the airspace. This would be extremely unlikely due to the presence of the heparin-binding domain in both human and mouse EC-SOD.

6.5. CONCLUSIONS

Proteolytic processing of the heparin-binding domain of EC-SOD, accompanied by depletion of this antioxidant from the lung parenchyma and accumulation in the airspaces, was observed in bleomycin- (207) and asbestos- (see Chapter 5) mediated lung disease. A similar depletion from the lungs was observed in response to hyperoxia (208). Since these disease processes are characterized by interstitial inflammation and remodeling, we hypothesized that these interstitial processes are responsible for the proteolysis and redistribution of EC-SOD. To test this hypothesis, we examined the proteolysis and localization of EC-SOD in a bacterial pneumonia/bacterial clearance model which lacks interstitial remodeling events and in which inflammation is limited to the airspaces.

As expected, our studies show that challenge of mice with inhaled *E. coli* bacteria leads to an inflammatory reaction 6 and 24 h later that is localized primarily to the airspaces. PMN leukocytes in particular were increased, as determined by histology, BAL fluid cell counts, myeloperoxidase, and MMP-9 activity. Notably, this neutrophilic influx is also observed in asbestos-induced interstitial lung disease.

We also found a significant increase in EC-SOD levels in the airspaces at 24 h, as measured in the BAL fluid. This accumulation is similar to that seen in the asbestos mouse model (see Chapter 5). However, in contrast to findings in interstitial lung diseases which show a loss of EC-SOD from the lung parenchyma, lung homogenates and immunohistochemistry did not show any change in EC-SOD in the lung parenchyma following bacterial pneumonia, in which the inflammatory response is limited to the airspaces.

Pulmonary fibrosis disease models have effects on both the interstitium (inflammation and either fibrosis or interstitial thickening) and the airspaces (inflammation). In contrast, bacterial pneumonias cause inflammation primarily in the airspaces. This difference may

underlie the lack of EC-SOD depletion from the lung parenchyma in bacteria-exposed mice. Interstitial inflammation or remodeling processes may lead to the elaboration of proteases that cleave the heparin-binding domain of EC-SOD in the lung parenchyma. Without a significant interstitial component to the disease, as in the pneumonia model, EC-SOD remains at normal levels in the lung parenchyma.

Notably, we observed EC-SOD accumulation in the airspaces during bacterial pneumonia in spite of the retention of EC-SOD in the lung parenchyma. This suggests that proteolysis and diffusion of EC-SOD from the matrix into the airspaces is not the source of EC-SOD that accumulates in alveolar lining fluid. As PMNs and macrophages are present in the airspaces in both interstitial lung diseases and pneumonia, and these cells possess large amounts of EC-SOD (184, 275), we hypothesized that these cells may be the source of the EC-SOD accumulation in airspaces after inflammatory injuries in the lung. We did observe that although neutrophils are significantly increased at 6 h, significant EC-SOD accumulation in BAL fluid does not occur until 24 h. It is likely that a period of time is required to accumulate enough EC-SOD to detect by western blotting and the activity assay. We also cannot rule out a role for macrophages, since they are significantly elevated at 24 h but not at 6 h. However, the large influx of neutrophils compared to macrophages implies a greater neutrophilic contribution to airspace EC-SOD.

In experiments with transgenic mice producing human and mouse EC-SOD in the lung and only mouse EC-SOD in all other cells and tissues, we found only mouse EC-SOD in the BAL fluid after a stimulus for inflammation and interstitial lung injury. This finding strongly suggests that inflammatory cells transport and release EC-SOD into the airspaces since a lung origin would lead to both human and mouse isoforms in the airspace. Other authors have suggested a role for neutrophils and macrophages in transporting EC-SOD into the lung (184).

However, we cannot rule out the less likely possibility that only mouse EC-SOD, but not human EC-SOD, is being redistributed to the airspace.

It is not yet known whether this increased EC-SOD in the BAL fluid represents a protective response. Proteolyzed EC-SOD retains its catalytic antioxidant capacity. Its release in sites of PMN infiltration may act to balance the large pro-oxidant activities of neutrophils. The release of EC-SOD may act to prevent widespread oxidative damage to alveolar airspace contents such as surfactant and epithelial cells. EC-SOD is also known to inhibit neutrophil influx in response to hyperoxia (197), LPS (201), and bleomycin (204). It was shown that some of these effects in the LPS model are mediated by alterations in cytokine production as well as endothelial selectins and adhesion molecules (201). Therefore, release of EC-SOD from neutrophils may serve as a mechanism to limit further neutrophil influx.

In conclusion, EC-SOD accumulates in the BAL fluid of mice following inhaled *E. coli* challenge. This is not accompanied by any depletion of EC-SOD from the lung parenchyma, indicating that PMN leukocytes and macrophages release this antioxidant into the airspaces. This pattern differs from that seen in interstitial lung diseases, where the presence of interstitial inflammation and remodeling may contribute to the depletion of EC-SOD from the pulmonary interstitium. Our data suggests differential regulation of this antioxidant in the progression of interstitial lung disease and bacterial pneumonia and that inflammatory cells are a source of airspace EC-SOD during pulmonary inflammatory responses.

7. EC-SOD KNOCKOUT MICE HAVE INCREASED SUSCEPTIBILITY TO ASBESTOS

Chapter 5 described the loss of EC-SOD from lung parenchyma after exposure to asbestos at both acute and chronic timepoints. Studies described in Chapters 5 and 6 demonstrated that this depletion is an event unique to pulmonary fibrosis likely due to interstitial processes occurring in that disease. Also, it was found that airspace EC-SOD can accumulate due to apparent release of the antioxidant from inflammatory cells. However, these studies did not directly examine the role of EC-SOD in the development of asbestosis. We hypothesized that EC-SOD has a protective effect on the lung and that its absence would lead to greater disease severity. Therefore, we examined asbestosis in mice that are null for the EC-SOD gene and do not produce any of this antioxidant.

7.1. EC-SOD KNOCKOUT MICE DEVELOP WORSE INFLAMMATION

Wild type and EC-SOD knockout mice were exposed to asbestos via intratracheal instillation and sacrificed at 1 and 28 days. BAL fluid from these mice revealed significantly increased BAL fluid protein in the knockout/asbestos mice versus the wild type/asbestos mice, indicating greater damage in the knockout mice (Figure 27). Inflammation was also increased, as neutrophil counts in the BAL fluid were also increased in the knockout mice (Figure 28). This data showed that the inflammatory response to asbestos is heightened when EC-SOD is not present in the lung.

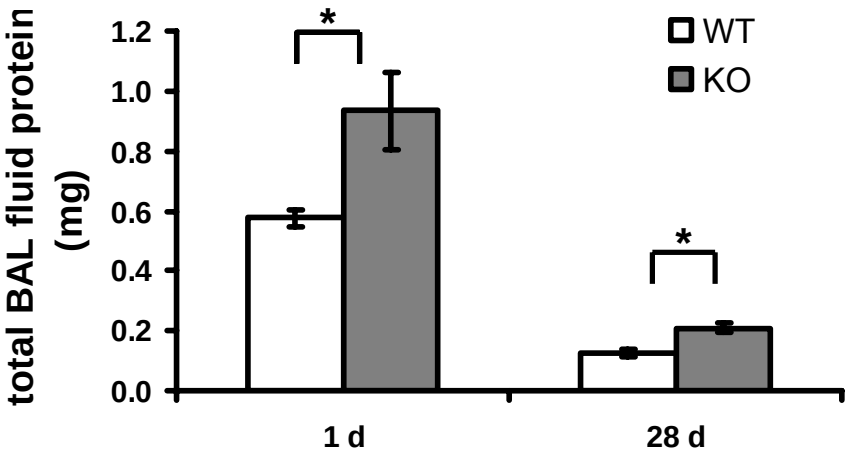

Figure 27. EC-SOD knockout mice have increased BAL fluid protein.

BAL fluid was recovered from mice intratracheally instilled with 0.1 mg crocidolite asbestos. Protein content was determined with the Coomassie Plus Protein Assay Reagent. Mice that do not express EC-SOD possess a greater amount of protein in their airspaces after asbestos instillation. * $p < 0.05$ Student's t test.

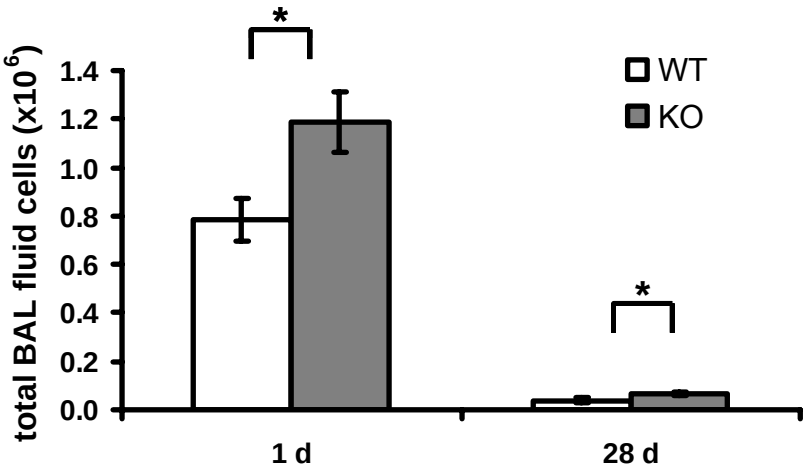

Figure 28. EC-SOD knockout mice have increased PMNs.

BAL fluid was recovered 1 or 28 days after asbestos instillation. Total cell counts were taken and differential counts performed on BAL fluid spun onto slides with a cytospin. Percentages of PMNs were multiplied by the total number of cells to get total PMN numbers in BAL fluid. EC-SOD knockout mice displayed greater PMN influx than the wild types.

*** $p < 0.05$ Student's t test.**

7.2. EC-SOD KNOCKOUT MICE DEVELOP WORSE FIBROSIS

To determine levels of fibrosis in EC-SOD knockout mice exposed to asbestos, histology and hydroxyproline analysis were undertaken. Histology revealed an increase in fibrosis at 28 days in knockout versus wild type mice when both were treated with asbestos (Figure 29). The pathology grade was significantly increased in the knockout mice over wild type mice. Hydroxyproline levels from lungs of EC-SOD knockout mice also confirmed these findings of increased fibrosis (Figure 30).

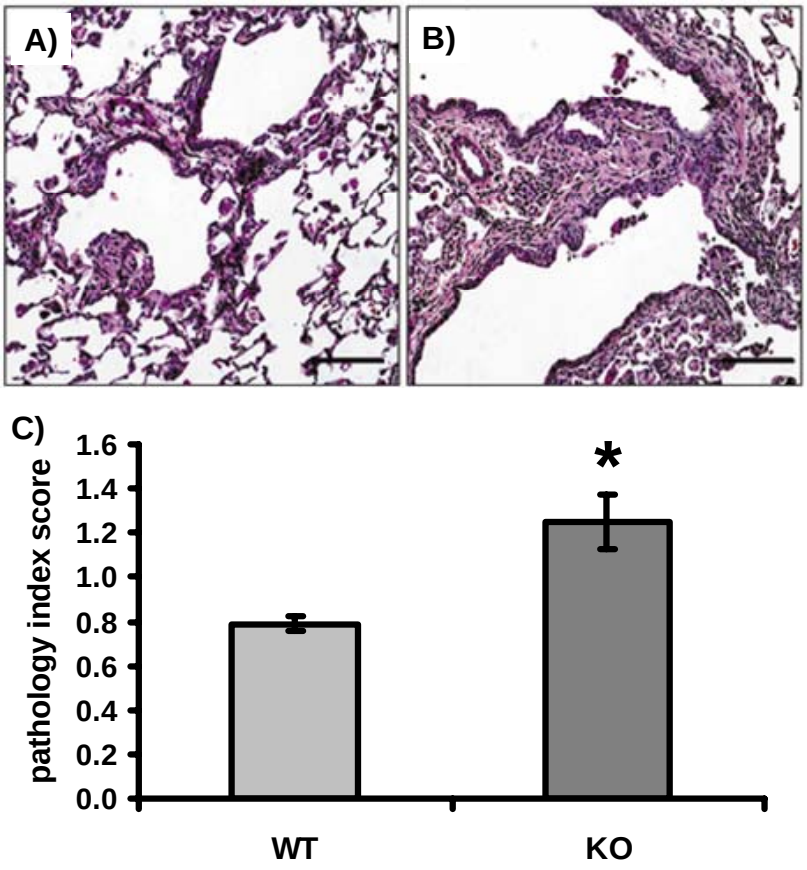

Figure 29. EC-SOD knockout mice exhibit worsened fibrosis after asbestos.

Wild type and EC-SOD knockout mice were euthanized 28 days after intratracheal administration of 0.1mg crocidolite asbestos. Histologically, hematoxylin and eosin staining revealed greater lung fibrosis in knockout mice (B) compared to wild types (A). Pathology index scores were assigned by a blinded pathologist (T.D.O.) and also indicated increased fibrosis in knockouts (C). Scoring: 0=no fibrosis, 1=0-25% fibrosis, 2=25-50%, 3=50-75%, 4=75-100%. * $p < 0.05$, Student's t test.

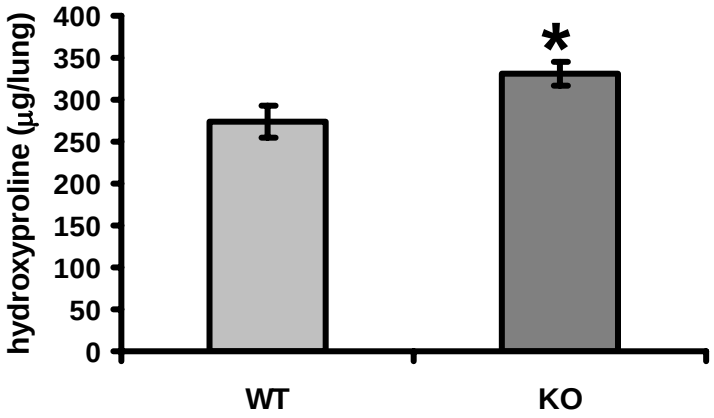

Figure 30. EC-SOD knockout mice have increased hydroxyproline levels at 28 days.

Mice were treated as Figure 29. After 28 days, mice were euthanized and lungs recovered. The lungs were acid hydrolyzed and hydroxyproline levels were determined as a measure of fibrosis.

*** $p < 0.05$, Student's t test.**

7.3. CONCLUSIONS

In Chapter 5, an alteration in EC-SOD localization was described after asbestos exposure in mice that involved a depletion of EC-SOD from lung parenchyma. Although removal from the lung would suggest that the lung would be more susceptible to increased oxidative stress and injury, it was not known whether this was the case. To definitely test the role of EC-SOD in the development of asbestosis, we examined EC-SOD knockout mice in our model system. It was hypothesized that EC-SOD knockout mice would develop worse disease in response to asbestos compared to wild type mice.

EC-SOD knockout mice were examined at 24 hours and 28 days post-asbestos exposure. BAL fluid revealed increased parameters of lung injury, as higher protein levels and PMNs accumulated in the airspaces of knockout mice compared to wild type mice. Knockout mice also exhibited greater levels of fibrosis as determined by histologic scoring and hydroxyproline analysis.

These results indicate that EC-SOD plays an important protective role in asbestos-induced pulmonary fibrosis. Both inflammation and fibrosis were increased when EC-SOD was absent from the lung, suggesting that our findings of depleted lung parenchymal EC-SOD from wild type mouse lungs after asbestos is in fact detrimental in this disease. It also suggests that the airspace accumulation of EC-SOD may also be protective, as the knockout mice would also not exhibit this accumulation. As discussed in Chapter 6.5, EC-SOD release from inflammatory cells could prevent further inflammation. The two fold effect of depletion from lung parenchyma and loss of airspace EC-SOD probably underlies the increased susceptibility of knockout mice to asbestos lung disease.

The targets of increased oxidative stress resulting from loss of EC-SOD remain to be determined. Matrix metalloproteinases are a potential target of oxidative stress because of their propensity to become activated after ROS exposure (229, 231, 276). The activity of these proteases is examined in Chapters 9 and 10. Collagen is another potential target of oxidative stress in asbestos lung injury and is present in high amounts in the extracellular matrix. Collagen fragments are known chemoattractants and activators of neutrophils (205, 206). Not only can ROS activate MMPs which cleave collagen (229, 231, 276), collagen itself can be directly fragmented by oxidative stress (277). EC-SOD has been shown to associate with type I collagen and can prevent its oxidative fragmentation *in vitro* (174) and *in vivo* (204). Depletion of EC-SOD from the lung parenchyma could lead to increased collagen fragmentation and increased neutrophil chemotaxis and activation. It has already been shown that EC-SOD can inhibit pulmonary inflammation in response to hyperoxia (197) and bleomycin (204). In further support of this hypothesis, it was found that neutrophil immigration into the lung coincides with loss of EC-SOD from the lung in asbestos-treated mice (see Figure 5, Figure 11, and Figure 15).

Neutrophils themselves can also produce large quantities of reactive oxygen species (which can lead to more collagen fragmentation) and proteases (which can cleave collagen and can also potentially cleave the heparin-binding domain of EC-SOD, leading to its release from the lung parenchyma) (115, 278).

Overall, loss of EC-SOD in asbestosis is likely to contribute to pathogenesis of the asbestosis and pulmonary fibrosis in general. Greater understanding of the targets of increased oxidative stress in the lung will greatly aid development of new therapies for the disease. Furthermore, treatment of patients with antioxidant therapy may improve symptoms and outcomes.

8. EC-SOD IN HUMAN IDIOPATHIC PULMONARY FIBROSIS

Although the results presented thus far indicate an important role for EC-SOD in the pathogenesis of experimentally-induced pulmonary fibrosis, it is unclear whether EC-SOD is involved in the development of human idiopathic pulmonary fibrosis. We examined lung tissue samples taken from IPF patients for the presence of EC-SOD, hypothesizing that patients with IPF had less EC-SOD in the lung than normal patient controls.

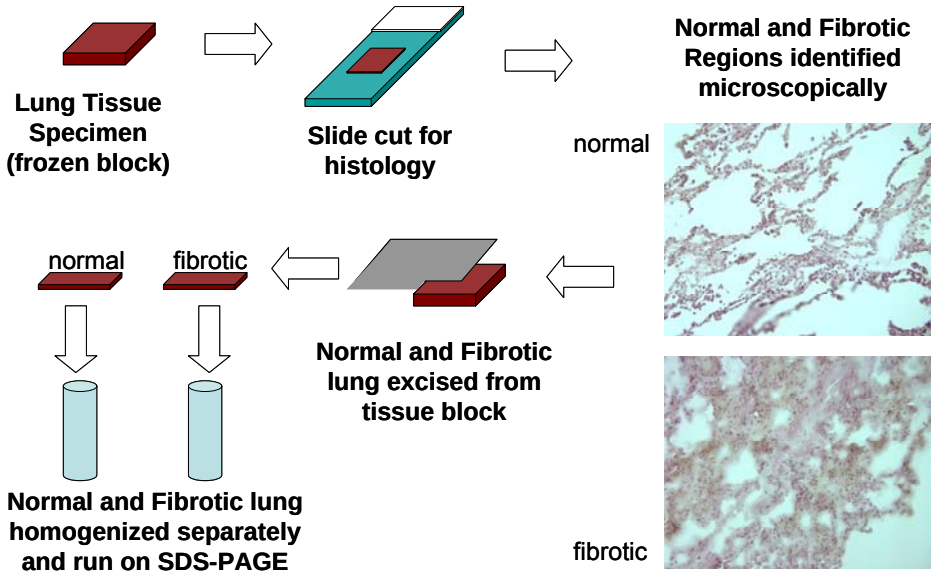

Figure 31. Technique for determination of EC-SOD levels in IPF lung.

To quantify the amount of EC-SOD in fibrotic versus normal regions of IPF lung, slides were cut from frozen blocks to identify these areas. Using this as a guide, the frozen blocks were dissected and normal and fibrotic areas isolated and homogenized separately.

EC-SOD was assessed via western blot analysis using both normal and IPF lung tissue homogenates. All lungs, normal and IPF, showed a large variability in the amount of EC-SOD isolated. We attempted a different analysis to correct for this variability. Instead of comparing normal controls versus IPF patients, we compared normal and fibrotic regions from the same IPF patient. After identifying these regions microscopically from sections cut from frozen blocks,

these regions were dissected from the blocks (Figure 31). The separate pieces were then individually homogenized and analyzed on western blots. As shown in Figure 32, when comparing normal and fibrotic areas from the same lung, EC-SOD was depleted in the fibrotic areas.

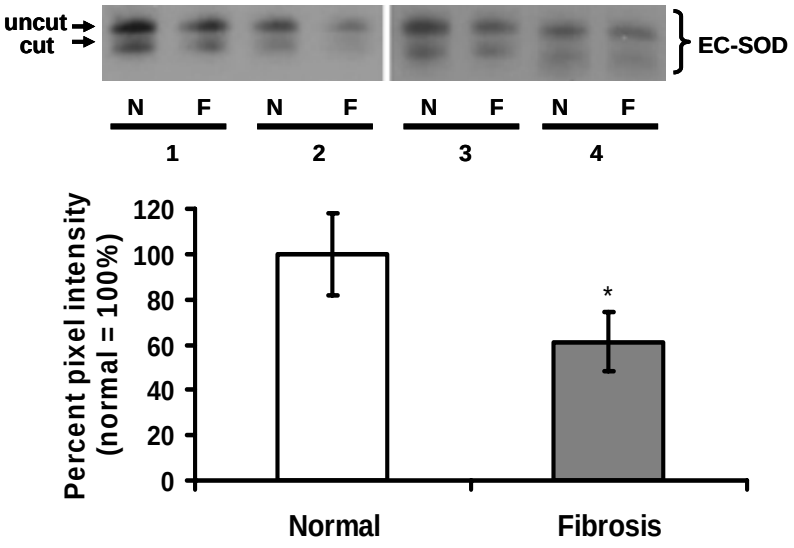

Figure 32. Fibrotic lung has less EC-SOD than normal lung from the same IPF patient.

Tissue homogenates isolated as described in Figure 31 were equal protein amounts (10 μg) subjected to SDS-PAGE and western blotting for EC-SOD. Samples from four IPF patients are shown (#1-4). The adjacent normal (N) and fibrotic (F) regions of the lung were compared. Densitometry was expressed as percent of normal, with normal equaling 100%. Fibrotic lung regions showed a decrease in EC-SOD levels.

*** $p < 0.05$, Student's t test.**

In collaboration with the laboratory of Vuokko Kinnula in Finland, immunohistochemistry was performed on sections from paraffin-embedded UIP patients. Immunohistochemical staining for EC-SOD in UIP lungs showed positive labeling in normal alveolar parenchyma that was noticeably absent from fibrotic areas of the lung. This data is consistent with our western blot findings in Figure 32.

8.1. CONCLUSIONS

Our results in IPF tissue samples show that similar events occur in both experimentally-induced and human pulmonary fibrosis. Namely, EC-SOD is depleted from the lung parenchyma during the development of pulmonary fibrosis in mice, and EC-SOD is also depleted from fibrotic lung in IPF patients in comparison to adjacent normal tissue. Loss of EC-SOD from these regions could contribute to an oxidant/antioxidant imbalance in the lung parenchyma. Potential targets of increased oxidative stress have already been discussed in Chapter 7.3, and the resulting damage could contribute to the development of fibrosis. Our data shows that there is less EC-SOD in the lung once fibrosis has developed. In theory, antioxidant therapy may reduce oxidative stress in fibrotic areas of the lung, and, more importantly supplement the EC-SOD already found in the normal areas of lung. This may help to limit progression of the disease by limiting oxidative stress and preventing normal lung development of fibrosis.

9. MATRIX METALLOPROTEINASES IN ASBESTOSIS

It is widely recognized that MMPs play an important role in normal and diseased lung (279). Their upregulation has been noted in a number of pulmonary conditions including bleomycin-induced and silica-induced pulmonary fibrosis (33, 261). However, the regulation of MMPs in asbestosis has not been examined previously. Furthermore, the relationships between oxidative stress, EC-SOD, and MMPs have not been specifically studied in any of the pulmonary fibrosis diseases. Therefore, we examined the levels and role of MMPs as well as their endogenous TIMP inhibitors in our asbestos-induced disease model.

9.1. MMP-2 AND MMP-9 ARE UPREGULATED IN ASBESTOSIS

MMP-2 and -9, also known as gelatinase A and B, respectively, were studied in our mouse model of pulmonary fibrosis. These two MMPs are thought to be involved in the development of pulmonary fibrosis because of their high expression in other lung diseases and because of their ability to degrade native type IV collagen (236). Since one of the earliest steps in the pathogenesis of this disease is the loss of epithelial barrier integrity (280) and since the epithelium lies upon the basement membrane rich in collagen type IV, the gelatinases could play an important role in degradation of this barrier. We hypothesized that MMP-2 and -9 would be upregulated in asbestosis.

A common technique used to study these two MMPs is gelatin zymography. Zymography is an SDS-PAGE technique in which gelatin is incorporated into the electrophoretic gel during its casting (272). Samples containing MMPs are electrophoresed under nonreducing denaturing conditions. After electrophoresis, the denaturing agent (SDS) is removed, activity is restored, and the MMPs are able to cleave the gelatin in the gel. Coomassie staining of the gel

after an incubation period reveals the location of MMPs as clear zones against a blue background. This technique allows for the quantification of both MMP-2 and MMP-9, as well as active versus latent forms, as these species migrate differently on SDS-PAGE. Zymograms are a better method than western blots because sensitivity is greater, generally in the picomolar range (281). Lung homogenates on zymograms typically show three major bands in the molecular weight region of MMP-2 and MMP-9. The 105kD band represents the latent form of MMP-9 while the active form is undetectable. Latent MMP-2 is approximately 72kD while active MMP-2 is 62kD, reflecting cleavage of the prodomain.

Figure 33 shows a zymogram containing equal protein amounts of lung homogenates from titanium dioxide-treated controls and mice euthanized at 1, 7, 14, and 28 days after intratracheal instillation of asbestos. The zymogram shown is representative of a larger sample set, and densitometry was performed on 3 to 6 samples for each group at each timepoint. The asbestos values were all normalized to the titanium dioxide-treated controls at that timepoint, so that control values always equaled one.

In lung homogenates, the two gelatinases show different kinetics of upregulation. MMP-9 has its greatest increase over control values acutely at 1 day and then returns to baseline at all other timepoints. In contrast, protein levels of MMP-2, particularly active MMP-2, are increased more chronically, beginning at 1 day but persisting even at 28 days with a peak at 7 and 14 days. The ratio of active to latent MMP-2 was also significantly increased at all timepoints due to the increase in active MMP-2. The identity of these bands as MMPs was confirmed because incubation of the gel with the zinc chelator, 1,10-phenanthroline, inhibited development of these bands.

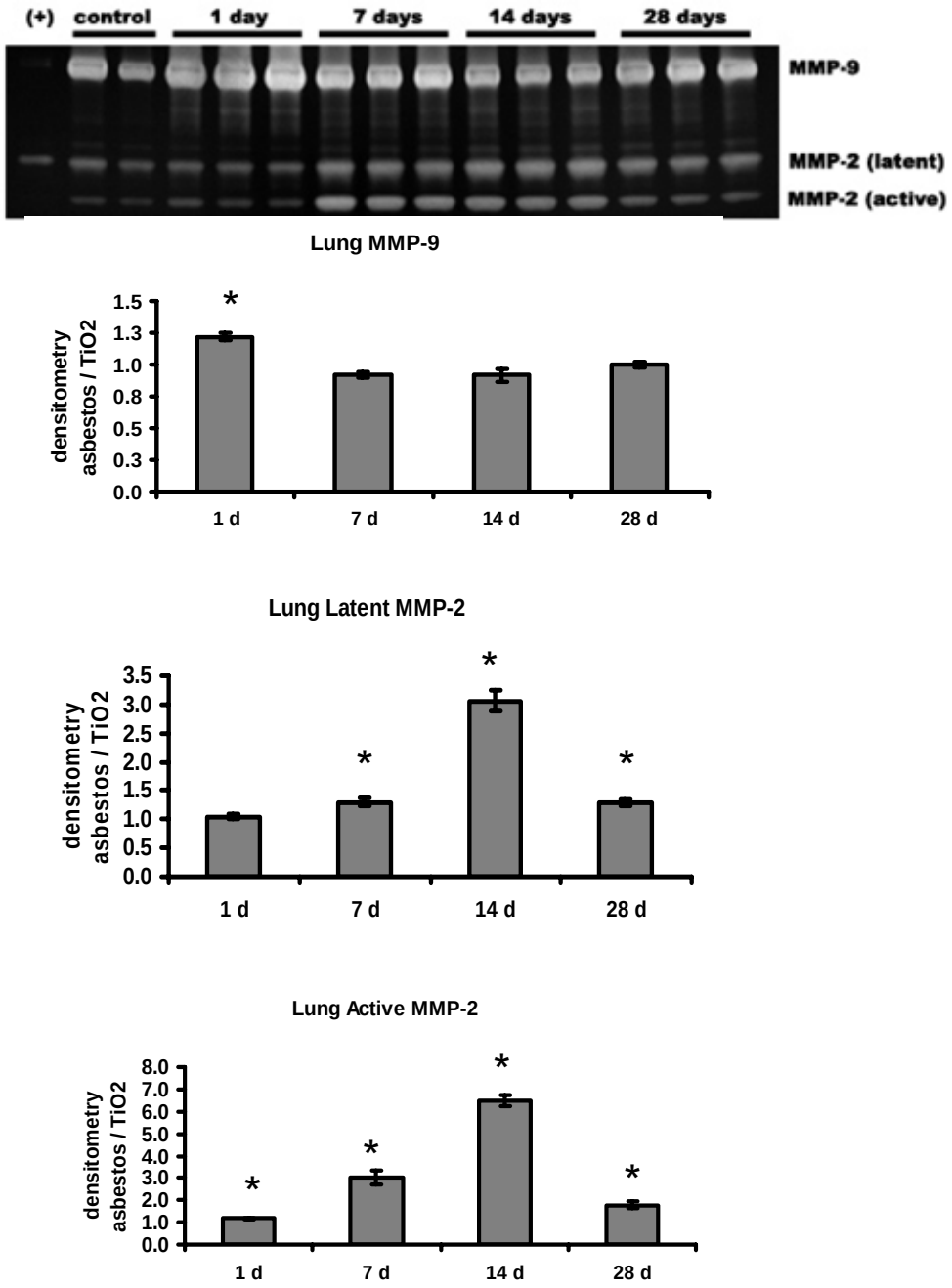

Figure 33. MMP-2 and MMP-9 are increased in lung homogenates after asbestos.

Wild type C57BL/6 mice were exposed to asbestos and euthanized at 1, 7, 14, and 28 days. Gelatin zymography of CHAPS-extracted (10 mM) lung homogenates (equal loading, 15 μg) was performed. A representative gel is shown but densitometry was performed on zymograms comparing controls and asbestos samples at each timepoint (N=3-6). Densitometry was normalized as the average intensity of the asbestos bands divided by the average of the control (titanium dioxide) bands at the same timepoint. The identification of bands as MMP-2 and MMP-9 was made through comparison with purified MMP-2 and MMP-9 (+). Latent and active MMP-2 are increased at all timepoints, while MMP-9 is significantly increased at 24 h only. *P<0.05 Student's t test, comparing asbestos to control at each timepoint.

BAL fluid samples from the same control and asbestos mice described above were also subjected to gelatin zymography (Figure 34). In the BAL fluid, latent MMP-9 and only the latent form of MMP-2 could be detected. While MMPs were nearly undetectable in control mice, MMP-2 and MMP-9 were significantly elevated at all timepoints following asbestos exposure. As in the lung, MMP-9 levels were particularly high at 1 day although titanium treatment also increased MMP-9 at this time, leading to a lower than expected ratio between asbestos to titanium. The highest MMP-2 levels were noted at 1-14 days. Overall, gelatin zymography revealed that MMP-9 is predominantly increased at 1 day, while MMP-2 has a more protracted increase in lung parenchyma and alveolar lining fluid after asbestos exposure.

Localization of these MMPs in asbestosis was determined through the use of immunohistochemistry. Although zymography can be adapted to detect gelatinase activity in lung sections, immunohistochemistry with separate antibodies for MMP-2 and MMP-9 allowed us to differentiate between the two gelatinases.

As we described previously, asbestos-exposed mice revealed neutrophilic influx and some edema and interstitial thickening at 1 day, followed by progressively worsening fibrosis at 7, 14, and 28 days (see Chapter 4). In the context of these histologic changes, we observed the most intense staining for MMP-9 at 1 day, and this was localized to the bronchiolar airspaces of asbestos-treated mice but not titanium dioxide-treated mice (Figure 35). Staining was associated with neutrophils aggregating around asbestos fibers. There was no observable increase in MMP-9 staining in alveolar septa of the asbestos-treated mice at any of the timepoints, although occasional MMP-9 staining was observed in airspaces at 7-28 days, again associated with bronchiolar neutrophils. This localization likely accounts for the transient increase at 1 day of

MMP-9 in lung homogenates and the more persistent expression of MMP-9 in BAL fluid as detected by zymography.

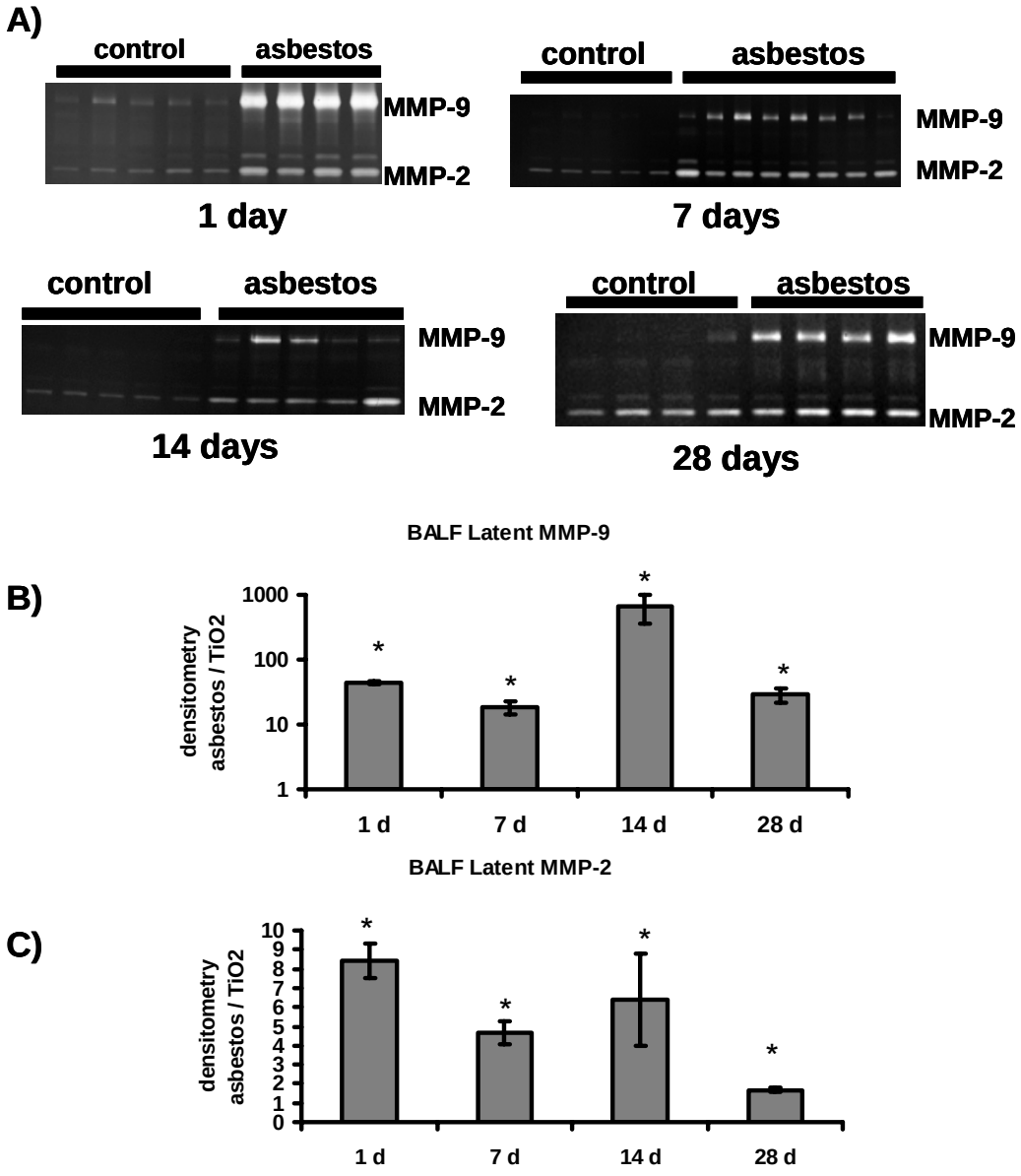

Figure 34. BAL fluid MMPs were increased after asbestos treatment.

MMP-2 and MMP-9 are increased in bronchoalveolar lavage (BAL) fluid after asbestos exposure. Gelatin zymography and densitometry was performed as in figure 1 on equal protein amounts of BAL fluid (5 μg). Only the latent forms of MMP-2 and MMP-9 were found in BAL fluid. There are significant increases in MMP-9 (B) and MMP-2 (C) at all timepoints following asbestos exposure. * $p < 0.05$, Student's t test, comparing asbestos and control.

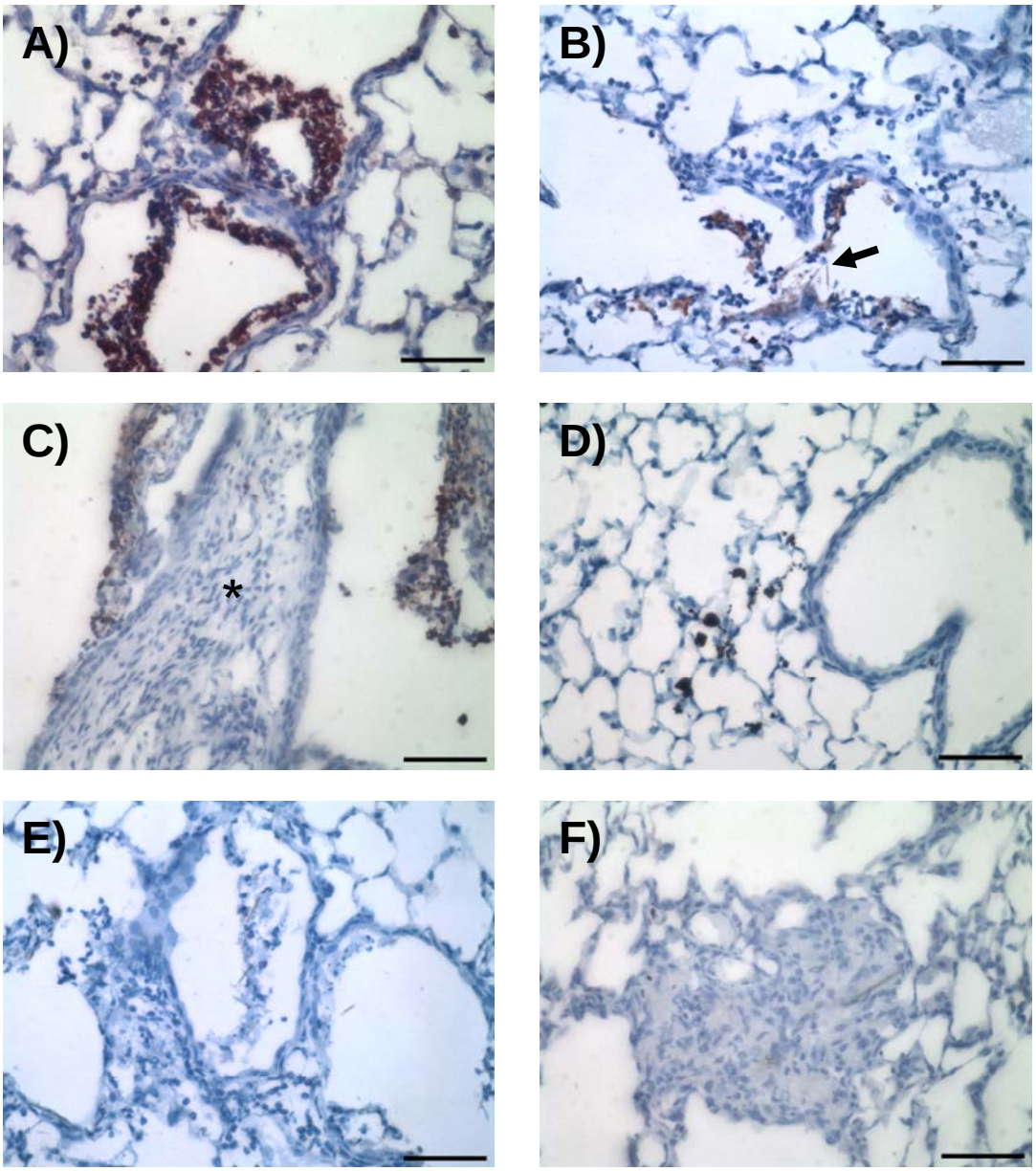

Figure 35. MMP-9 immunohistochemistry in asbestos-exposed mouse lungs.

Mouse lungs were inflation fixed in formalin at 1, 7, 14, and 28 days after intratracheal instillation of 0.1 mg asbestos. Sections were incubated with anti-MMP-9 antibody (A-C, E) from R&D Systems or with normal IgG as a negative control (D,F). Line equals 50 μm.

(A,B) One day after asbestos exposure, bronchiolar neutrophils surrounding visible asbestos fibers (fibers at arrows) stained strongly for MMP-9 (red color).

(C) Bronchiolar neutrophils retained MMP-9 positive staining at 14 d. However, no interstitial MMP-9 was observed, either in normal alveolar septa or in areas of fibrosis (asterisk). Identical staining patterns were observed at 7 and 28 d.

(D) Titanium dioxide-treated mice did not display any MMP-9 staining. Macrophages that have engulfed these particles are clearly visible.

(E, F) Normal goat IgG revealed no staining at 24 hours (E) or 14 days (F) or at any timepoint.

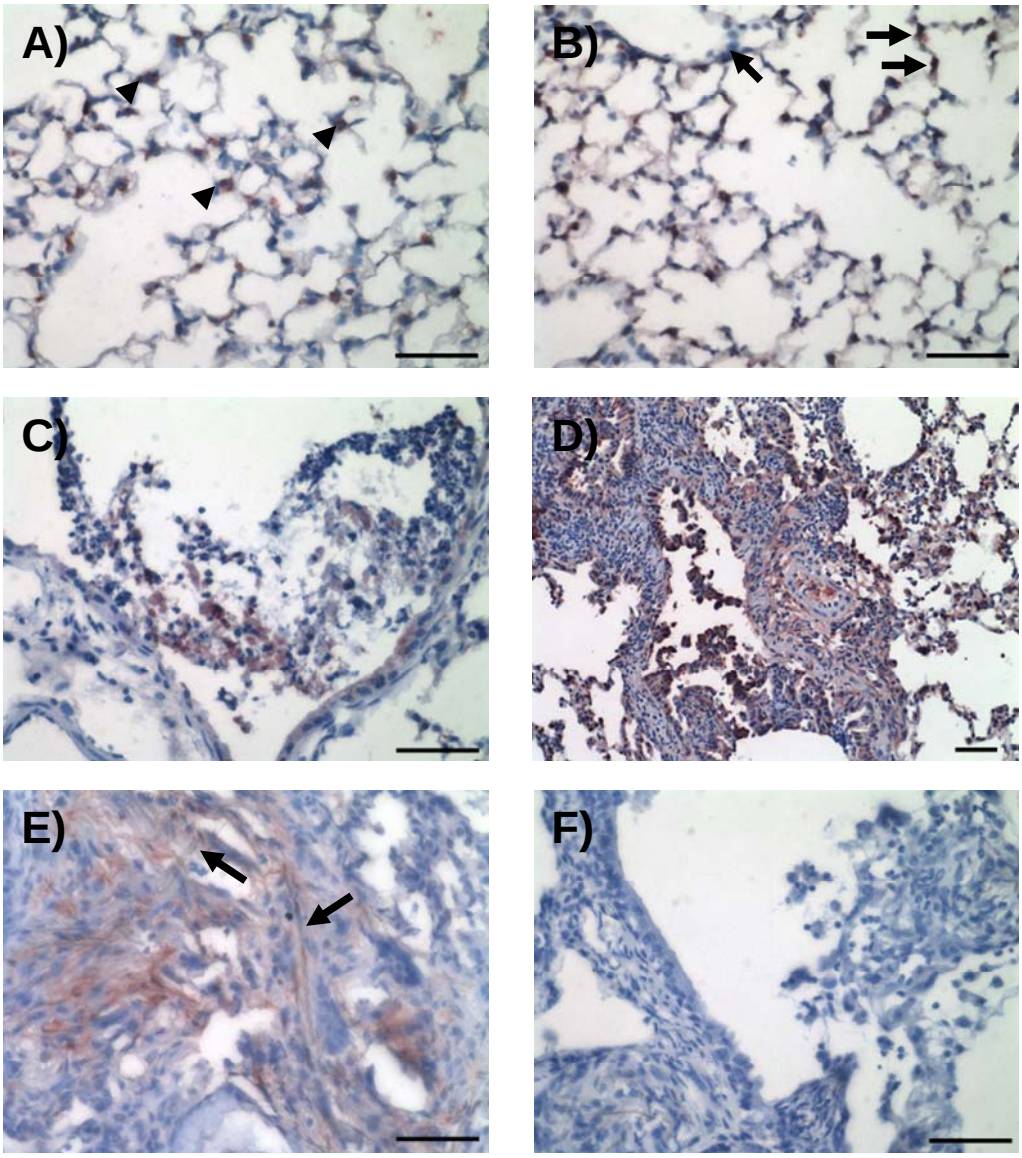

Figure 36. MMP-2 immunohistochemistry in asbestos-exposed mouse lung.

Sections were incubated with anti-MMP-2 antibody (R&D Systems) as described in Materials and Methods. Line equals 50 μm.

(A) Titanium dioxide-treated mice exhibited punctuate localization of MMP-2 in type II epithelial cells (arrowheads).

(B) At 1 d, asbestos-treated mice exhibited the same type II staining but in addition had a more diffuse staining over alveolar septa (arrows).

(C) Also at 1 d, asbestos-treated mice had MMP-2 around bronchiolar neutrophils.

(D) After 7 d, there is a significant increase in interstitial MMP-2 in areas of fibrosis.

(E) As late as 28 d, fibrotic regions retain MMP-2 expression, here in fibrosis with visible asbestos fibers (arrows).

(F) Nonimmune IgG revealed no staining.

While titanium dioxide-treated mice exhibited punctuate intracellular staining for MMP-2 localizing to type II epithelial cells and bronchiolar epithelium, asbestos-treated mice exhibited a more diffuse and often extracellular localization over alveolar surfaces (Figure 36). MMP-2 also had a more protracted expression pattern, as it was located in both normal alveoli and particularly in fibrotic areas of lung at 7, 14, and 28 days. MMP-2 also localized to areas showing inflammation, as was seen for MMP-9. This localization corroborates our findings from gelatin zymography showing that MMP-2 is more predominant during development of fibrosis in the lung.

9.2. TIMPs ARE UPREGULATED IN ASBESTOS-EXPOSED LUNGS

The tissue inhibitors of metalloproteinases (TIMPs) are endogenous antiproteases directed against MMPs. While other functions for TIMPs are being identified, it is clear that these TIMPs have the ability to potently inhibit, and in some cases, activate MMPs through binding in 1:1 stoichiometry. Analysis of their abundance is therefore important when considering MMP activity. TIMP-1 and TIMP-2 are known to associate strongly with and inhibit MMP-9 and MMP-2, respectively. However, these TIMPs are not limited to these MMPs, and it is important to note that in the right local concentrations, TIMPs can essentially inhibit any MMP.

Lung homogenates from asbestos-exposed mice were subjected to western blotting for TIMP-1 and TIMP-2. Levels of both inhibitors increased over the timecourse of asbestos treatment (Figure 37). This may indicate a role in compensating for the increased gelatinases found in asbestosis. However, it may also indicate that these TIMPs are inhibiting the activity of other collagenases. The TIMP upregulation could therefore skew the profibrotic/antifibrotic balance towards the deposition of collagen.

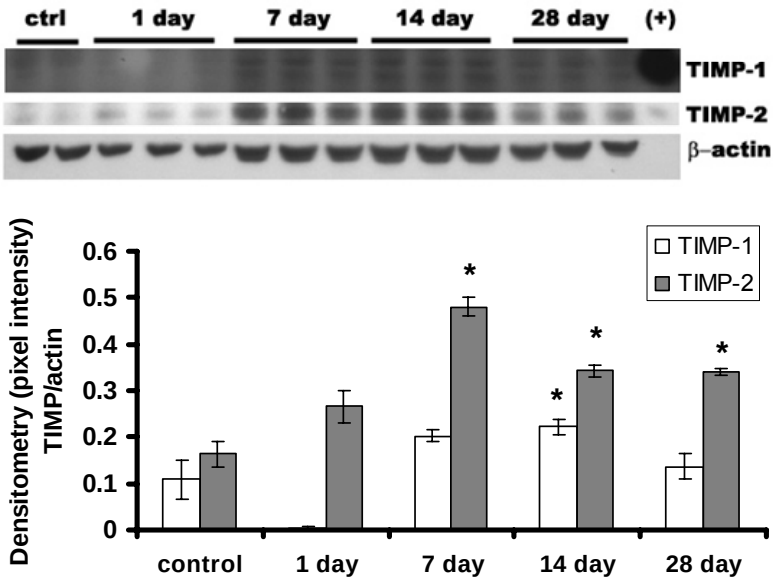

Figure 37. TIMP-1 and -2 are increased after asbestos exposure.

Western blotting was performed on soluble fraction (non-CHAPS-containing) lung homogenates (10 μg) from mice exposed to asbestos fibers. TIMP-1 (1:1,000 antibody dilution, purchased from Triple Point Biologics), TIMP-2 (1:200, Chemicon), and beta-actin (1:5,000, Sigma) were all probed from the same blot. * $p < 0.05$, one way ANOVA and Tukey's post test.

9.3. MMP INHIBITION ATTENUATES ASBESTOSIS

The drug GM6001 has been used *in vivo* by other investigators and was notably shown to inhibit both MMP activity and disease development in murine models of asthma (282) and emphysema (283). GM6001 is a reversible hydroxamic acid-based global MMP inhibitor. GM6001 was intraperitoneally injected (0.2 mg per mouse, ~8.8 mg/kg) every day over the course of 14 days, beginning on day 0. Mice were intratracheally instilled with asbestos on day 1 and sacrificed on day 13.

Daily doses of MMP inhibitor reduced the inflammation and lung damage found 13 days after asbestos. Although BAL fluid protein was not significantly different between asbestos/vehicle and asbestos/GM6001 mice, the mice with MMP inhibition did have a trend towards less protein in the BAL (Figure 38). Notably, while mice treated with asbestos had

significant elevations in the number of inflammatory cells in the BAL fluid, this inflammatory response was attenuated in asbestos-exposed mice treated with the MMP inhibitor (Figure 39). Differentials were performed on BAL fluid cytospins and revealed a significant increase in PMN in all asbestos-treated mice (Figure 40). Macrophages, on the other hand, were significantly decreased in all of these mice. However, the increase in PMN in the asbestos/GM6001 group is significantly attenuated in the airspaces of asbestos/GM6001 mice versus the asbestos/vehicle group.

MMP inhibition also ameliorated the development of pulmonary fibrosis. Measurements of total hydroxyproline were used as an indicator of collagen deposition in the lungs of mice treated with asbestos. Although both the asbestos/vehicle and asbestos/GM6001 groups exhibited significant increases in fibrosis compared to titanium controls, the asbestos/GM6001 group had a significant reduction (15%) in fibrosis compared to asbestos/vehicle ($P<0.01$, ANOVA with Tukey's post-test) (Figure 41). Therefore, inhibition of MMPs leads to a reduction in both inflammation and fibrosis in our experimental model of asbestosis.

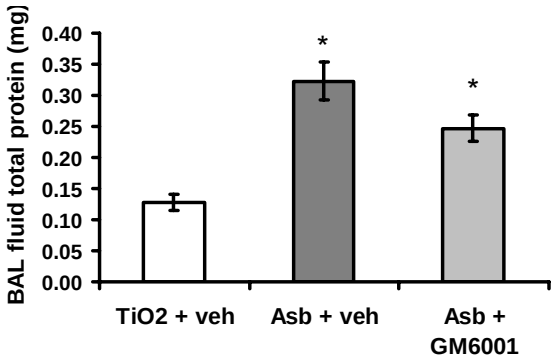

Figure 38. BAL fluid protein accumulation shows a trend to decrease after MMP inhibition.

Wild type mice were injected daily (i.p.) with vehicle (veh) or the broad-spectrum MMP inhibitor GM6001 beginning on day 0. Mice were exposed to asbestos (Asb) on day 1 and euthanized on day 13. BAL fluid protein was determined and found to be significantly increased over titanium controls in all asbestos treated mice, regardless of MMP inhibition. However, BAL fluid from the MMP inhibited mice had a trend towards lower protein accumulation. * $p < 0.05$ compared to TiO2 + vehicle group, one way ANOVA with Tukey's post test.

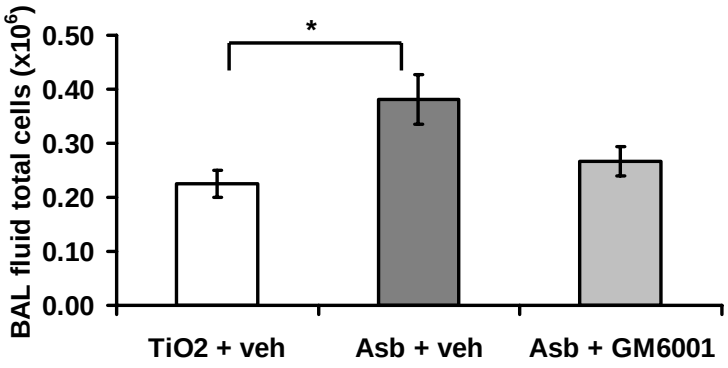

Figure 39. MMP inhibition reduces BAL fluid total cells after asbestos.

Mice were treated as in Figure 38. Although total BAL fluid cells in asbestos + vehicle group was increased compared to the titanium control, the cell counts were not significantly increased in the asbestos + GM6001 group compared to TiO2 + vehicle controls. * p < 0.05, one way ANOVA with Tukey's post test.

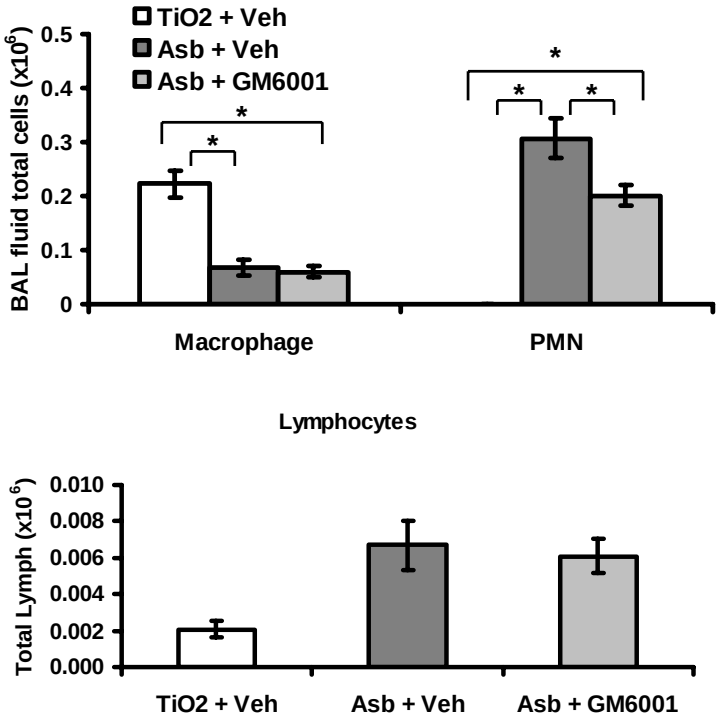

Figure 40. MMP inhibition reduces PMN numbers in BAL fluid.

Differentials counts of BAL fluid total cells were performed to determine total numbers of white blood cell types in the lung airspaces. Lymphocytes are shown on a separate graph due to their low overall numbers. After asbestos, macrophages are significantly decreased. PMNs and lymphocytes are increased in all mice treated with asbestos, but this increase is attenuated in MMP-inhibited mice. * p < 0.05, one way ANOVA and Tukey's post test.

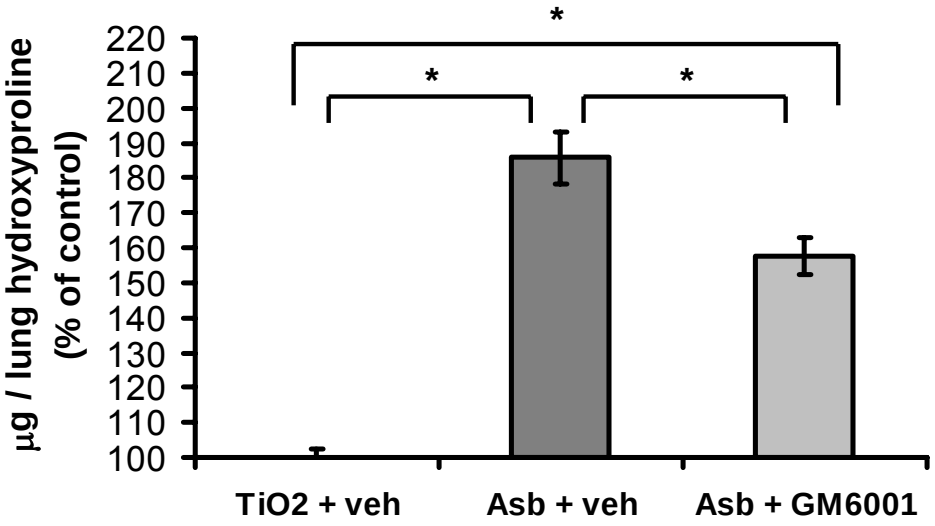

Figure 41. MMP inhibition attenuates fibrosis.

Mice were treated as in Figure 38. Lungs were recovered, acid hydrolyzed, and hydroxyproline analysis was performed on the hydrolysates. Values were expressed as % of control, with the TiO2 + vehicle controls equaling 100%. Daily injections of GM6001 significantly reduced fibrosis development at 13 days. * $p < 0.05$, one way ANOVA, Tukey's post test.

9.4. CONCLUSIONS

Matrix metalloproteinases (MMPs) have been implicated in both human idiopathic pulmonary fibrosis (76) and experimental models of pulmonary fibrosis, including bleomycin- (33) and silica-induced models (261). However, the MMPs have never been studied in the context of asbestosis. Previous *in vivo* studies utilized the less fibrogenic chrysotile fibers instead of amphiboles, and these investigators did not observe any fibrosis at 4 weeks (260). These studies also did not examine protein levels, relying on mRNA analysis instead. In this study, we sought to determine whether MMPs are increased in response to a single intratracheal instillation of amphibole (crocidolite) asbestos and what the role of MMPs are in the development of asbestosis.

We here describe increases in MMP-2 and MMP-9 after crocidolite asbestos instillation. MMP-9 was increased in lung homogenates only at day 1, but latent and active MMP-2 was increased over all timepoints (Figure 33). Importantly, the increase in active MMP-2 was particularly large at 7, 14, and 28 days, indicating potential for high proteolytic activity due to this MMP during the chronic fibrosis phase of this model. The latent forms of MMP-2 and -9 were also increased in airspaces, as sampled by BAL fluid (Figure 34). As in the lung homogenates, the most profound increase in MMP-9 was at day 1 while MMP-2 remained high after this timepoint.

Immunohistochemistry supported these results, as the strongest MMP-9 staining was found 1 day after asbestos while MMP-2 had a more protracted expression pattern (Figure 35). The MMP-9 localized to bronchiolar airspaces in conjunction with neutrophils and asbestos fibers. Since neutrophils can express this MMP (274), it is likely that these cells are the source of the MMP-9. Furthermore, it has been shown that asbestos fibers can induce the release of collagenases *in vitro*, although the collagenase was not identified (259).

MMP-2 in control mice was expressed in a few type II epithelial cells (Figure 36). After asbestos injury, staining was more diffuse over the alveolar septa, implying release from the cell. MMP-2 was also found in bronchiolar neutrophilic aggregates and most strikingly was observed throughout areas of fibrosis. MMP-2 is kown to be expressed by fibroblasts, which may explain this distribution. Furthermore, our results indicate that MMP-2 plays a significant role in the development of fibrosis in the lung, while MMP-9 activity appears to be important in the inflammatory component of the disease.

To determine whether endogenous inhibitors were upregulated in conjunction with or as a compensatory response to these proteases, tissue inhibitor of metalloproteinase (TIMP) levels

were examined using western blotting (Figure 37). These studies focused on TIMP-1 and TIMP-2, which are known to most efficiently inhibit MMP-9 and MMP-2, respectively. While these TIMPs were expressed at low levels in controls and at 1 day post-asbestos exposure, large increases in these inhibitors were found at 7 and 14 days with a lesser increase at 28 days. Other investigators have found similar upregulation of TIMPs at later stages of non-asbestos models of fibrosis with TIMP-2 being especially highly expressed (33, 76, 257). While it was proposed that TIMPs opposed the collagenolytic activity of MMPs, thus leading to a profibrotic environment (284), it is also possible that TIMP-2 participates in the activation of MMPs. TIMP-2 is known to associate with MMP-2 and lead to its activation by a separate membrane bound MT-MMP1 (228, 258).

MMP inhibition has been used as an experimental therapy in animal studies of a number of pulmonary diseases, including asthma (282), emphysema (283), and bleomycin-induced pulmonary fibrosis (28). We utilized a broad spectrum MMP inhibitor, GM6001, using daily intraperitoneal injections to attempt to ameliorate disease. These studies indicate that MMP inhibition significantly protected against asbestos-induced lung injury by inhibiting both inflammation and fibrosis.

While these results may seem counterintuitive, as MMP degradation of ECM components such as collagen may oppose fibrosis development, other investigators have found similar protection with MMP inhibition in other models of fibrosis (28). Our findings suggest that one mechanism by which MMP inhibition is protective is by dampening of inflammatory responses to asbestos. Based on our zymography and immunohistochemistry, inhibition of MMP-9 could inhibit inflammation, perhaps through reduction of basement membrane degradation and subsequent migration of inflammatory cells. However, it should be noted that in the bleomycin

model, MMP-9 null mice were not significantly protected from fibrosis and only had an observed deficit in alveolar bronchiolization (219). This does not rule out that MMP-9 activity is pathogenic in asbestosis as there are no published reports examining this injury in MMP-9 knockout mice.

On the other hand, MMP-2 was predominantly associated with fibrosis instead of inflammation. Inhibition of this MMP could directly reduce the migration of fibroblasts in the lung and reduce fibrosis. The role of this MMP could be studied with MMP-2 knockout mice.

Broad spectrum MMP inhibition could exert other effects which require further studies to evaluate. MMP inhibition could reduce MMP-7 activity, which is highly proinflammatory in the lung (29, 244). Inhibition of MMPs could also reduce the production of collagen fragments, which are potent chemoattractants for neutrophils (206). MMPs could also play a role in regulating the localization of the antioxidant enzyme EC-SOD, a possibility that is examined in further detail in Chapter 10. Furthermore, it must be noted that GM6001 is a broad spectrum inhibitor, and also inhibits members of the ADAM (A Disintigrin and Metalloproteinase) family.

In conclusion, we observed large increases in MMP-2, MMP-9, TIMP-1, and TIMP-2 in the course of experimentally-induced asbestosis in mice. While MMP-9 appeared to be related to inflammation in the lung, MMP-2 was more strongly associated with development of fibrosis. MMP inhibition reduced both inflammation and fibrosis, and revealed a contributory role for these MMPs in antioxidant regulation. These studies reveal a pathogenic role for MMPs in asbestosis and suggest a potential role in other particulate lung diseases. These studies also indicate that a mechanism must exist to lead to MMP upregulation in asbestosis and other fibrotic lung diseases. The role of EC-SOD in this upregulation will be evaluated in the following chapter.

10. RELATIONSHIP BETWEEN EC-SOD AND MMP UPREGULATION

While the studies described in Chapters 5 and 9 indicate that both EC-SOD and MMPs are altered in either localization or abundance in asbestosis, it remains to be seen whether the events are directly connected. That is, whether changes in EC-SOD affect MMPs and vice versa. This question is relevant because MMPs are known to be activated by reactive oxygen species. Since EC-SOD is depleted from the lungs of mice exposed to asbestos, the resulting increased oxidative stress could activate MMPs. Furthermore, clearance of EC-SOD is associated with cleavage of the protein's heparin binding domain. The protease responsible for this cleavage *in vivo* in pulmonary fibrosis is unknown. MMPs are highly upregulated in this disease and can therefore potentially proteolyze EC-SOD. The colocalization of EC-SOD with collagen (172), a substrate for many MMPs, further strengthens this idea.

It was hypothesized that EC-SOD and MMPs are related in function and localization in pulmonary fibrosis. To examine this question, the timecourse of EC-SOD and MMP upregulation in both the bleomycin and asbestos models of pulmonary fibrosis were examined. The role that EC-SOD plays in MMP activity through the use of EC-SOD knockout mice was then assessed. The role of MMPs in pulmonary EC-SOD regulation was determined with MMP inhibition.

10.1. EC-SOD AND MMP CHANGES COINCIDE IN PULMONARY FIBROSIS

The localization and relative levels of EC-SOD and MMPs in the asbestos model was described in Chapters 5 and 9, respectively. EC-SOD is depleted from lungs beginning at 24 hours and remains depleted until at least 28 days (Figure 12 and Figure 15). Coincident with this loss is accumulation of EC-SOD in the airspaces at the same timepoints (Figure 14 and Figure

16). As described in Chapter 9, MMPs are increased at the same time that these EC-SOD localization changes are observed. Specifically, MMP-9 and active MMP-2 are increased at 24 hours, with MMP-2 remaining at high levels at 7, 14, and 28 days (Figure 33 and Figure 34). The simultaneous occurrence of these events suggests a possible relationship between EC-SOD localization and MMP upregulation in asbestosis.

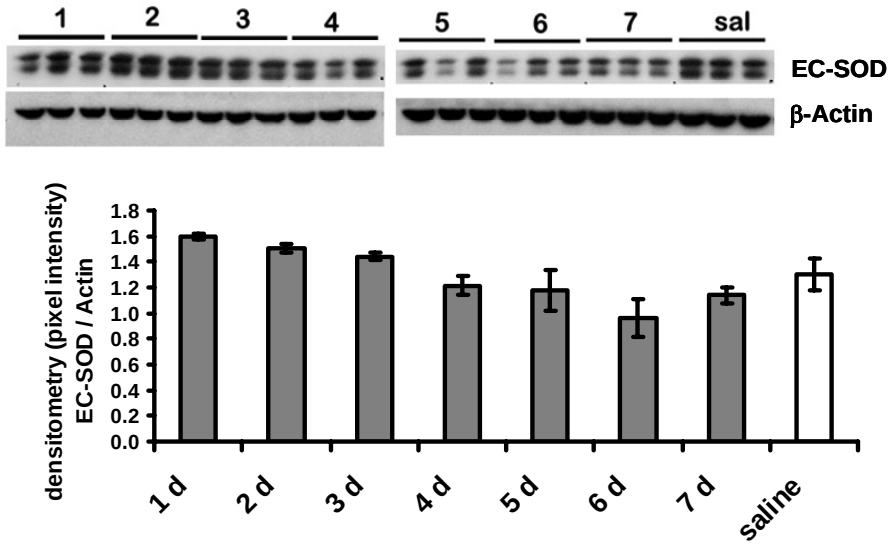

Figure 42. Timecourse of EC-SOD depletion from the lung after bleomycin treatment.

Western blots were performed for EC-SOD on lung homogenates (10 μg) from mice intratracheally instilled with saline vehicle (sal) or with bleomycin (0.06 U/mouse). Mice were sacrificed every day for 7 days. Densitometry was performed and normalized to β-actin as a loading control.

In a bleomycin model of fibrosis, the relationship between EC-SOD and MMPs was further examined. In these experiments, mice were given a single intratracheal instillation of bleomycin and sacrificed every day for seven days. This detailed timecourse revealed that depletion of EC-SOD from the lung (Figure 42) and accumulation in the BAL fluid (Figure 43) coincided with upregulation of MMPs (Figure 44), beginning at 3-4 days and continuing to at least 7 days. The fact that these events are simultaneous in two models of pulmonary fibrosis

suggests that they may be related events. Notably, PMNs were also increased at the same time as EC-SOD redistribution and MMP upregulation in the bleomycin model (Figure 45) and at all timepoints tested in the asbestos model (Figure 7) and may be the common link between these proteins. As noted above, PMNs are a source of both EC-SOD and MMPs (184, 276, 285).

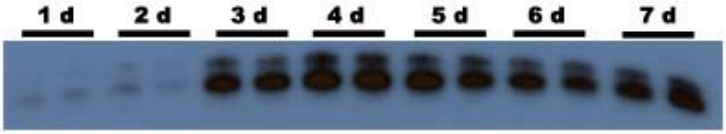

Figure 43. Timecourse of EC-SOD accumulation in BAL after bleomycin.

Western blots were performed for EC-SOD in BAL fluid from mice treated with 0.06 U bleomycin and sacrificed over a 7 day timecourse. Equal volumes (5 μL) of BAL fluid were loaded for this blot.

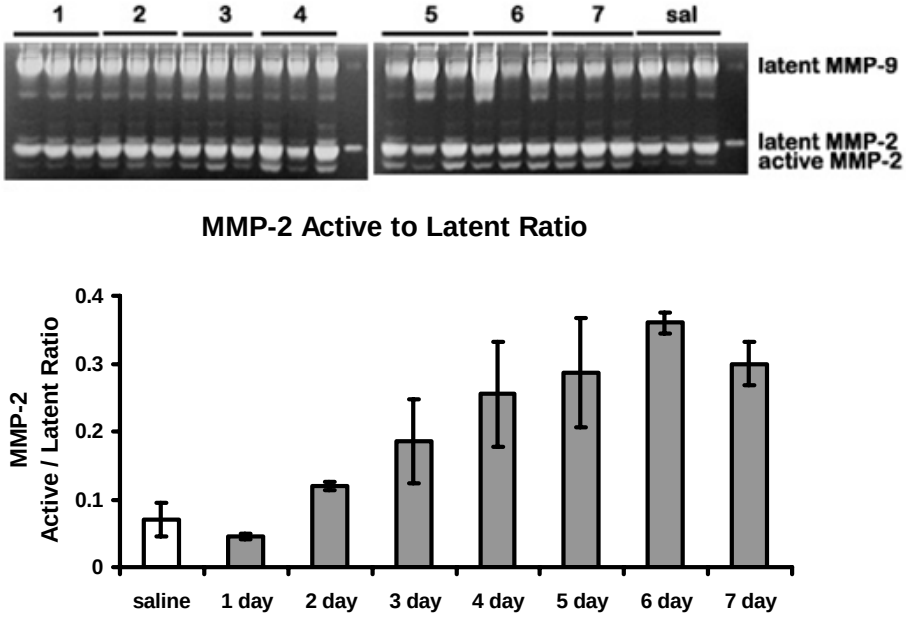

Figure 44. Gelatinase activity in mice after exposure to bleomycin.

Gelatin zymography was performed on CHAPS-extracted lung homogenates (30 μg) from the same mice described in Figure 42 and Figure 43. While no significant changes in MMP-9 were detected, levels of active MMP-2 did increase beginning at day 2-3. Densitometry data is expressed as pixel intensity of active MMP-2 divided by intensity of latent MMP-2.

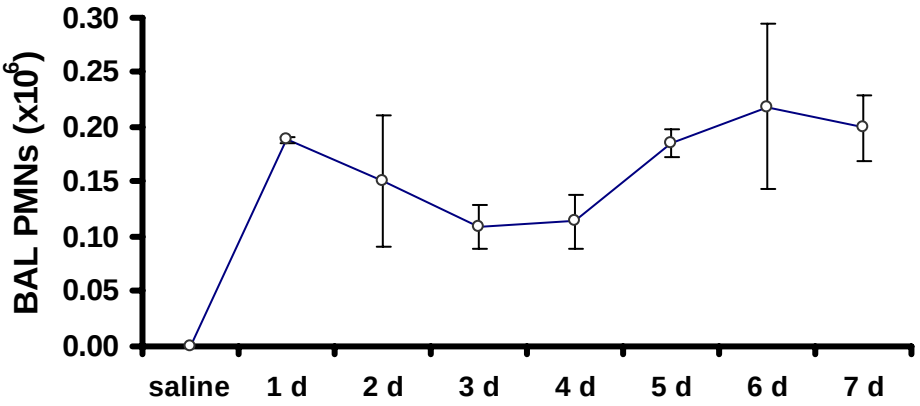

Figure 45. PMNs in BAL fluid after bleomycin.

BAL fluid was recovered from mice during a 7 day timecourse after bleomycin instillation (0.06U/mouse). PMNs were counted from cytospins of the BAL, and differential counts were multiplied by the total number of cells in the BAL to get absolute numbers of PMNs. N=3 for each timepoint.

10.2. EC-SOD KNOCKOUTS AND MMP ACTIVITY

To definitively test whether EC-SOD is involved in the observed changes in MMPs, pulmonary fibrosis was induced in EC-SOD knockout mice. EC-SOD knockout mice were examined in the asbestos model for MMP activity. Using gelatin zymography as an indicator of MMP-2 and -9 activation, no differences could be found in MMP-2 or MMP-9 at 1, 7, 14, or 28 days post asbestos exposure in the lung (Figure 46) or BAL fluid (Figure 47). This does not rule out effects earlier than 24 hours, however, as those timepoints were not yet tested. The largely negative effects of EC-SOD deficiency on MMP activity suggest that there is not a direct effect on these proteases by EC-SOD in asbestosis. However, it is possible that wild type mice already have maximal activation of MMPs and that knockout mice cannot develop increased activation. More complete studies would require testing of EC-SOD transgenic overexpressors to determine if MMP activity is decreased. Unfortunately, these mice were not available at the time of these experiments and must instead be studied in future directions.

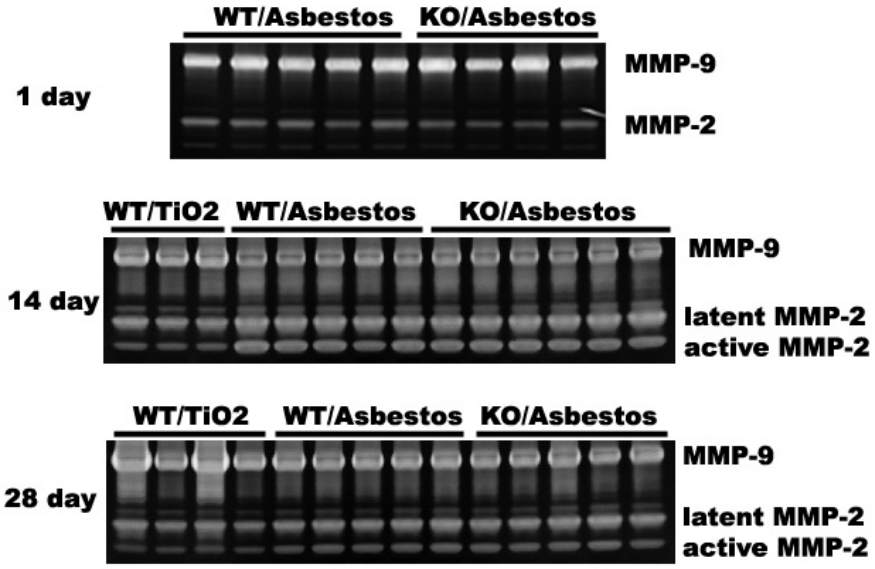

Figure 46. Lung homogenate MMP activity in EC-SOD knockout mice treated with asbestos.

Gelatin zymograms were performed on CHAPS detergent-extracted lung homogenates (equal protein loaded, 15 μg) from wild type and EC-SOD knockout mice treated with 0.1 mg crocidolite asbestos and euthanized at the timepoints indicated. Although MMPs increase in asbestos mice compared to titanium controls, there was no difference in MMP-2 or -9 levels in knockouts versus wild types when both were treated with asbestos.

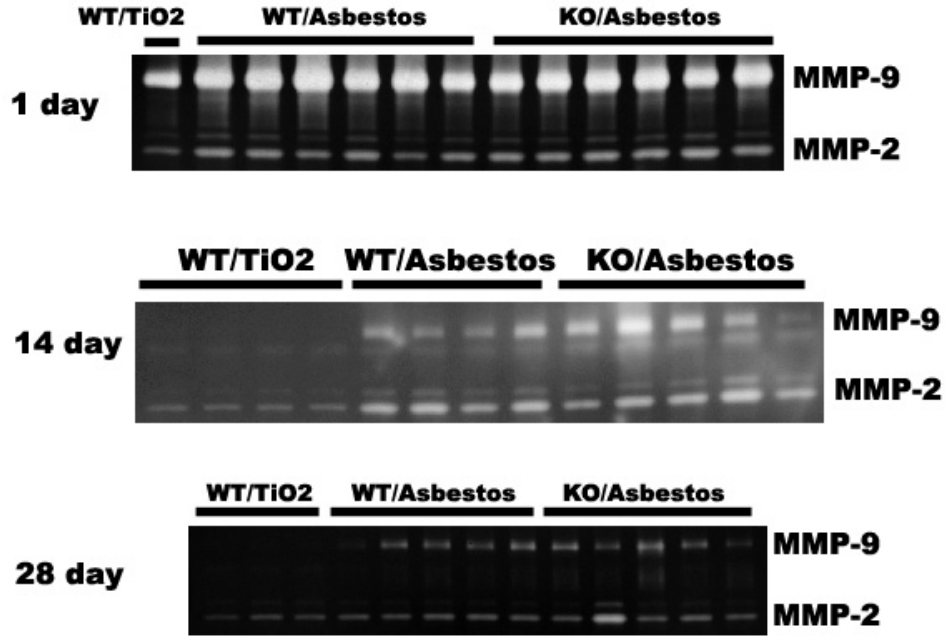

Figure 47. BAL fluid MMP activity in EC-SOD knockout mice treated with asbestos.

Gelatin zymograms were performed on BAL fluid (equal protein loaded, 2 μg) from wild type and EC-SOD knockout mice treated with 0.1 mg crocidolite asbestos and euthanized at the timepoints indicated. No differences were observed in either MMP-2 or -9 comparing wild type and knockout mice treated with asbestos.

In the bleomycin model, initial studies found no difference in gelatinase activity 7 days after treatment in either the lungs or BAL fluid (Figure 48 and Figure 49). However, when earlier timepoints were examined, a significant increase in MMP-9 was detected in BAL fluid at 1 day in knockouts versus wild types. This upregulation of MMP-9 was associated with an increase in PMN infiltration into the lung airspaces at 24 hours in knockout mice (Figure 50). As PMN can produce MMP-9 (274), this shows that EC-SOD can have an indirect effect to increase MMP-9 levels through increases in inflammation.

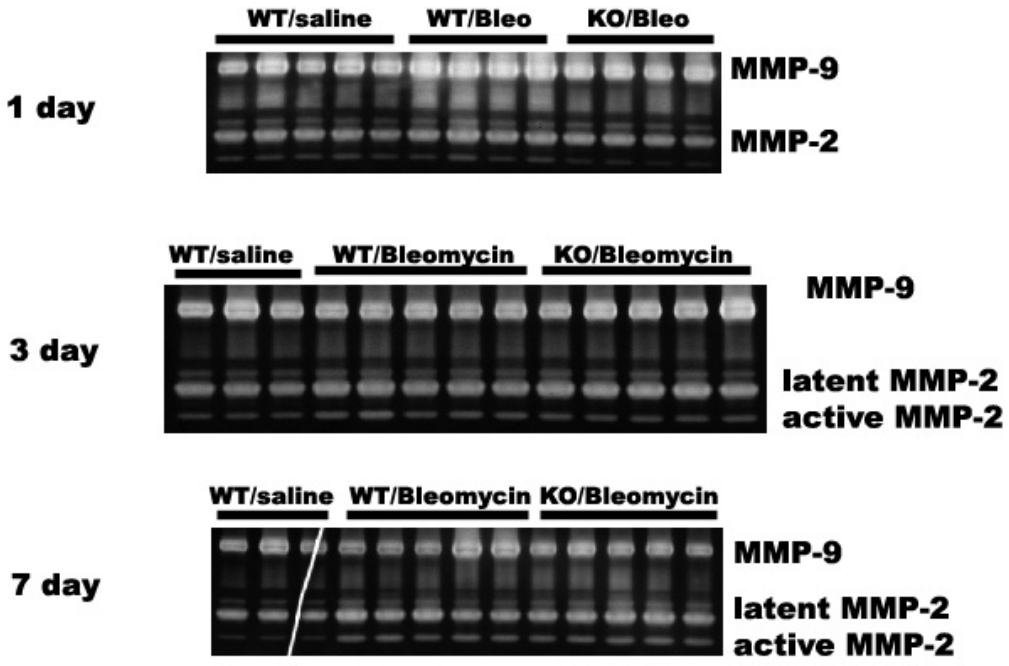

Figure 48. EC-SOD knockout mice do not have differences in MMP activity in lung homogenates after bleomycin treatment

Lungs were recovered from wild type and EC-SOD knockout mice at the times indicated after intratracheal bleomycin (0.06U/mouse) instillation. Gelatin zymography was performed on equal protein amounts (15 μg) of CHAPS-extracted lung homogenates. No significant differences were observed or measured by densitometry between wild type mice and knockout mice treated with bleomycin.

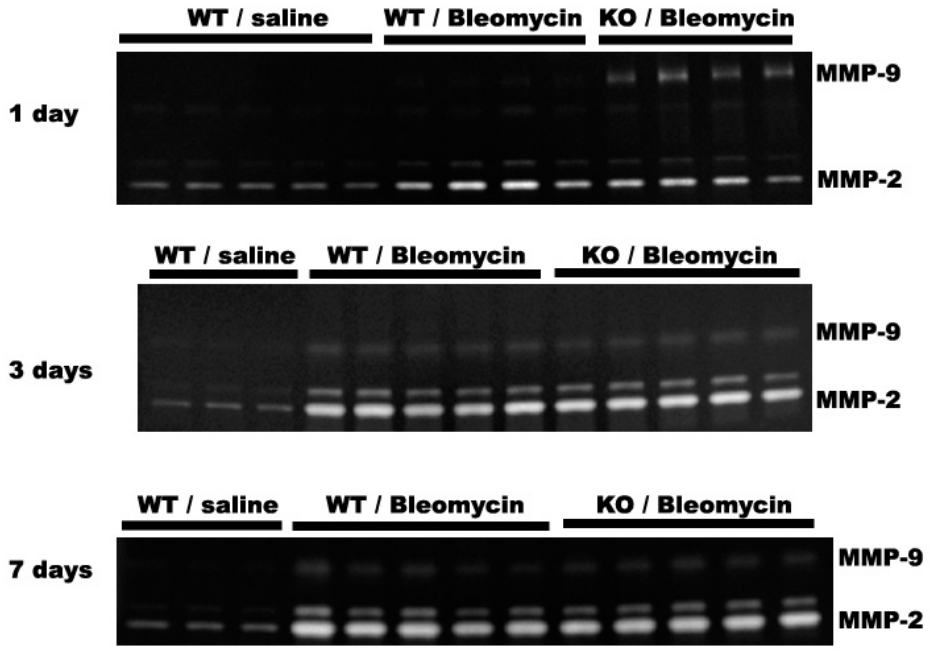

Figure 49. EC-SOD knockouts have increased MMP-9 but not MMP-2 at 24 hours after bleomycin.

Gelatin zymography was performed on equal protein amounts (5 μg) of BAL fluid recovered at the times indicated after intratracheal bleomycin (0.06 U/mouse) instillation. Note the increase in MMP-9 in knockout mice at 1 day. No other differences between bleomycin-treated wild types and knockouts were observed

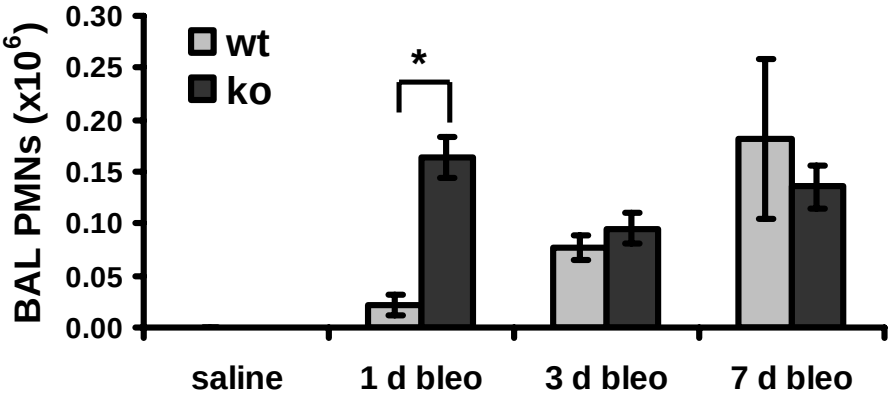

Figure 50. EC-SOD knockout mice have increased PMNs at 1 day post-bleomycin exposure.

PMNs were counted in BAL fluid at the times indicated after bleomycin treatment (0.04 U/mouse) in wild type (wt) and EC-SOD knockout (ko) mice. There are significantly more PMNs at 1 day after bleomycin in ko vs wt. * $p < 0.05$, one-way ANOVA and Tukey's post test comparing saline and 1 day bleomycin values.

10.3. MMP INHIBITION IN ASBESTOSIS

MMPs were examined for their ability to regulate the localization of EC-SOD. Since numerous MMPs could theoretically be involved in this regulation, we chose to use a broad-spectrum global MMP inhibitor (GM6001) in our asbestos studies. These studies were described in Chapter 9.3. Western blotting was performed for EC-SOD in the BAL fluid of mice exposed to asbestos with or without MMP inhibitor treatment (Figure 51). Although EC-SOD is increased in the asbestos + vehicle group compared to the titanium dioxide group, there was no significant increase in the asbestos + GM6001 group. The GM6001 group also displayed significant decreases in PMN infiltration . Our pneumonia studies indicated that PMNs are the predominant source of the EC-SOD that accumulates in the airspaces (Figure 40). Thus, these results suggest that MMPs regulate the localization of EC-SOD in the airspaces through reduction of PMN-dominated inflammation after asbestos.

10.4. CONCLUSIONS

Links between EC-SOD and matrix metalloproteinases have not been previously examined, particularly in the case of asbestos lung injury. It is thought that both oxidant/antioxidant and protease/antiprotease imbalances are involved in the development of pulmonary fibrosis. Reactive oxygen species can affect MMPs through oxidation of the cysteine switch in the proenzyme leading to activation. Furthermore, protease/antiprotease imbalances could lead to the clearance of EC-SOD from lung parenchyma through proteolysis of the heparin-binding domain. It was hypothesized that EC-SOD and MMPs are related in function and localization in pulmonary fibrosis. These studies utilized both the asbestos- and bleomycin-models of pulmonary fibrosis to evaluate this possibility.

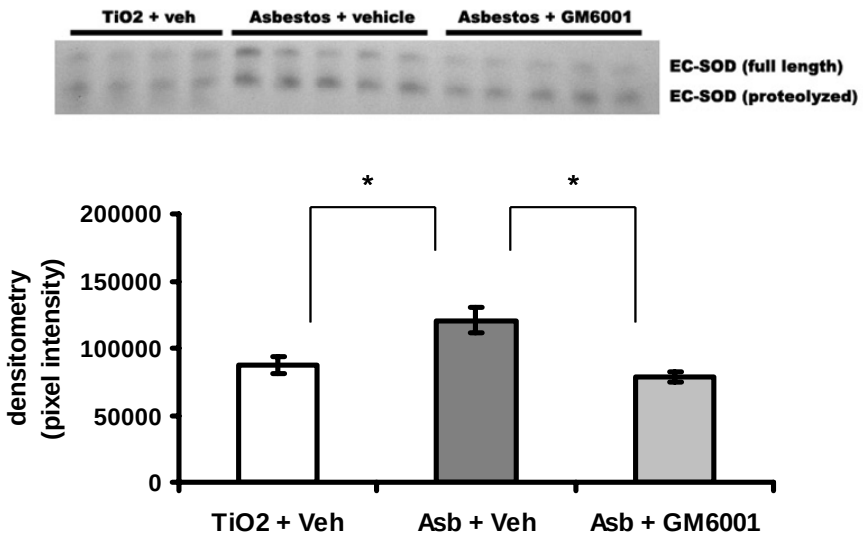

Figure 51. MMP inhibition reduces airspace accumulation of EC-SOD.

Mice were intratracheally instilled with 0.1 mg titanium dioxide or asbestos. Concurrently, one group was treated with daily intraperitoneal injections of 0.2 mgGM6001, a broad spectrum MMP inhibitor, beginning the day before intratracheal instillation. Mice were sacrificed at day 13 and BAL fluid collected. EC-SOD was evaluated by western blotting loading equal protein amounts of BAL fluid (5 μg). The Asbestos+GM6001 group accumulated less EC-SOD in BAL fluid than the Asbestos+Vehicle group. * $p < 0.05$, one way ANOVA with Tukey's post test.

In support of this hypothesis, it was found that the asbestos- or bleomycin-induced depletion of EC-SOD from the lung parenchyma in wild type mice was associated with increases in active MMP-2 in lung homogenates at the same time in two models of pulmonary fibrosis (Figure 42 and Figure 44; Figure 11, Figure 15, and Figure 33). Loss of EC-SOD may increase oxidative stress in the lung and lead to oxidative activation of latent MMP-2. Although we also know that EC-SOD accumulates in the airspaces, we did not observe any differences in airspace MMP activation. The caveat to this finding is that in general the active MMPs are not found in the BAL fluid. From these experiments in wild type animals we therefore cannot determine whether the airspace accumulation of EC-SOD has a direct effect on preventing MMP activation in the airspace. However, the studies in EC-SOD knockout mice also did not reveal additional MMP activation in the BAL fluid, indicating that airspace EC-SOD has negligible effects on

MMPs in that location. While simultaneous alterations of EC-SOD and MMPs do not prove an association between the two proteins, it does suggest that they may be related in regulation.

To more directly test the role of EC-SOD in MMP activation, pulmonary fibrosis was induced in EC-SOD knockout mice. In the asbestos model, although MMPs were always increased after exposure, we did not find any differences in MMP-2 and MMP-9 when knockout mice were compared to wild type mice at 1, 14, and 28 days in either the BAL fluid or lung homogenates (Figure 46 and Figure 47).

The bleomycin model also revealed largely negative effects of EC-SOD on MMPs. However, at 24 hours after bleomycin injury, a significant increase was found in BAL fluid MMP-9 in knockouts versus wild types at 24 hours (Figure 49). This increase was associated with a significant increase in PMNs in the knockout mice over the wild type mice that was not present at later timepoints, suggesting that these PMNs are the source of the MMP-9 (Figure 50). Overall, we found that EC-SOD does not have a direct effect on MMP activation but can have a modulatory role on inflammation that leads to differential MMP expression.

To examine the converse question of whether MMPs play a role in EC-SOD localization, we treated wild type mice with asbestos and a global MMP inhibitor, GM6001. Treatment with this inhibitor reduced asbestos disease severity, including a decrease in neutrophil influx and fibrosis (Figure 40 and Figure 41). In addition levels of airspace EC-SOD were reduced, suggesting that airspace EC-SOD is regulated by MMPs, likely due to the influx of PMNs.

The data presented above indicate a central role for inflammation in the regulation of both EC-SOD and MMPs in pulmonary fibrosis. When EC-SOD is absent from the lungs, greater inflammation is observed after challenge. These findings not only apply to our models of pulmonary fibrosis, but to other pulmonary injuries such as hyperoxia, oil fly ash, LPS-induced,

and hemorrhage induced lung damage (197, 199, 201, 286). It has been proposed that these increases in inflammation are related to effects on TNF-α and vascular endothelial selectins, two factors critical to leukocyte infiltration into the lung. In the bleomycin model, an increase in MMP-9 is found at 24 hours in knockout mice compared to bleomycin- or saline-treated wild type mice. Since MMP-9 can be released from PMNs (274), it is likely that these cells are releasing MMP-9 into the airspace. Therefore EC-SOD can decrease levels of MMP-9 in the lung by antagonizing influx of PMNs.

It is unexpected that the asbestos model does not follow the same pattern as the bleomycin model. No increases in MMP-9 are noted at 1 or 28 days in the airspaces of EC-SOD knockout mice in spite of increases in PMN at these timepoints compared to wild type mice. It is possible that the bleomycin effect is an acute one, and that increased MMP-9 appears earlier in asbestos injury at a timepoint before 24 hours. Also, the bleomycin experiment in EC-SOD knockouts showed only a small increase in MMP-9 activity at a time (1 day) when the wild type mice had no MMP-9 at all. In the asbestos model, there is a large amount of MMP-9 in both wild type and EC-SOD knockout mice after exposure. A small increase in MMP-9 might be obscured by the larger overall increases observed.

The higher level of MMP-9 in EC-SOD knockout mice could indicate a role for MMP-9 in the greater inflammation and fibrosis observed in these mice. MMP-9 could be used by the inflammatory cells in migration into the lung. Our studies showing that MMP inhibition reduces inflammation support this idea. Although studies by Betsuyaku et al., shows that MMP-9 null mice are not protected from bleomycin-induced pulmonary fibrosis (219), it is possible that other MMPs compensate for loss of MMP-9. The role of MMP-9 as either a contributor or bystander to lung injury remains to be determined.

Inflammation also appears to play a role in EC-SOD localization, as MMP inhibition reduces both inflammation and EC-SOD accumulation in the BAL fluid. Our results from Chapter 6 showed that inflammatory cells are a major source of this antioxidant in the airspaces in pulmonary fibrosis. Other investigators have also indicated that inflammatory cells can produce EC-SOD (184). The significance of this loss of EC-SOD from the airspaces is unclear since mice given the MMP inhibitor are protected from disease. Although we had proposed that airspace EC-SOD is protective against inflammation-induced lung damage, it is possible that airspace EC-SOD is pathogenic by a function not previously described. In all likelihood however, decreases in airspace EC-SOD after MMP inhibition simply reflects the fact that fewer leukocytes are in the airspace to release it. Protection may be achieved from overall reduction in inflammation. Nevertheless, these results indicate that EC-SOD localization can be influenced by MMP inhibition indirectly through modulation of inflammation.

11. DISCUSSION AND FUTURE DIRECTIONS

Idiopathic pulmonary fibrosis and asbestosis are debilitating lung diseases characterized by a progressive disease course and poor prognosis. The only known cure for these diseases is lung transplantation, a treatment limited by the availability of donated organs and the complications inherent in organ transplantation. Enhanced understanding of the pathogenesis of this disease would aid in the development of more conventional therapies for pulmonary fibrosis. Based on evidence in humans and in experimental models, it is thought that both oxidant/antioxidant and protease/antiprotease imbalances are critical to the development of pulmonary fibrosis. In our study, we examined the regulation of the EC-SOD antioxidant and the matrix metalloproteinases in animal models of pulmonary fibrosis. EC-SOD is abundant in the lung and is known to be protective in a variety of lung injury models. It localizes to the extracellular matrices of the lung due to the presence of a heparin-binding domain that confers affinity for the matrix. Clearance of EC-SOD from the lung parenchyma has been observed in disease states, likely due to cleavage of this domain. While the *in vivo* protease responsible for this event in pulmonary fibrosis is unknown, it is known that members of the MMP family of proteases are upregulated in the disease process and could therefore contribute to this regulation of EC-SOD.

It was hypothesized that depletion of EC-SOD from the lung and interrelated increases in MMP activity contribute to the development of pulmonary fibrosis. To examine this hypothesis, an asbestos model was characterized that closely resembled human IPF histopathologically. We found that EC-SOD is depleted from the lung parenchyma and accumulates in the airspaces after induction of lung injury in this model. MMPs were increased in both lung parenchyma and airspaces in response to asbestos. Our studies also determined that the presence of inflammation could in part explain these alterations in EC-SOD localization and MMP activity.

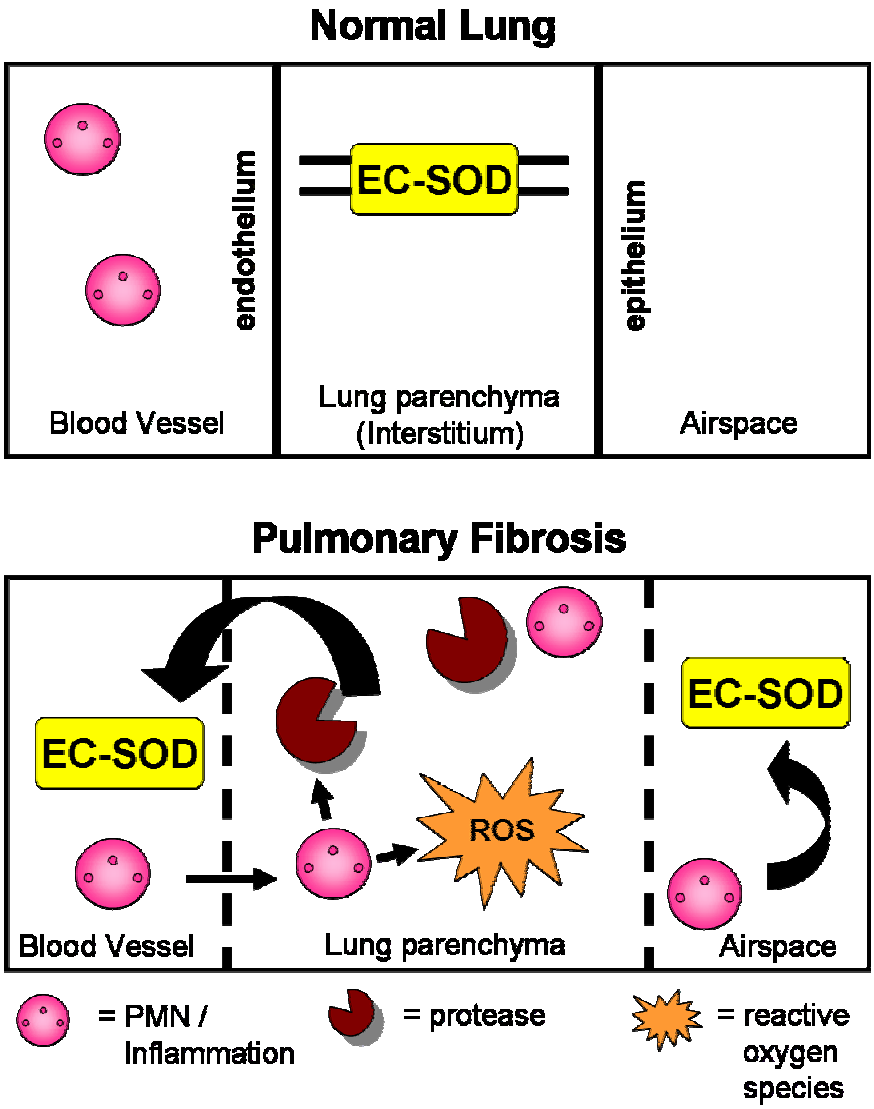

Figure 52. Model for regulation of EC-SOD in lung in pulmonary fibrosis.

The normal lung (top) has intact vascular endothelium and alveolar epithelium. EC-SOD with its heparin-binding domains sticks to the extracellular matrix of the lung parenchyma (interstitium) and protects the lung from oxidative stress. Inflammatory cells are not present in the lung but circulate in the bloodstream.

In pulmonary fibrosis (bottom), endothelial and epithelial permeability increases and the interstitium expands due to edema or fibrosis. Inflammatory cells emigrate into the parenchyma, releasing proteases and ROS. Resident macrophages, epithelium, and fibroblasts can also release proteases and ROS. The heparin-binding domain of EC-SOD is cleaved, and EC-SOD either diffuses into the plasma or is proteolyzed, increasing susceptibility of the lung parenchyma to oxidative stress and potentially leading to propagation of inflammation. It was also shown that EC-SOD expression is decreased after asbestos, which may further contribute to decreased lung parenchymal levels. Inflammatory cells that have reached the airspaces release EC-SOD into the alveolar lining fluid which could help to prevent further inflammation.

11.1. EC-SOD LOCALIZATION IN ASBESTOSIS

These studies first characterized an asbestos-induced model of pulmonary fibrosis that more closely simulates the development of asbestosis and IPF than the more common bleomycin method. In this model, airspace and interstitial inflammation progressed to interstitial fibrosis. We found that EC-SOD was depleted from the lung parenchyma in a sustained fashion throughout the inflammatory and fibrotic phases of the disease. Concurrently, EC-SOD accumulated in the BAL fluid. Although the origin of the airspace EC-SOD was unknown, our findings initially suggested that EC-SOD that was removed from the lung parenchyma redistributes into the airspaces.

In order to determine the source of this EC-SOD, experiments were performed in a model of airspace inflammation that is not complicated by the presence of interstitial inflammation or matrix remodeling. It was observed in this bacterial model that EC-SOD accumulated in the airspaces in the absence of depletion from the lung parenchyma. These studies revealed that airspace EC-SOD is likely due to the airspace inflammation and not the redistribution from the lung parenchyma. This was confirmed by the presence of only mouse EC-SOD in the airspaces of asbestos-treated transgenic mice expressing the human form of EC-SOD in the lung. This is a major advance in the understanding of the regulation of EC-SOD in lung disease as it has not been previously demonstrated that inflammation is responsible for transport and release of EC-SOD in the lung airspaces. In addition, this model demonstrated that interstitial processes such as inflammation and matrix remodeling are responsible for the clearance of EC-SOD from the lung parenchyma. These processes are unique to pulmonary fibrosis and cannot be recapitulated with airspace inflammation alone. Our overall understanding of the regulation of EC-SOD in pulmonary fibrosis is modeled in Figure 52.

11.1.1. EC-SOD depletion from the lung parenchyma

Proteolytic cleavage and decreased mRNA expression is likely responsible for the depletion of EC-SOD from the lung parenchyma. The heparin-binding domain is unique to this isoform of SOD and is particularly sensitive to cleavage by a number of proteases (176). It has been shown that the half-life of EC-SOD in tissues dramatically decreases when its heparin-binding domain is cut (287). Decreased expression of EC-SOD has not been previously demonstrated in interstitial lung injuries, indicating that asbestos has unique effects on the expression of this antioxidant.

Loss of EC-SOD should increase oxidative stress in the lung parenchyma as EC-SOD is the major extracellular antioxidant enzyme in the lung. The functional consequence of this may be to contribute to the progression of the disease. Indeed, when EC-SOD knockout mice were challenged with asbestos, they developed worse inflammation and fibrosis compared to similarly treated wild type mice. This mechanism of increased oxidative stress through removal of EC-SOD from the lung parenchyma demonstrates the importance of antioxidant protection in pulmonary fibrosis and suggests that antioxidants may be viable treatment modalities for patients with IPF.

11.1.1.1. Future Directions: Protease Inhibition

Since EC-SOD is protective in asbestos- and bleomycin-induced lung injury, methods by which to facilitate retention of EC-SOD in the matrix may be therapeutic. As proteolytic removal of the heparin-binding domain is the most likely mechanism for EC-SOD clearance from tissues, protease inhibition may be an effective method to achieve this goal. Experiments aimed at determining which protease or proteases are cleaving EC-SOD *in vivo* are currently being performed. Unfortunately, the positively-charged heparin-binding domain is particularly

sensitive to cleavage and has been shown to be cut by many different classes of proteases *in vitro*. Therefore, protease inhibition *in vivo* will have to target numerous proteases in order to be successful. Dichloroisocoumarin, E-64, and GM6001 or 1,10-phenanthroline as inhibitors of the serine, cysteine, and metallo-proteases, respectively, are being tested in conjunction with asbestos treatment in mice. Prevention of EC-SOD removal from the lung with any of these inhibitors would indicate that a particular class of proteases contains the enzyme responsible for proteolysis. More specific inhibitors can then be applied in these experiments. Unfortunately, it should be noted that complete protease inhibition can be difficult to achieve *in vivo*. Negative results could either mean that the proteases inhibited play no role in the endpoint being examined, or that the inhibitor was not delivered at the optimal concentration or cannot gain access to the correct location. Furthermore, toxicity of the inhibitors complicates these experiments as many proteases are involved in normal homeostatic processes such as coagulation. Depending on the target protease, the side effects of inhibition will likely decrease as more specific inhibitors are utilized.

To circumvent problems with pharmacologic inhibition of proteases, we are also assessing EC-SOD clearance in mice that are knockouts for various proteases. In collaboration with Dr. Wendy Mars, we have already examined this question in mice that do not express plasminogen (the precursor to plasmin), urokinase plasminogen activator, and tissue plasminogen activator. MMP-9 knockout mice have also been examined. So far, no single knockout mouse has been shown to prevent the loss of EC-SOD during the development of pulmonary fibrosis. These studies are continuing with mice that are null for MMP-7, an important MMP that is upregulated highly in IPF. This MMP can cleave syndecans in the extracellular matrix. Syndecans bind to heparan sulfate, to which full-length EC-SOD can

adhere. MMP-7 may cut syndecans in the extracellular matrix, leading to clearance of the syndecans and associated EC-SOD from the lung parenchyma. Furthermore, MMP-7 could directly proteolyze the heparin-binding domain of EC-SOD or could facilitate cleavage by another protease through release of syndecans from the matrix.

11.1.1.2. Future Directions: Effects of EC-SOD on inflammation in asbestosis

The mechanisms of EC-SOD's modulation of inflammation are not completely understood. One investigation found that EC-SOD is related to the expression of TNF-alpha and endothelial selectins after LPS-injury in the lung (201). Additional studies of other cytokines such as IL-1 and IL-6 and chemokines such as KC (IL-8 in humans) and their changes in response to loss of EC-SOD are warranted.

It is also known that type I collagen can be fragmented by exposure to reactive oxygen species (277). EC-SOD has been shown to co-localize with type I collagen in the lung (172). It has been demonstrated that EC-SOD can directly bind to and protect collagen from oxidative fragmentation *in vitro* (174), and EC-SOD knockout mice have increased levels of oxidative collagen fragmentation in the lung *in vivo* (204). Collagen fragments can be chemoattractants and activators of PMNs (205, 206). Examination of oxidative fragmentation of collagen through measurement of oxidized proline residues by HPLC will be performed in our asbestos model. Higher levels would indicate a potential role in PMN chemotaxis. The role of collagen fragments *in vivo* would be tested with commercially available antibodies that block PMN cell surface receptors for collagen, such as β1 integrins or discoidin domain receptor 1 (288, 289). Preliminary data in our lab shows that these antibodies block PMN chemotaxis to oxidized collagen *in vitro*.

11.1.2. EC-SOD accumulation in airspaces

Our data in the pneumonia model revealed that accumulation of EC-SOD in the BAL fluid was not due to clearance from the lung parenchyma. Rather, this EC-SOD originated from the inflammatory cells infiltrating the airspaces. This finding was confirmed by the examination of airspace protein accumulation in mice that have lung-specific expression of human EC-SOD. After asbestos exposure, the EC-SOD present in the BAL fluid was the mouse isoform, indicating an extrapulmonary source (i.e. inflammatory cells) of EC-SOD. The purpose for release of EC-SOD from inflammatory cells is currently unknown. It is hypothesized that EC-SOD is anti-inflammatory as EC-SOD knockout mice develop worse inflammation in the lung while EC-SOD transgenic overexpressors exhibit attenuated inflammation after challenge. Release of EC-SOD by leukocytes may act as molecular brakes to limit further influx of PMNs. These studies also show that EC-SOD can prevent increases in MMP levels in the lung. It is also possible that EC-SOD release compensates for the large amount of ROS released from activated inflammatory cells. EC-SOD may prevent inadvertent damage to the lung while still allowing for immunological defense utilizing ROS.

11.1.2.1. Future Directions: Neutrophil and Macrophage Depletion

To test further which inflammatory cells are releasing EC-SOD in this disease, selective depletion of leukocyte subtypes will be performed. PMNs and macrophages are two sources of EC-SOD that are being investigated. Since PMNs are present in much higher levels in asbestosis, current experiments are aimed at depleting these cells first. PMNs can be depleted through use of an anti-neutrophil antibody that causes complement-mediated lysis and has been used successfully in a hyperoxic lung injury model (197). This antibody is currently being tested

in our own asbestos model to determine effects on EC-SOD airspace accumulation. If PMN depletion does not reduce EC-SOD in the BAL fluid, alveolar macrophage depletion will be attempted with clodronate (290).

To test the functional relevance of this leukocyte-derived EC-SOD, an experiment is being designed to examine the inflammatory response in mice whose leukocytes do not possess EC-SOD. Wild type mice will be irradiated to ablate their bone marrow and prevent granulopoiesis. These mice will then receive bone marrow transplants from EC-SOD knockout donors. The leukocytes derived from this transplanted bone marrow will not have the ability to produce EC-SOD. It is hypothesized that the resulting inflammatory response induced by asbestos will be greater than that produced by control mice with wild type bone marrow transplants. Furthermore, it is expected that greater damage will occur to airspace components because of loss of the protective EC-SOD released from the inflammatory cells. Markers of oxidative stress in proteins (carbonyl modifications and nitrotyrosine) and lipids (TBARS) will be assessed to determine this. These experiments will help to determine why leukocytes carry and release EC-SOD in sites of active inflammation. Other bone marrow stem cells from the EC-SOD knockout mice may also have an effect on the disease process. While this is a confounder to the inflammation studies, it also presents an opportunity to determine whether EC-SOD has a role in these stem cells as well.

Depletion of leukocytes also provides an opportunity to determine disease progression in the relative absence of inflammation. These cells can produce a number of pathogenic mediators, such as ROS, proteases, and proinflammatory cytokines and chemokines to attract even more inflammatory cells and fibroblasts. Furthermore, our studies have not ruled out that interstitial inflammation (not airspace inflammation) is responsible for the proteolytic removal of

EC-SOD from lung parenchyma. This hypothesis can be directly examined in experiments with PMN-depleted mice. Eliminating or reducing these cells may confer a protective benefit against development of disease through any or all of these mechanisms.

However, a recent report also shows that leukocytes can downregulate the immune response. When alveolar macrophages were depleted before LPS challenge in rats, PMN recruitment was increased by 320% (290). This indicates that these macrophages have an important role for downregulating immune responses in the lung. Importantly, we have observed that macrophage numbers are markedly decreased in response to crocidolite asbestos (Figure 7 and Figure 40). Depletion of these cells may promote the development of PMN inflammation.

11.2. MMP UPREGULATION IN ASBESTOSIS

These studies revealed that MMP-2 and MMP-9 are increased after asbestos exposure in mice. MMP inhibition was also able to ameliorate the development of fibrosis and inflammation. An exhaustive literature search did not reveal any previously published reports reporting an increase in MMP-2 and MMP-9 in asbestos-related fibrotic lung disease in humans or animals. Furthermore, MMP inhibition has not been examined previously in this disease. Overall it appears that MMPs do play a pathogenic role in the development of asbestosis.

11.2.1. Consequences of increased MMP-2 and MMP-9

Although their substrate specificity for type IV collagen would suggest a role in basement membrane degredation, these MMPs have multiple substrates and potential roles that remain to be evaluated in the context of asbestosis. Basement membrane degredation may enable inflammatory cells and fibroblasts, two of the major effectors of asbestos-induced lung

injury, to migrate into the lung. In the case of inflammation, greater numbers of leukocytes could initiate damage through their elaboration of proteases and ROS. Fibroblast migration, on the other hand, would lead to the extensive fibrosis characteristic of the disease. The degredation of basement membrane could also contribute to fibrogenesis through impaired reepithelialization.

11.2.1.1. Future Directions: *in situ* zymography

Another important step in the studies of these MMPs is to examine their activity in the tissues. Although MMP-2 and MMP-9 were observed to be upregulated by zymographic analysis, the TIMPs were also increased. Whether these TIMPs are playing any role in inactivating the MMPs will be determined through *in situ* zymographic analysis. This technique localizes active gelatinase activity in histological sections of tissue. If these MMPs are being inhibited by TIMPs, they will not be detectable. This technique therefore allows for the determination of levels of activity in the tissue itself.

11.2.1.2. Future Directions: MMP-9 knockout experiments

While it has been shown that MMP-9 null mice do not have a significant phenotype change in response to bleomycin (219), compensation by other MMPs was not examined and this does not rule out a role for MMP-9 in asbestosis. MMP-9 knockout mice are currently being examined to determine their role in asbestos-induced pulmonary fibrosis, testing the hypothesis that these mice will be protected from disease progression. If protection is found, the mechanisms by which this benefit is mediated will be examined. Apart from its collagen-

degrading capabilities, MMP-9 can also inactivate alpha-1-proteinase inhibitor and cleave IL-1β. These proteins can be assayed by activity assay and ELISA, respectively. Alpha-1-proteinase inhibitor is already known to play a role in emphysema and has been postulated to play a role in pulmonary fibrosis. It is also known for its sensitivity to oxidative inactivation, perhaps indicating a target of converging pathways involving both EC-SOD and MMPs. IL-1β is a proinflammatory cytokine capable of promote development of pulmonary fibrosis. The MMP-9 knockout will allow us to determine whether MMP-9 plays a role in the activity of these proteins.

11.2.1.3. Future Directions: MMP-7 knockout mice

MMP-7 (matrilysin) was shown to have a surprising role in the development of bleomycin-induced pulmonary fibrosis as well as in human IPF. This MMP has not yet been studied in asbestosis. MMP-7 null mice are now being bred in the animal facility and the role of MMP-7 in development of inflammation and fibrosis will be assessed. We hypothesize that the knockout mice will be protected against the development of fibrosis. It has been shown that MMP-7 cleaves syndecan, upon which a neutrophil chemoattractant, KC, is bound. KC is the murine homologue of human IL-8. This cleavage helps to set up a chemotactic gradient for the neutrophil in response to KC in bleomycin-induced lung injury. The same mechanism will be examined in asbestosis, as well as measure endpoints such as inflammation and fibrosis. Ongoing studies in our laboratory have failed to identify the same increases in MMP-7 in asbestosis as is seen in the bleomycin model. While this may be due to the low levels of MMP-7 transcripts in the lung, it could also indicate that MMP-7 does not play a role in asbestosis. This discovery would indicate that there are differences between asbestosis from IPF despite their

histologic similarities and suggest that different mechanisms may contribute to the pathogenesis of these diseases.

11.3. INFLAMMATION IN THE REGULATION OF EC-SOD AND MMPS

These results indicate that EC-SOD can modulate levels of MMPs through effects on inflammation. Increased inflammation led to greater MMP-9 levels in the BAL fluid. Conversely, MMP inhibition also had inhibitory effects on lung inflammation, and this played a role in the accumulation of EC-SOD in the airspaces. The implications and future directions related to increased MMPs and EC-SOD were already discussed above. These studies for the first time show that EC-SOD and MMPs may regulate each other in the lung through effects on inflammation. These findings increase our understanding of the interrelationships and convering pathways due to oxidant/antioxidant imbalances and protease/antiprotease imbalances in diseases of the lung.

11.4. CLINICAL IMPLICATIONS

The discovery of potential involvement of EC-SOD and MMPs in the development of asbestosis and pulmonary fibrosis in general suggests a number of clinical implications for therapy. The finding of decreased EC-SOD in lung parenchyma supports the continued research into N-acetylcysteine and other antioxidants as treatments for the disease. Similarly MMP inhibition can have a protective effect by inhibiting the development of fibrosis. While it is true that the experimental results with MMP inhibition were observed when inhibition was given before the addition of asbestos, this study is not irrelevant for a human disease in which patients present with the disease already in development. IPF is a relentlessly progressive disease. MMP

inhibition could slow the progression of the disease by slowing the development of new fibrosis. In the same way, antioxidant therapies would prevent progression after a patient has presented. Since asbestos involves continued production of ROS from iron-laden asbestos fibers over the course of the disease, this type of therapy may be even more beneficial in the setting of asbestos fibers. In any event, it is critical that the molecular mechanisms of pulmonary fibrosis be more fully understood so that rational decisions about experimental therapies can be made. It is hoped that the research described in this thesis can contribute to this understanding so that future studies will have a firm foundation upon which to develop novel therapies for pulmonary fibrosis and other lung diseases.

BIBLIOGRAPHY

1. Lynch III, J. P., and G. B. Toews. 1998. Idiopathic Pulmonary Fibrosis. *In* A. P. Fishman, editor. Fishman's Pulmonary Diseases and Disorders, 3rd ed. McGraw Hill, New York. 1069-84.

2. Mossman, B. T., and A. Churg. Mechanisms in the pathogenesis of asbestosis and silicosis. *Am J Respir Crit Care Med* 1998; 157(5 Pt 1):1666-80.

3. Thrall, R. S., and P. J. Scalise. 1995. Bleomycin. *In* S. H. Phan and R. S. Thrall, editors. Pulmonary Fibrosis, Lung Biology in Health and Disease, 1st ed. Marcel Dekker, New York. 231-292.

4. Pickrell, J. A., and A. B. Abdel-Mageed. 1995. Radiation-Induced Pulmonary Fibrosis. *In* S. H. Phan and R. S. Thrall, editors. Pulmonary Fibrosis, Lung Biology in Health and Disease. Marcel Dekker, Inc., New York. 363-382.

5. Michalski, J. P., C. C. McCombs, E. Scopelitis, J. J. Biundo, Jr., and T. A. Medsger, Jr. Alpha 1-antitrypsin phenotypes, including M subtypes, in pulmonary disease associated with rheumatoid arthritis and systemic sclerosis. *Arthritis Rheum* 1986; 29(5):586-91.

6. Thomas, A. Q., K. Lane, J. Phillips, 3rd, M. Prince, C. Markin, M. Speer, D. A. Schwartz, R. Gaddipati, A. Marney, J. Johnson, R. Roberts, J. Haines, M. Stahlman, and J. E. Loyd. Heterozygosity for a surfactant protein C gene mutation associated with usual interstitial pneumonitis and cellular nonspecific interstitial pneumonitis in one kindred. *Am J Respir Crit Care Med* 2002; 165(9):1322-8.

7. Selman, M., V. J. Thannickal, A. Pardo, D. A. Zisman, F. J. Martinez, and J. P. Lynch, 3rd. Idiopathic pulmonary fibrosis: pathogenesis and therapeutic approaches. *Drugs* 2004; 64(4):405-30.

8. Coultas, D. B., and R. Hubbard. 2004. Epidemiology of Idiopathic Pulmonary Fibrosis. *In* J. P. Lynch III, editor. Idiopathic Pulmonary Fibrosis, Lung Biology in Health and Disease. Marcel Dekker, Inc., New York. 1-30.

9. Coultas, D. B., R. E. Zumwalt, W. C. Black, and R. E. Sobonya. The epidemiology of interstitial lung diseases. *Am J Respir Crit Care Med* 1994; 150(4):967-72.

10. West, J. B. 1995. Respiratory Physiology - the essentials, 5th ed. Williams & Williams, Baltimore.

11. Burkitt, H. G., B. Young, J. W. Heath, and P. J. Deakin. 1993. Wheater's Functional Histology, 3rd ed. Churchhill Livingstone, Inc., New York.

12. Panos, R. J., R. L. Mortenson, S. A. Niccoli, and T. E. King, Jr. Clinical deterioration in patients with idiopathic pulmonary fibrosis: causes and assessment. *Am J Med* 1990; 88(4):396-404.

13. Hubbard, R., I. Johnston, and J. Britton. Survival in patients with cryptogenic fibrosing alveolitis: a population-based cohort study. *Chest* 1998; 113(2):396-400.

14. Travis, W. D. 2004. Pathology of Usual Interstitial Pneumonia. *In* J. P. Lynch III, editor. Idiopathic Pulmonary Fibrosis, Lung Biology in Health and Disease. Marcel Dekker, Inc., New York. 81-100.

15. Douglas, W. W., J. H. Ryu, and D. R. Schroeder. Idiopathic pulmonary fibrosis: Impact of oxygen and colchicine, prednisone, or no therapy on survival. *Am J Respir Crit Care Med* 2000; 161(4 Pt 1):1172-8.

16. Raghu, G., W. J. Depaso, K. Cain, S. P. Hammar, C. E. Wetzel, D. F. Dreis, J. Hutchinson, N. E. Pardee, and R. H. Winterbauer. Azathioprine combined with prednisone in the treatment of idiopathic pulmonary fibrosis: a prospective double-blind, randomized, placebo-controlled clinical trial. *Am Rev Respir Dis* 1991; 144(2):291-6.

17. Selman, M., G. Carrillo, J. Salas, R. P. Padilla, R. Perez-Chavira, R. Sansores, and R. Chapela. Colchicine, D-penicillamine, and prednisone in the treatment of idiopathic pulmonary fibrosis: a controlled clinical trial. *Chest* 1998; 114(2):507-12.

18. Raghu, G., K. K. Brown, W. Z. Bradford, K. Starko, P. W. Noble, D. A. Schwartz, and T. E. King, Jr. A placebo-controlled trial of interferon gamma-1b in patients with idiopathic pulmonary fibrosis. *N Engl J Med* 2004; 350(2):125-33.

19. Kinnula, V. L., C. L. Fattman, R. J. Tan, and T. D. Oury. Oxidative stress in pulmonary fibrosis: a possible role for redox modulatory therapy. *Am J Respir Crit Care Med* 2005; 172(4):417-22.

20. Behr, J., K. Maier, B. Degenkolb, F. Krombach, and C. Vogelmeier. Antioxidative and clinical effects of high-dose N-acetylcysteine in fibrosing alveolitis. Adjunctive therapy to maintenance immunosuppression. *Am J Respir Crit Care Med* 1997; 156(6):1897-901.

21. Sporn, T. A., and V. L. Roggli. 2004. Asbestosis. *In* V. L. Roggli, T. D. Oury and T. A. Sporn, editors. Pathology of Asbestos-Associated Diseases, 2nd ed. Springer, New York. 71-103.

22. Darcey, D. J., and T. Alleman. 2004. Occupational and Environmental Exposure to Asbestos. *In* V. L. Roggli, T. D. Oury and T. A. Sporn, editors. Pathology of Asbestos-Associated Diseases, 2nd ed. Springer, New York. 17-33.

23. Manning, C. B., V. Vallyathan, and B. T. Mossman. Diseases caused by asbestos: mechanisms of injury and disease development. *Int Immunopharmacol* 2002; 2(2-3):191-200.

24. Kamp, D. W., and S. A. Weitzman. The molecular basis of asbestos induced lung injury. *Thorax* 1999; 54(7):638-52.

25. Niklinski, J., W. Niklinska, E. Chyczewska, J. Laudanski, W. Naumnik, L. Chyczewski, and E. Pluygers. The epidemiology of asbestos-related diseases. *Lung Cancer* 2004; 45 Suppl 1:S7-S15.

26. Roggli, V. L. 2004. Asbestos Bodies and Nonasbestos Ferruginous Bodies. *In* V. L. Roggli, T. D. Oury and T. A. Sporn, editors. Pathology of Asbestos-Associated Diseases, 2nd ed. Springer, New York. 34-70.

27. Lazo, J. S., D. G. Hoyt, S. M. Sebti, and B. R. Pitt. Bleomycin: a pharmacologic tool in the study of the pathogenesis of interstitial pulmonary fibrosis. *Pharmacol Ther* 1990; 47(3):347-58.

28. Corbel, M., S. Caulet-Maugendre, N. Germain, S. Molet, V. Lagente, and E. Boichot. Inhibition of bleomycin-induced pulmonary fibrosis in mice by the matrix metalloproteinase inhibitor batimastat. *J Pathol* 2001; 193(4):538-45.

29. Li, Q., P. W. Park, C. L. Wilson, and W. C. Parks. Matrilysin shedding of syndecan-1 regulates chemokine mobilization and transepithelial efflux of neutrophils in acute lung injury. *Cell* 2002; 111(5):635-46.

30. Phan, S. H., R. S. Thrall, and C. Williams. Bleomycin-induced pulmonary fibrosis. Effects of steroid on lung collagen metabolism. *Am Rev Respir Dis* 1981; 124(4):428-34.

31. Schrier, D. J., R. G. Kunkel, and S. H. Phan. The role of strain variation in murine bleomycin-induced pulmonary fibrosis. *Am Rev Respir Dis* 1983; 127(1):63-6.

32. Mitsuhashi, H., S. Asano, T. Nonaka, I. Hamamura, K. Masuda, and M. Kiyoki. Administration of truncated secretory leukoprotease inhibitor ameliorates bleomycin-induced pulmonary fibrosis in hamsters. *Am J Respir Crit Care Med* 1996; 153(1):369-74.

33. Yaguchi, T., Y. Fukuda, M. Ishizaki, and N. Yamanaka. Immunohistochemical and gelatin zymography studies for matrix metalloproteinases in bleomycin-induced pulmonary fibrosis. *Pathol Int* 1998; 48(12):954-63.

34. Fattman, C. L., C. T. Chu, and T. D. Oury. 2004. Experimental Models of Asbestos-Related Diseases. *In* V. L. Roggli, T. D. Oury and T. A. Sporn, editors. Pathology of Asbestos-Associated Diseases, 2nd ed. Springer, New York. 256-308.

35. Dorger, M., A. M. Allmeling, R. Kiefmann, S. Munzing, K. Messmer, and F. Krombach. Early inflammatory response to asbestos exposure in rat and hamster lungs: role of inducible nitric oxide synthase. *Toxicol Appl Pharmacol* 2002; 181(2):93-105.

36. Prieditis, H., and I. Y. Adamson. Alveolar macrophage kinetics and multinucleated giant cell formation after lung injury. *J Leukoc Biol* 1996; 59(4):534-8.

37. Kamp, D. W., V. Panduri, S. A. Weitzman, and N. Chandel. Asbestos-induced alveolar epithelial cell apoptosis: role of mitochondrial dysfunction caused by iron-derived free radicals. *Mol Cell Biochem* 2002; 234-235(1-2):153-60.

38. Adamson, I. Y., and D. H. Bowden. Response of mouse lung to crocidolite asbestos. 2. Pulmonary fibrosis after long fibres. *J Pathol* 1987; 152(2):109-17.

39. Brody, A. R., J. Y. Liu, D. Brass, and M. Corti. Analyzing the genes and peptide growth factors expressed in lung cells in vivo consequent to asbestos exposure and in vitro. *Environ Health Perspect* 1997; 105 Suppl 5:1165-71.

40. Middleton, A. P., S. T. Beckett, and J. M. Davis. Further observations on the short-term retention and clearance of asbestos by rats, using UICC reference samples. *Ann Occup Hyg* 1979; 22(2):141-52.

41. Adamson, I. Y., and D. H. Bowden. Response of mouse lung to crocidolite asbestos. 1. Minimal fibrotic reaction to short fibres. *J Pathol* 1987; 152(2):99-107.

42. Perdue, T. D., and A. R. Brody. Distribution of transforming growth factor-beta 1, fibronectin, and smooth muscle actin in asbestos-induced pulmonary fibrosis in rats. *J Histochem Cytochem* 1994; 42(8):1061-70.

43. Fox-Dewhurst, R., M. K. Alberts, O. Kajikawa, E. Caldwell, M. C. Johnson, 2nd, S. J. Skerrett, R. B. Goodman, J. T. Ruzinski, V. A. Wong, E. Y. Chi, and T. R. Martin. Pulmonary and systemic inflammatory responses in rabbits with gram-negative pneumonia. *Am J Respir Crit Care Med* 1997; 155(6):2030-40.

44. Thannickal, V. J., G. B. Toews, E. S. White, J. P. Lynch, 3rd, and F. J. Martinez. Mechanisms of pulmonary fibrosis. *Annu Rev Med* 2004; 55:395-417.

45. Maeyama, T., K. Kuwano, M. Kawasaki, R. Kunitake, N. Hagimoto, T. Matsuba, M. Yoshimi, I. Inoshima, K. Yoshida, and N. Hara. Upregulation of Fas-signalling molecules in lung epithelial cells from patients with idiopathic pulmonary fibrosis. *Eur Respir J* 2001; 17(2):180-9.

46. Hagimoto, N., K. Kuwano, I. Inoshima, M. Yoshimi, N. Nakamura, M. Fujita, T. Maeyama, and N. Hara. TGF-beta 1 as an enhancer of Fas-mediated apoptosis of lung epithelial cells. *J Immunol* 2002; 168(12):6470-8.

47. Wang, R., A. Zagariya, E. Ang, O. Ibarra-Sunga, and B. D. Uhal. Fas-induced apoptosis of alveolar epithelial cells requires ANG II generation and receptor interaction. *Am J Physiol* 1999; 277(6 Pt 1):L1245-50.

48. Hojo, S., J. Fujita, T. Yoshinouchi, H. Yamanouchi, T. Kamei, I. Yamadori, Y. Otsuki, N. Ueda, and J. Takahara. Hepatocyte growth factor and neutrophil elastase in idiopathic pulmonary fibrosis. *Respir Med* 1997; 91(9):511-6.

49. Yaekashiwa, M., S. Nakayama, K. Ohnuma, T. Sakai, T. Abe, K. Satoh, K. Matsumoto, T. Nakamura, T. Takahashi, and T. Nukiwa. Simultaneous or delayed administration of hepatocyte growth factor equally represses the fibrotic changes in murine lung injury induced by bleomycin. A morphologic study. *Am J Respir Crit Care Med* 1997; 156(6):1937-44.

50. Kasper, M., and G. Haroske. Alterations in the alveolar epithelium after injury leading to pulmonary fibrosis. *Histol Histopathol* 1996; 11(2):463-83.

51. Eitzman, D. T., R. D. McCoy, X. Zheng, W. P. Fay, T. Shen, D. Ginsburg, and R. H. Simon. Bleomycin-induced pulmonary fibrosis in transgenic mice that either lack or overexpress the murine plasminogen activator inhibitor-1 gene. *J Clin Invest* 1996; 97(1):232-7.

52. Rakic, J. M., C. Maillard, M. Jost, K. Bajou, V. Masson, L. Devy, V. Lambert, J. M. Foidart, and A. Noel. Role of plasminogen activator-plasmin system in tumor angiogenesis. *Cell Mol Life Sci* 2003; 60(3):463-73.

53. Swaisgood, C. M., E. L. French, C. Noga, R. H. Simon, and V. A. Ploplis. The development of bleomycin-induced pulmonary fibrosis in mice deficient for components of the fibrinolytic system. *Am J Pathol* 2000; 157(1):177-87.

54. Sisson, T. H., N. Hattori, Y. Xu, and R. H. Simon. Treatment of bleomycin-induced pulmonary fibrosis by transfer of urokinase-type plasminogen activator genes. *Hum Gene Ther* 1999; 10(14):2315-23.

55. Chapman, H. A., C. L. Allen, and O. L. Stone. Abnormalities in pathways of alveolar fibrin turnover among patients with interstitial lung disease. *Am Rev Respir Dis* 1986; 133(3):437-43.

56. Hattori, N., J. L. Degen, T. H. Sisson, H. Liu, B. B. Moore, R. G. Pandrangi, R. H. Simon, and A. F. Drew. Bleomycin-induced pulmonary fibrosis in fibrinogen-null mice. *J Clin Invest* 2000; 106(11):1341-50.

57. George, S. J., J. L. Johnson, M. A. Smith, G. D. Angelini, and C. L. Jackson. Transforming growth factor-beta is activated by plasmin and inhibits smooth muscle cell death in human saphenous vein. *J Vasc Res* 2005; 42(3):247-54.

58. Ramos-DeSimone, N., E. Hahn-Dantona, J. Sipley, H. Nagase, D. L. French, and J. P. Quigley. Activation of matrix metalloproteinase-9 (MMP-9) via a converging plasmin/stromelysin-1 cascade enhances tumor cell invasion. *J Biol Chem* 1999; 274(19):13066-76.

59. Hattori, N., S. Mizuno, Y. Yoshida, K. Chin, M. Mishima, T. H. Sisson, R. H. Simon, T. Nakamura, and M. Miyake. The plasminogen activation system reduces fibrosis in the lung by a hepatocyte growth factor-dependent mechanism. *Am J Pathol* 2004; 164(3):1091-8.

60. Khalil, N., R. N. O'Connor, K. C. Flanders, and H. Unruh. TGF-beta 1, but not TGF-beta 2 or TGF-beta 3, is differentially present in epithelial cells of advanced pulmonary fibrosis: an immunohistochemical study. *Am J Respir Cell Mol Biol* 1996; 14(2):131-8.

61. Xu, Y. D., J. Hua, A. Mui, R. O'Connor, G. Grotendorst, and N. Khalil. Release of biologically active TGF-beta1 by alveolar epithelial cells results in pulmonary fibrosis. *Am J Physiol Lung Cell Mol Physiol* 2003; 285(3):L527-39.

62. Venkatesan, N., L. Pini, and M. S. Ludwig. Changes in Smad expression and subcellular localization in bleomycin-induced pulmonary fibrosis. *Am J Physiol Lung Cell Mol Physiol* 2004; 287(6):L1342-7.

63. Verrecchia, F., M. L. Chu, and A. Mauviel. Identification of novel TGF-beta /Smad gene targets in dermal fibroblasts using a combined cDNA microarray/promoter transactivation approach. *J Biol Chem* 2001; 276(20):17058-62.

64. Wen, F. Q., X. Liu, T. Kobayashi, S. Abe, Q. Fang, T. Kohyama, R. Ertl, Y. Terasaki, L. Manouilova, and S. I. Rennard. Interferon-gamma inhibits transforming growth factor-beta production in human airway epithelial cells by targeting Smads. *Am J Respir Cell Mol Biol* 2004; 30(6):816-22.

65. Gurujeyalakshmi, G., and S. N. Giri. Molecular mechanisms of antifibrotic effect of interferon gamma in bleomycin-mouse model of lung fibrosis: downregulation of TGF-beta and procollagen I and III gene expression. *Exp Lung Res* 1995; 21(5):791-808.

66. Korfhagen, T. R., R. J. Swantz, S. E. Wert, J. M. McCarty, C. B. Kerlakian, S. W. Glasser, and J. A. Whitsett. Respiratory epithelial cell expression of human transforming growth factor-alpha induces lung fibrosis in transgenic mice. *J Clin Invest* 1994; 93(4):1691-9.

67. Antoniades, H. N., M. A. Bravo, R. E. Avila, T. Galanopoulos, J. Neville-Golden, M. Maxwell, and M. Selman. Platelet-derived growth factor in idiopathic pulmonary fibrosis. *J Clin Invest* 1990; 86(4):1055-64.

68. Miyazaki, Y., K. Araki, C. Vesin, I. Garcia, Y. Kapanci, J. A. Whitsett, P. F. Piguet, and P. Vassalli. Expression of a tumor necrosis factor-alpha transgene in murine lung causes lymphocytic and fibrosing alveolitis. A mouse model of progressive pulmonary fibrosis. *J Clin Invest* 1995; 96(1):250-9.

69. Borok, Z., A. Gillissen, R. Buhl, R. F. Hoyt, R. C. Hubbard, T. Ozaki, S. I. Rennard, and R. G. Crystal. Augmentation of functional prostaglandin E levels on the respiratory epithelial surface by aerosol administration of prostaglandin E. *Am Rev Respir Dis* 1991; 144(5):1080-4.

70. Crystal, R. G., P. B. Bitterman, B. Mossman, M. I. Schwarz, D. Sheppard, L. Almasy, H. A. Chapman, S. L. Friedman, T. E. King, Jr., L. A. Leinwand, L. Liotta, G. R. Martin, D. A. Schwartz, G. S. Schultz, C. R. Wagner, and R. A. Musson. Future research directions in idiopathic pulmonary fibrosis: summary of a National Heart, Lung, and Blood Institute working group. *Am J Respir Crit Care Med* 2002; 166(2):236-46.

71. Raghu, G., Y. Y. Chen, V. Rusch, and P. S. Rabinovitch. Differential proliferation of fibroblasts cultured from normal and fibrotic human lungs. *Am Rev Respir Dis* 1988; 138(3):703-8.

72. Torry, D. J., C. D. Richards, T. J. Podor, and J. Gauldie. Anchorage-independent colony growth of pulmonary fibroblasts derived from fibrotic human lung tissue. *J Clin Invest* 1994; 93(4):1525-32.

73. Lappi-Blanco, E., Y. Soini, and P. Paakko. Apoptotic activity is increased in the newly formed fibromyxoid connective tissue in bronchiolitis obliterans organizing pneumonia. *Lung* 1999; 177(6):367-76.

74. Kuhn, C., 3rd, J. Boldt, T. E. King, Jr., E. Crouch, T. Vartio, and J. A. McDonald. An immunohistochemical study of architectural remodeling and connective tissue synthesis in pulmonary fibrosis. *Am Rev Respir Dis* 1989; 140(6):1693-703.

75. Hayashi, T., W. G. Stetler-Stevenson, M. V. Fleming, N. Fishback, M. N. Koss, L. A. Liotta, V. J. Ferrans, and W. D. Travis. Immunohistochemical study of metalloproteinases and their tissue inhibitors in the lungs of patients with diffuse alveolar damage and idiopathic pulmonary fibrosis. *Am J Pathol* 1996; 149(4):1241-56.

76. Fukuda, Y., M. Ishizaki, S. Kudoh, M. Kitaichi, and N. Yamanaka. Localization of matrix metalloproteinases-1, -2, and -9 and tissue inhibitor of metalloproteinase-2 in interstitial lung diseases. *Lab Invest* 1998; 78(6):687-98.

77. Zhang, K., M. D. Rekhter, D. Gordon, and S. H. Phan. Myofibroblasts and their role in lung collagen gene expression during pulmonary fibrosis. A combined immunohistochemical and in situ hybridization study. *Am J Pathol* 1994; 145(1):114-25.

78. Walker, G. A., I. A. Guerrero, and L. A. Leinwand. Myofibroblasts: molecular crossdressers. *Curr Top Dev Biol* 2001; 51:91-107.

79. Finlay, G. A., V. J. Thannickal, B. L. Fanburg, and K. E. Paulson. Transforming growth factor-beta 1-induced activation of the ERK pathway/activator protein-1 in human lung fibroblasts requires the autocrine induction of basic fibroblast growth factor. *J Biol Chem* 2000; 275(36):27650-6.

80. Phan, S. H., K. Zhang, H. Y. Zhang, and M. Gharaee-Kermani. The myofibroblast as an inflammatory cell in pulmonary fibrosis. *Curr Top Pathol* 1999; 93:173-82.

81. Mezzano, S. A., M. A. Droguett, M. E. Burgos, L. G. Ardiles, C. A. Aros, I. Caorsi, and J. Egido. Overexpression of chemokines, fibrogenic cytokines, and myofibroblasts in human membranous nephropathy. *Kidney Int* 2000; 57(1):147-58.

82. Thannickal, V. J., K. D. Aldweib, and B. L. Fanburg. Tyrosine phosphorylation regulates H2O2 production in lung fibroblasts stimulated by transforming growth factor beta1. *J Biol Chem* 1998; 273(36):23611-5.

83. Thannickal, V. J., and B. L. Fanburg. Activation of an H2O2-generating NADH oxidase in human lung fibroblasts by transforming growth factor beta 1. *J Biol Chem* 1995; 270(51):30334-8.

84. Selman, M., T. E. King, and A. Pardo. Idiopathic pulmonary fibrosis: prevailing and evolving hypotheses about its pathogenesis and implications for therapy. *Ann Intern Med* 2001; 134(2):136-51.

85. Rahman, I., E. Skwarska, M. Henry, M. Davis, C. M. O'Connor, M. X. FitzGerald, A. Greening, and W. MacNee. Systemic and pulmonary oxidative stress in idiopathic pulmonary fibrosis. *Free Radic Biol Med* 1999; 27(1-2):60-8.

86. Comhair, S. A., and S. C. Erzurum. Antioxidant responses to oxidant-mediated lung diseases. *Am J Physiol Lung Cell Mol Physiol* 2002; 283(2):L246-55.

87. Bruckdorfer, R. The basics about nitric oxide. *Mol Aspects Med* 2005; 26(1-2):3-31.

88. Oury, T. D., L. Tatro, A. J. Ghio, and C. A. Piantadosi. Nitration of tyrosine by hydrogen peroxide and nitrite. *Free Radic Res* 1995; 23(6):537-47.

89. Geiszt, M., and T. L. Leto. The Nox family of NAD(P)H oxidases: host defense and beyond. *J Biol Chem* 2004; 279(50):51715-8.

90. Meneshian, A., and G. B. Bulkley. The physiology of endothelial xanthine oxidase: from urate catabolism to reperfusion injury to inflammatory signal transduction. *Microcirculation* 2002; 9(3):161-75.

91. Chow, C. W., M. T. Herrera Abreu, T. Suzuki, and G. P. Downey. Oxidative stress and acute lung injury. *Am J Respir Cell Mol Biol* 2003; 29(4):427-31.

92. Levine, R. L., and E. R. Stadtman. Oxidative modification of proteins during aging. *Exp Gerontol* 2001; 36(9):1495-502.

93. Laukkanen, M. O., P. Lehtolainen, P. Turunen, S. Aittomaki, P. Oikari, S. L. Marklund, and S. Yla-Herttuala. Rabbit extracellular superoxide dismutase: expression and effect on LDL oxidation. *Gene* 2000; 254(1-2):173-9.

94. Fukai, T., Z. S. Galis, X. P. Meng, S. Parthasarathy, and D. G. Harrison. Vascular expression of extracellular superoxide dismutase in atherosclerosis. *J Clin Invest* 1998; 101(10):2101-11.

95. Callio, J., T. D. Oury, and C. T. Chu. Manganese superoxide dismutase protects against 6-hydroxydopamine injury in mouse brains. *J Biol Chem* 2005; 280(18):18536-42.

96. Kinnula, V. L., T. Torkkeli, P. Kristo, R. Sormunen, Y. Soini, P. Paakko, T. Ollikainen, K. Kahlos, A. Hirvonen, and S. Knuutila. Ultrastructural and chromosomal studies on manganese superoxide dismutase in malignant mesothelioma. *Am J Respir Cell Mol Biol* 2004; 31(2):147-53.

97. Karihtala, P., V. L. Kinnula, and Y. Soini. Antioxidative response for nitric oxide production in breast carcinoma. *Oncol Rep* 2004; 12(4):755-9.

98. Sanders, L. M., C. E. Henderson, M. Y. Hong, R. Barhoumi, R. C. Burghardt, R. J. Carroll, N. D. Turner, R. S. Chapkin, and J. R. Lupton. Pro-oxidant environment of the colon compared to the small intestine may contribute to greater cancer susceptibility. *Cancer Lett* 2004; 208(2):155-61.

99. Wickens, A. P. Ageing and the free radical theory. *Respir Physiol* 2001; 128(3):379-91.

100. Davies, M. J., and R. T. Dean. 1997. Formation and chemistry of radicals involved in amino acid, peptide, and protein oxidation. Radical-Mediated Protein Oxidation. Oxford University Press, Inc., New York. 25-120.

101. Goldstein, S., and G. Czapski. The reaction of NO. with O2.- and HO2.: a pulse radiolysis study. *Free Radic Biol Med* 1995; 19(4):505-10.

102. Tanaka, S., N. Choe, D. R. Hemenway, S. Zhu, S. Matalon, and E. Kagan. Asbestos inhalation induces reactive nitrogen species and nitrotyrosine formation in the lungs and pleura of the rat. *J Clin Invest* 1998; 102(2):445-54.

103. Saleh, D., P. J. Barnes, and A. Giaid. Increased production of the potent oxidant peroxynitrite in the lungs of patients with idiopathic pulmonary fibrosis. *Am J Respir Crit Care Med* 1997; 155(5):1763-9.

104. Montaldo, C., E. Cannas, M. Ledda, L. Rosetti, L. Congiu, and L. Atzori. Bronchoalveolar glutathione and nitrite/nitrate in idiopathic pulmonary fibrosis and sarcoidosis. *Sarcoidosis Vasc Diffuse Lung Dis* 2002; 19(1):54-8.

105. Kehrer, J. P. The Haber-Weiss reaction and mechanisms of toxicity. *Toxicology* 2000; 149(1):43-50.

106. Bryk, R., P. Griffin, and C. Nathan. Peroxynitrite reductase activity of bacterial peroxiredoxins. *Nature* 2000; 407(6801):211-5.

107. Reynolds, M. R., R. W. Berry, and L. I. Binder. Site-specific nitration and oxidative dityrosine bridging of the tau protein by peroxynitrite: implications for Alzheimer's disease. *Biochemistry* 2005; 44(5):1690-700.

108. Singer, II, D. W. Kawka, S. Scott, J. R. Weidner, R. A. Mumford, T. E. Riehl, and W. F. Stenson. Expression of inducible nitric oxide synthase and nitrotyrosine in colonic epithelium in inflammatory bowel disease. *Gastroenterology* 1996; 111(4):871-85.

109. Pfeilschifter, J., W. Eberhardt, and K. F. Beck. Regulation of gene expression by nitric oxide. *Pflugers Arch* 2001; 442(4):479-86.

110. Kinnula, V. L., and J. D. Crapo. Superoxide dismutases in the lung and human lung diseases. *Am J Respir Crit Care Med* 2003; 167(12):1600-19.

111. Cantin, A. M., S. L. North, R. C. Hubbard, and R. G. Crystal. Normal alveolar epithelial lining fluid contains high levels of glutathione. *J Appl Physiol* 1987; 63(1):152-7.

112. Fattman, C. L., L. M. Schaefer, and T. D. Oury. Extracellular superoxide dismutase in biology and medicine. *Free Radic Biol Med* 2003; 35(3):236-56.

113. Montuschi, P., G. Ciabattoni, P. Paredi, P. Pantelidis, R. M. du Bois, S. A. Kharitonov, and P. J. Barnes. 8-Isoprostane as a biomarker of oxidative stress in interstitial lung diseases. *Am J Respir Crit Care Med* 1998; 158(5 Pt 1):1524-7.

114. Hallgren, R., L. Bjermer, R. Lundgren, and P. Venge. The eosinophil component of the alveolitis in idiopathic pulmonary fibrosis. Signs of eosinophil activation in the lung are related to impaired lung function. *Am Rev Respir Dis* 1989; 139(2):373-7.

115. Cantin, A. M., S. L. North, G. A. Fells, R. C. Hubbard, and R. G. Crystal. Oxidant-mediated epithelial cell injury in idiopathic pulmonary fibrosis. *J Clin Invest* 1987; 79(6):1665-73.

116. Strausz, J., J. Muller-Quernheim, H. Steppling, and R. Ferlinz. Oxygen radical production by alveolar inflammatory cells in idiopathic pulmonary fibrosis. *Am Rev Respir Dis* 1990; 141(1):124-8.

117. Lakari, E., Y. Soini, M. Saily, P. Koistinen, P. Paakko, and V. L. Kinnula. Inducible nitric oxide synthase, but not xanthine oxidase, is highly expressed in interstitial pneumonias and granulomatous diseases of human lung. *Am J Clin Pathol* 2002; 117(1):132-42.

118. Behr, J., B. Degenkolb, F. Krombach, and C. Vogelmeier. Intracellular glutathione and bronchoalveolar cells in fibrosing alveolitis: effects of N-acetylcysteine. *Eur Respir J* 2002; 19(5):906-11.

119. Lakari, E., P. Paakko, P. Pietarinen-Runtti, and V. L. Kinnula. Manganese superoxide dismutase and catalase are coordinately expressed in the alveolar region in chronic interstitial pneumonias and granulomatous diseases of the lung. *Am J Respir Crit Care Med* 2000; 161(2 Pt 1):615-21.

120. Oury, T. D., K. Thakker, M. Menache, L. Y. Chang, J. D. Crapo, and B. J. Day. Attenuation of bleomycin-induced pulmonary fibrosis by a catalytic antioxidant metalloporphyrin. *Am J Respir Cell Mol Biol* 2001; 25(2):164-9.

121. Hoshino, T., H. Nakamura, M. Okamoto, S. Kato, S. Araya, K. Nomiyama, K. Oizumi, H. A. Young, H. Aizawa, and J. Yodoi. Redox-active protein thioredoxin prevents proinflammatory cytokine- or bleomycin-induced lung injury. *Am J Respir Crit Care Med* 2003; 168(9):1075-83.

122. Wang, H. D., M. Yamaya, S. Okinaga, Y. X. Jia, M. Kamanaka, H. Takahashi, L. Y. Guo, T. Ohrui, and H. Sasaki. Bilirubin ameliorates bleomycin-induced pulmonary fibrosis in rats. *Am J Respir Crit Care Med* 2002; 165(3):406-11.

123. Arslan, S. O., M. Zerin, H. Vural, and A. Coskun. The effect of melatonin on bleomycin-induced pulmonary fibrosis in rats. *J Pineal Res* 2002; 32(1):21-5.

124. Punithavathi, D., N. Venkatesan, and M. Babu. Curcumin inhibition of bleomycin-induced pulmonary fibrosis in rats. *Br J Pharmacol* 2000; 131(2):169-72.

125. Giri, S. N., I. Biring, T. Nguyen, Q. Wang, and D. M. Hyde. Abrogation of bleomycin-induced lung fibrosis by nitric oxide synthase inhibitor, aminoguanidine in mice. *Nitric Oxide* 2002; 7(2):109-18.

126. Davis, D. W., D. A. Weidner, A. Holian, and D. J. McConkey. Nitric oxide-dependent activation of p53 suppresses bleomycin-induced apoptosis in the lung. *J Exp Med* 2000; 192(6):857-69.

127. Buhl, R., A. Meyer, and C. Vogelmeier. Oxidant-protease interaction in the lung. Prospects for antioxidant therapy. *Chest* 1996; 110(6 Suppl):267S-272S.

128. Van Wart, H. E., and H. Birkedal-Hansen. The cysteine switch: a principle of regulation of metalloproteinase activity with potential applicability to the entire matrix metalloproteinase gene family. *Proc Natl Acad Sci U S A* 1990; 87(14):5578-82.

129. Frears, E. R., Z. Zhang, D. R. Blake, J. P. O'Connell, and P. G. Winyard. Inactivation of tissue inhibitor of metalloproteinase-1 by peroxynitrite. *FEBS Lett* 1996; 381(1-2):21-4.

130. Wu, S. M., and S. V. Pizzo. Mechanism of hypochlorite-mediated inactivation of proteinase inhibition by alpha 2-macroglobulin. *Biochemistry* 1999; 38(42):13983-90.

131. Cavarra, E., M. Lucattelli, F. Gambelli, B. Bartalesi, S. Fineschi, A. Szarka, F. Giannerini, P. A. Martorana, and G. Lungarella. Human SLPI inactivation after cigarette smoke

exposure in a new in vivo model of pulmonary oxidative stress. *Am J Physiol Lung Cell Mol Physiol* 2001; 281(2):L412-7.

132. Carp, H., and A. Janoff. In vitro suppression of serum elastase-inhibitory capacity by reactive oxygen species generated by phagocytosing polymorphonuclear leukocytes. *J Clin Invest* 1979; 63(4):793-7.

133. Janoff, A., H. Carp, D. K. Lee, and R. T. Drew. Cigarette smoke inhalation decreases alpha 1-antitrypsin activity in rat lung. *Science* 1979; 206(4424):1313-4.

134. Kim, H., L. Lepler, A. Daniels, and Y. Phillips. alpha 1-antitrypsin deficiency and idiopathic pulmonary fibrosis in a family. *South Med J* 1996; 89(10):1008-10.

135. Chan, E. D., A. H. Ralston, and L. Shapiro. Does reduced alpha(1)-antitrypsin activity explain the link between cigarette smoking and idiopathic pulmonary fibrosis? *Chest* 2001; 120(1 Suppl):72S-74S.

136. Bellocq, A., E. Azoulay, S. Marullo, A. Flahault, B. Fouqueray, C. Philippe, J. Cadranel, and L. Baud. Reactive oxygen and nitrogen intermediates increase transforming growth factor-beta1 release from human epithelial alveolar cells through two different mechanisms. *Am J Respir Cell Mol Biol* 1999; 21(1):128-36.

137. Barcellos-Hoff, M. H., and T. A. Dix. Redox-mediated activation of latent transforming growth factor-beta 1. *Mol Endocrinol* 1996; 10(9):1077-83.

138. Cho, H. Y., S. P. Reddy, M. Yamamoto, and S. R. Kleeberger. The transcription factor NRF2 protects against pulmonary fibrosis. *Faseb J* 2004; 18(11):1258-60.

139. Serrano-Mollar, A., D. Closa, N. Prats, S. Blesa, M. Martinez-Losa, J. Cortijo, J. M. Estrela, E. J. Morcillo, and O. Bulbena. In vivo antioxidant treatment protects against bleomycin-induced lung damage in rats. *Br J Pharmacol* 2003; 138(6):1037-48.

140. Meyer, A., R. Buhl, and H. Magnussen. The effect of oral N-acetylcysteine on lung glutathione levels in idiopathic pulmonary fibrosis. *Eur Respir J* 1994; 7(3):431-6.

141. Demedts, M., J. Behr, R. Buhl, and el al. IFIGENIA: effects of N-acetylcysteine (NAC) on primary end points VC and Dlco [abstract]. *Am J Respir Crit Care Med* 2003; 167:A988.

142. Liu, J. Y., and A. R. Brody. Increased TGF-beta1 in the lungs of asbestos-exposed rats and mice: reduced expression in TNF-alpha receptor knockout mice. *J Environ Pathol Toxicol Oncol* 2001; 20(2):97-108.

143. Jagirdar, J., T. C. Lee, J. Reibman, L. I. Gold, C. Aston, R. Begin, and W. N. Rom. Immunohistochemical localization of transforming growth factor beta isoforms in asbestos-related diseases. *Environ Health Perspect* 1997; 105 Suppl 5:1197-203.

144. Dai, J., B. Gilks, K. Price, and A. Churg. Mineral dusts directly induce epithelial and interstitial fibrogenic mediators and matrix components in the airway wall. *Am J Respir Crit Care Med* 1998; 158(6):1907-13.

145. Lemaire, I., H. Beaudoin, S. Masse, and C. Grondin. Alveolar macrophage stimulation of lung fibroblast growth in asbestos-induced pulmonary fibrosis. *Am J Pathol* 1986; 122(2):205-11.

146. Dai, J., and A. Churg. Relationship of fiber surface iron and active oxygen species to expression of procollagen, PDGF-A, and TGF-beta(1) in tracheal explants exposed to amosite asbestos. *Am J Respir Cell Mol Biol* 2001; 24(4):427-35.

147. Lasky, J. A., B. Tonthat, J. Y. Liu, M. Friedman, and A. R. Brody. Upregulation of the PDGF-alpha receptor precedes asbestos-induced lung fibrosis in rats. *Am J Respir Crit Care Med* 1998; 157(5 Pt 1):1652-7.

148. Garcia, J. G., D. E. Griffith, A. B. Cohen, and K. S. Callahan. Alveolar macrophages from patients with asbestos exposure release increased levels of leukotriene B4. *Am Rev Respir Dis* 1989; 139(6):1494-501.

149. Mossman, B. T., J. P. Marsh, A. Sesko, S. Hill, M. A. Shatos, J. Doherty, J. Petruska, K. B. Adler, D. Hemenway, R. Mickey, and et al. Inhibition of lung injury, inflammation, and interstitial pulmonary fibrosis by polyethylene glycol-conjugated catalase in a rapid inhalation model of asbestosis. *Am Rev Respir Dis* 1990; 141(5 Pt 1):1266-71.

150. Treadwell, M. D., B. T. Mossman, and A. Barchowsky. Increased neutrophil adherence to endothelial cells exposed to asbestos. *Toxicol Appl Pharmacol* 1996; 139(1):62-70.

151. Driscoll, K. E., D. G. Hassenbein, J. Carter, J. Poynter, T. N. Asquith, R. A. Grant, J. Whitten, M. P. Purdon, and R. Takigiku. Macrophage inflammatory proteins 1 and 2: expression by rat alveolar macrophages, fibroblasts, and epithelial cells and in rat lung after mineral dust exposure. *Am J Respir Cell Mol Biol* 1993; 8(3):311-8.

152. Rosenthal, G. J., D. R. Germolec, M. E. Blazka, E. Corsini, P. Simeonova, P. Pollock, L. Y. Kong, J. Kwon, and M. I. Luster. Asbestos stimulates IL-8 production from human lung epithelial cells. *J Immunol* 1994; 153(7):3237-44.

153. Driscoll, K. E., J. K. Maurer, J. Higgins, and J. Poynter. Alveolar macrophage cytokine and growth factor production in a rat model of crocidolite-induced pulmonary inflammation and fibrosis. *J Toxicol Environ Health* 1995; 46(2):155-69.

154. Simeonova, P. P., and M. I. Luster. Iron and reactive oxygen species in the asbestos-induced tumor necrosis factor-alpha response from alveolar macrophages. *Am J Respir Cell Mol Biol* 1995; 12(6):676-83.

155. Vallyathan, V., J. F. Mega, X. Shi, and N. S. Dalal. Enhanced generation of free radicals from phagocytes induced by mineral dusts. *Am J Respir Cell Mol Biol* 1992; 6(4):404-13.

156. Hansen, K., and B. T. Mossman. Generation of superoxide (O2-.) from alveolar macrophages exposed to asbestiform and nonfibrous particles. *Cancer Res* 1987; 47(6):1681-6.

157. Ghio, A. J., M. B. Kadiiska, Q. H. Xiang, and R. P. Mason. In vivo evidence of free radical formation after asbestos instillation: an ESR spin trapping investigation. *Free Radic Biol Med* 1998; 24(1):11-7.

158. Schapira, R. M., A. J. Ghio, R. M. Effros, J. Morrisey, C. A. Dawson, and A. D. Hacker. Hydroxyl radicals are formed in the rat lung after asbestos instillation in vivo. *Am J Respir Cell Mol Biol* 1994; 10(5):573-9.

159. Quinlan, T. R., K. A. BeruBe, M. P. Hacker, D. J. Taatjes, C. R. Timblin, J. Goldberg, P. Kimberley, P. O'Shaughnessy, D. Hemenway, J. Torino, L. A. Jimenez, and B. T. Mossman. Mechanisms of asbestos-induced nitric oxide production by rat alveolar macrophages in inhalation and in vitro models. *Free Radic Biol Med* 1998; 24(5):778-88.

160. Goodglick, L. A., and A. B. Kane. Cytotoxicity of long and short crocidolite asbestos fibers in vitro and in vivo. *Cancer Res* 1990; 50(16):5153-63.

161. Janssen, Y. M., J. P. Marsh, M. P. Absher, D. Hemenway, P. M. Vacek, K. O. Leslie, P. J. Borm, and B. T. Mossman. Expression of antioxidant enzymes in rat lungs after inhalation of asbestos or silica. *J Biol Chem* 1992; 267(15):10625-30.

162. Chu, C. T., D. J. Levinthal, S. M. Kulich, E. M. Chalovich, and D. B. DeFranco. Oxidative neuronal injury. The dark side of ERK1/2. *Eur J Biochem* 2004; 271(11):2060-6.

163. Kamp, D. W., V. A. Israbian, S. E. Preusen, C. X. Zhang, and S. A. Weitzman. Asbestos causes DNA strand breaks in cultured pulmonary epithelial cells: role of iron-catalyzed free radicals. *Am J Physiol* 1995; 268(3 Pt 1):L471-80.

164. Chao, C. C., S. H. Park, and A. E. Aust. Participation of nitric oxide and iron in the oxidation of DNA in asbestos-treated human lung epithelial cells. *Arch Biochem Biophys* 1996; 326(1):152-7.

165. Aljandali, A., H. Pollack, A. Yeldandi, Y. Li, S. A. Weitzman, and D. W. Kamp. Asbestos causes apoptosis in alveolar epithelial cells: role of iron-induced free radicals. *J Lab Clin Med* 2001; 137(5):330-9.

166. Mossman, B. T., P. Surinrut, B. T. Brinton, J. P. Marsh, N. H. Heintz, B. Lindau-Shepard, and J. B. Shaffer. Transfection of a manganese-containing superoxide dismutase gene into hamster tracheal epithelial cells ameliorates asbestos-mediated cytotoxicity. *Free Radic Biol Med* 1996; 21(2):125-31.

167. McCord, J. M., and I. Fridovich. Superoxide dismutase. An enzymic function for erythrocuprein (hemocuprein). *J Biol Chem* 1969; 244(22):6049-55.

168. Weisiger, R. A., and I. Fridovich. Superoxide dismutase. Organelle specificity. *J Biol Chem* 1973; 248(10):3582-92.

169. Marklund, S. L. Human copper-containing superoxide dismutase of high molecular weight. *Proc Natl Acad Sci U S A* 1982; 79(24):7634-8.

170. Oury, T. D., J. D. Crapo, Z. Valnickova, and J. J. Enghild. Human extracellular superoxide dismutase is a tetramer composed of two disulphide-linked dimers: a simplified, high-yield purification of extracellular superoxide dismutase. *Biochem J* 1996; 317 (Pt 1):51-7.

171. Carlsson, L. M., S. L. Marklund, and T. Edlund. The rat extracellular superoxide dismutase dimer is converted to a tetramer by the exchange of a single amino acid. *Proc Natl Acad Sci U S A* 1996; 93(11):5219-22.

172. Oury, T. D., B. J. Day, and J. D. Crapo. Extracellular superoxide dismutase: a regulator of nitric oxide bioavailability. *Lab Invest* 1996; 75(5):617-36.

173. Sandstrom, J., K. Karlsson, T. Edlund, and S. L. Marklund. Heparin-affinity patterns and composition of extracellular superoxide dismutase in human plasma and tissues. *Biochem J* 1993; 294 (Pt 3):853-7.

174. Petersen, S. V., T. D. Oury, L. Ostergaard, Z. Valnickova, J. Wegrzyn, I. B. Thogersen, C. Jacobsen, R. P. Bowler, C. L. Fattman, J. D. Crapo, and J. J. Enghild. Extracellular superoxide dismutase (EC-SOD) binds to type I collagen and protects against oxidative fragmentation. *J Biol Chem* 2004; 279(14):13705-10.

175. Sandstrom, J., P. Nilsson, K. Karlsson, and S. L. Marklund. 10-fold increase in human plasma extracellular superoxide dismutase content caused by a mutation in heparin-binding domain. *J Biol Chem* 1994; 269(29):19163-6.

176. Karlsson, K., A. Edlund, J. Sandstrom, and S. L. Marklund. Proteolytic modification of the heparin-binding affinity of extracellular superoxide dismutase. *Biochem J* 1993; 290 (Pt 2):623-6.

177. Bowler, R. P., M. Nicks, D. A. Olsen, I. B. Thogersen, Z. Valnickova, P. Hojrup, A. Franzusoff, J. J. Enghild, and J. D. Crapo. Furin proteolytically processes the heparin-binding region of extracellular superoxide dismutase. *J Biol Chem* 2002; 277(19):16505-11.

178. Enghild, J. J., I. B. Thogersen, T. D. Oury, Z. Valnickova, P. Hojrup, and J. D. Crapo. The heparin-binding domain of extracellular superoxide dismutase is proteolytically processed intracellularly during biosynthesis. *J Biol Chem* 1999; 274(21):14818-22.

179. Petersen, S. V., T. D. Oury, Z. Valnickova, I. B. Thogersen, P. Hojrup, J. D. Crapo, and J. J. Enghild. The dual nature of human extracellular superoxide dismutase: one sequence and two structures. *Proc Natl Acad Sci U S A* 2003; 100(24):13875-80.

180. Hendrickson, D. J., J. H. Fisher, C. Jones, and Y. S. Ho. Regional localization of human extracellular superoxide dismutase gene to 4pter-q21. *Genomics* 1990; 8(4):736-8.

181. Folz, R. J., and J. D. Crapo. Extracellular superoxide dismutase (SOD3): tissue-specific expression, genomic characterization, and computer-assisted sequence analysis of the human EC SOD gene. *Genomics* 1994; 22(1):162-71.

182. Marklund, S. L. Regulation by cytokines of extracellular superoxide dismutase and other superoxide dismutase isoenzymes in fibroblasts. *J Biol Chem* 1992; 267(10):6696-701.

183. Oury, T. D., B. J. Day, and J. D. Crapo. Extracellular superoxide dismutase in vessels and airways of humans and baboons. *Free Radic Biol Med* 1996; 20(7):957-65.

184. Loenders, B., E. Van Mechelen, S. Nicolai, N. Buyssens, N. Van Osselaer, P. G. Jorens, J. Willems, A. G. Herman, and H. Slegers. Localization of extracellular superoxide dismutase in rat lung: neutrophils and macrophages as carriers of the enzyme. *Free Radic Biol Med* 1998; 24(7-8):1097-106.

185. Oury, T. D., L. Y. Chang, S. L. Marklund, B. J. Day, and J. D. Crapo. Immunocytochemical localization of extracellular superoxide dismutase in human lung. *Lab Invest* 1994; 70(6):889-98.

186. Ookawara, T., N. Imazeki, O. Matsubara, T. Kizaki, S. Oh-Ishi, C. Nakao, Y. Sato, and H. Ohno. Tissue distribution of immunoreactive mouse extracellular superoxide dismutase. *Am J Physiol* 1998; 275(3 Pt 1):C840-7.

187. Marklund, S. L. Extracellular superoxide dismutase in human tissues and human cell lines. *J Clin Invest* 1984; 74(4):1398-403.

188. Landmesser, U., R. Merten, S. Spiekermann, K. Buttner, H. Drexler, and B. Hornig. Vascular extracellular superoxide dismutase activity in patients with coronary artery disease: relation to endothelium-dependent vasodilation. *Circulation* 2000; 101(19):2264-70.

189. Juul, K., A. Tybjaerg-Hansen, S. Marklund, N. H. Heegaard, R. Steffensen, H. Sillesen, G. Jensen, and B. G. Nordestgaard. Genetically reduced antioxidative protection and increased ischemic heart disease risk: the Copenhagen City Heart Study. *Circulation* 2004; 109(1):59-65.

190. Sheng, H., T. C. Brady, R. D. Pearlstein, J. D. Crapo, and D. S. Warner. Extracellular superoxide dismutase deficiency worsens outcome from focal cerebral ischemia in the mouse. *Neurosci Lett* 1999; 267(1):13-6.

191. Sheng, H., R. D. Bart, T. D. Oury, R. D. Pearlstein, J. D. Crapo, and D. S. Warner. Mice overexpressing extracellular superoxide dismutase have increased resistance to focal cerebral ischemia. *Neuroscience* 1999; 88(1):185-91.

192. Sjoquist, P. O., L. Carlsson, G. Jonason, S. L. Marklund, and T. Abrahamsson. Cardioprotective effects of recombinant human extracellular-superoxide dismutase type C in rat isolated heart subjected to ischemia and reperfusion. *J Cardiovasc Pharmacol* 1991; 17(4):678-83.

193. Thiels, E., N. N. Urban, G. R. Gonzalez-Burgos, B. I. Kanterewicz, G. Barrionuevo, C. T. Chu, T. D. Oury, and E. Klann. Impairment of long-term potentiation and associative memory in mice that overexpress extracellular superoxide dismutase. *J Neurosci* 2000; 20(20):7631-9.

194. Marklund, S. L., A. Bjelle, and L. G. Elmqvist. Superoxide dismutase isoenzymes of the synovial fluid in rheumatoid arthritis and in reactive arthritides. *Ann Rheum Dis* 1986; 45(10):847-51.

195. Folz, R. J., J. Guan, M. F. Seldin, T. D. Oury, J. J. Enghild, and J. D. Crapo. Mouse extracellular superoxide dismutase: primary structure, tissue-specific gene expression, chromosomal localization, and lung in situ hybridization. *Am J Respir Cell Mol Biol* 1997; 17(4):393-403.

196. Carlsson, L. M., J. Jonsson, T. Edlund, and S. L. Marklund. Mice lacking extracellular superoxide dismutase are more sensitive to hyperoxia. *Proc Natl Acad Sci U S A* 1995; 92(14):6264-8.

197. Folz, R. J., A. M. Abushamaa, and H. B. Suliman. Extracellular superoxide dismutase in the airways of transgenic mice reduces inflammation and attenuates lung toxicity following hyperoxia. *J Clin Invest* 1999; 103(7):1055-66.

198. Ahmed, M. N., H. B. Suliman, R. J. Folz, E. Nozik-Grayck, M. L. Golson, S. N. Mason, and R. L. Auten. Extracellular superoxide dismutase protects lung development in hyperoxia-exposed newborn mice. *Am J Respir Crit Care Med* 2003; 167(3):400-5.

199. Ghio, A. J., H. B. Suliman, J. D. Carter, A. M. Abushamaa, and R. J. Folz. Overexpression of extracellular superoxide dismutase decreases lung injury after exposure to oil fly ash. *Am J Physiol Lung Cell Mol Physiol* 2002; 283(1):L211-8.

200. Bowler, R. P., J. Arcaroli, E. Abraham, M. Patel, L. Y. Chang, and J. D. Crapo. Evidence for extracellular superoxide dismutase as a mediator of hemorrhage-induced lung injury. *Am J Physiol Lung Cell Mol Physiol* 2003; 284(4):L680-7.

201. Bowler, R. P., M. Nicks, K. Tran, G. Tanner, L. Y. Chang, S. K. Young, and G. S. Worthen. Extracellular superoxide dismutase attenuates lipopolysaccharide-induced neutrophilic inflammation. *Am J Respir Cell Mol Biol* 2004; 31(4):432-9.

202. Bowler, R. P., M. Nicks, K. Warnick, and J. D. Crapo. Role of extracellular superoxide dismutase in bleomycin-induced pulmonary fibrosis. *Am J Physiol Lung Cell Mol Physiol* 2002; 282(4):L719-26.

203. Tamagawa, K., Y. Taooka, A. Maeda, K. Hiyama, S. Ishioka, and M. Yamakido. Inhibitory effects of a lecithinized superoxide dismutase on bleomycin-induced pulmonary fibrosis in mice. *Am J Respir Crit Care Med* 2000; 161(4 Pt 1):1279-84.

204. Fattman, C. L., L. Y. Chang, T. A. Termin, L. Petersen, J. J. Enghild, and T. D. Oury. Enhanced bleomycin-induced pulmonary damage in mice lacking extracellular superoxide dismutase. *Free Radic Biol Med* 2003; 35(7):763-71.

205. Monboisse, J. C., G. Bellon, J. Dufer, A. Randoux, and J. P. Borel. Collagen activates superoxide anion production by human polymorphonuclear neutrophils. *Biochem J* 1987; 246(3):599-603.

206. Monboisse, J. C., G. Bellon, A. Randoux, J. Dufer, and J. P. Borel. Activation of human neutrophils by type I collagen. Requirement of two different sequences. *Biochem J* 1990; 270(2):459-62.

207. Fattman, C. L., C. T. Chu, S. M. Kulich, J. J. Enghild, and T. D. Oury. Altered expression of extracellular superoxide dismutase in mouse lung after bleomycin treatment. *Free Radic Biol Med* 2001; 31(10):1198-207.

208. Oury, T. D., L. M. Schaefer, C. L. Fattman, A. Choi, K. E. Weck, and S. C. Watkins. Depletion of pulmonary EC-SOD after exposure to hyperoxia. *Am J Physiol Lung Cell Mol Physiol* 2002; 283(4):L777-84.

209. Gross, J., and C. M. Lapiere. Collagenolytic activity in amphibian tissues: a tissue culture assay. *Proc Natl Acad Sci U S A* 1962; 48:1014-22.

210. Parks, W. C., C. L. Wilson, and Y. S. Lopez-Boado. Matrix metalloproteinases as modulators of inflammation and innate immunity. *Nat Rev Immunol* 2004; 4(8):617-29.

211. Pardo, A., and M. Selman. MMP-1: the elder of the family. *Int J Biochem Cell Biol* 2005; 37(2):283-8.

212. Overall, C. M., J. L. Wrana, and J. Sodek. Transcriptional and post-transcriptional regulation of 72-kDa gelatinase/type IV collagenase by transforming growth factor-beta 1 in human fibroblasts. Comparisons with collagenase and tissue inhibitor of matrix metalloproteinase gene expression. *J Biol Chem* 1991; 266(21):14064-71.

213. Segura-Valdez, L., A. Pardo, M. Gaxiola, B. D. Uhal, C. Becerril, and M. Selman. Upregulation of gelatinases A and B, collagenases 1 and 2, and increased parenchymal cell death in COPD. *Chest* 2000; 117(3):684-94.

214. Hipps, D. S., R. M. Hembry, A. J. Docherty, J. J. Reynolds, and G. Murphy. Purification and characterization of human 72-kDa gelatinase (type IV collagenase). Use of immunolocalisation to demonstrate the non-coordinate regulation of the 72-kDa and 95-kDa gelatinases by human fibroblasts. *Biol Chem Hoppe Seyler* 1991; 372(4):287-96.

215. Xia, T., K. Akers, A. Z. Eisen, and J. L. Seltzer. Comparison of cleavage site specificity of gelatinases A and B using collagenous peptides. *Biochim Biophys Acta* 1996; 1293(2):259-66.

216. Liu, Z., X. Zhou, S. D. Shapiro, J. M. Shipley, S. S. Twining, L. A. Diaz, R. M. Senior, and Z. Werb. The serpin alpha1-proteinase inhibitor is a critical substrate for gelatinase B/MMP-9 in vivo. *Cell* 2000; 102(5):647-55.

217. Betsuyaku, T., J. M. Shipley, Z. Liu, and R. M. Senior. Gelatinase B deficiency does not protect against lipopolysaccharide-induced acute lung injury. *Chest* 1999; 116(1 Suppl):17S-18S.

218. Buckley, S., B. Driscoll, W. Shi, K. Anderson, and D. Warburton. Migration and gelatinases in cultured fetal, adult, and hyperoxic alveolar epithelial cells. *Am J Physiol Lung Cell Mol Physiol* 2001; 281(2):L427-34.

219. Betsuyaku, T., Y. Fukuda, W. C. Parks, J. M. Shipley, and R. M. Senior. Gelatinase B is required for alveolar bronchiolization after intratracheal bleomycin. *Am J Pathol* 2000; 157(2):525-35.

220. McGuire, J. K., Q. Li, and W. C. Parks. Matrilysin (matrix metalloproteinase-7) mediates E-cadherin ectodomain shedding in injured lung epithelium. *Am J Pathol* 2003; 162(6):1831-43.

221. Powell, W. C., B. Fingleton, C. L. Wilson, M. Boothby, and L. M. Matrisian. The metalloproteinase matrilysin proteolytically generates active soluble Fas ligand and potentiates epithelial cell apoptosis. *Curr Biol* 1999; 9(24):1441-7.

222. Wilson, C. L., A. J. Ouellette, D. P. Satchell, T. Ayabe, Y. S. Lopez-Boado, J. L. Stratman, S. J. Hultgren, L. M. Matrisian, and W. C. Parks. Regulation of intestinal alpha-defensin activation by the metalloproteinase matrilysin in innate host defense. *Science* 1999; 286(5437):113-7.

223. Sires, U. I., G. Murphy, V. M. Baragi, C. J. Fliszar, H. G. Welgus, and R. M. Senior. Matrilysin is much more efficient than other matrix metalloproteinases in the proteolytic inactivation of alpha 1-antitrypsin. *Biochem Biophys Res Commun* 1994; 204(2):613-20.

224. Wilson, C. L., and L. M. Matrisian. Matrilysin: an epithelial matrix metalloproteinase with potentially novel functions. *Int J Biochem Cell Biol* 1996; 28(2):123-36.

225. Pei, D., and S. J. Weiss. Furin-dependent intracellular activation of the human stromelysin-3 zymogen. *Nature* 1995; 375(6528):244-7.

226. Nagase, H., J. J. Enghild, K. Suzuki, and G. Salvesen. Stepwise activation mechanisms of the precursor of matrix metalloproteinase 3 (stromelysin) by proteinases and (4-aminophenyl)mercuric acetate. *Biochemistry* 1990; 29(24):5783-9.

227. von Bredow, D. C., A. E. Cress, E. W. Howard, G. T. Bowden, and R. B. Nagle. Activation of gelatinase-tissue-inhibitors-of-metalloproteinase complexes by matrilysin. *Biochem J* 1998; 331 (Pt 3):965-72.

228. Strongin, A. Y., I. Collier, G. Bannikov, B. L. Marmer, G. A. Grant, and G. I. Goldberg. Mechanism of cell surface activation of 72-kDa type IV collagenase. Isolation of the activated form of the membrane metalloprotease. *J Biol Chem* 1995; 270(10):5331-8.

229. Fu, X., S. Y. Kassim, W. C. Parks, and J. W. Heinecke. Hypochlorous acid oxygenates the cysteine switch domain of pro-matrilysin (MMP-7). A mechanism for matrix metalloproteinase activation and atherosclerotic plaque rupture by myeloperoxidase. *J Biol Chem* 2001; 276(44):41279-87.

230. Siwik, D. A., P. J. Pagano, and W. S. Colucci. Oxidative stress regulates collagen synthesis and matrix metalloproteinase activity in cardiac fibroblasts. *Am J Physiol Cell Physiol* 2001; 280(1):C53-60.

231. Rajagopalan, S., X. P. Meng, S. Ramasamy, D. G. Harrison, and Z. S. Galis. Reactive oxygen species produced by macrophage-derived foam cells regulate the activity of vascular matrix metalloproteinases in vitro. Implications for atherosclerotic plaque stability. *J Clin Invest* 1996; 98(11):2572-9.

232. Gu, Z., M. Kaul, B. Yan, S. J. Kridel, J. Cui, A. Strongin, J. W. Smith, R. C. Liddington, and S. A. Lipton. S-nitrosylation of matrix metalloproteinases: signaling pathway to neuronal cell death. *Science* 2002; 297(5584):1186-90.

233. Nelson, K. K., and J. A. Melendez. Mitochondrial redox control of matrix metalloproteinases. *Free Radic Biol Med* 2004; 37(6):768-84.

234. Michaelis, J., M. C. Vissers, and C. C. Winterbourn. Different effects of hypochlorous acid on human neutrophil metalloproteinases: activation of collagenase and inactivation of collagenase and gelatinase. *Arch Biochem Biophys* 1992; 292(2):555-62.

235. Fu, X., J. L. Kao, C. Bergt, S. Y. Kassim, N. P. Huq, A. d'Avignon, W. C. Parks, R. P. Mecham, and J. W. Heinecke. Oxidative cross-linking of tryptophan to glycine restrains matrix metalloproteinase activity: specific structural motifs control protein oxidation. *J Biol Chem* 2004; 279(8):6209-12.

236. Yu, A. E., A. N. Murphy, and W. G. Stetler-Stevenson. 1998. 72-kDa Gelatinase (Gelatinase A): Structure, Activation, Regulation, and Substrate Specificity. *In* W. C. Parks and R. P. Mecham, editors. Matrix Metalloproteinases. Academic Press, San Diego. 85-112.

237. Chu, C. T., G. C. Howard, U. K. Misra, and S. V. Pizzo. Alpha 2-macroglobulin: a sensor for proteolysis. *Ann N Y Acad Sci* 1994; 737:291-307.

238. Banyai, L., H. Tordai, and L. Patthy. The gelatin-binding site of human 72 kDa type IV collagenase (gelatinase A). *Biochem J* 1994; 298 (Pt 2):403-7.

239. Seltzer, J. L., S. A. Adams, G. A. Grant, and A. Z. Eisen. Purification and properties of a gelatin-specific neutral protease from human skin. *J Biol Chem* 1981; 256(9):4662-8.

240. Fessler, L. I., K. G. Duncan, J. H. Fessler, T. Salo, and K. Tryggvason. Characterization of the procollagen IV cleavage products produced by a specific tumor collagenase. *J Biol Chem* 1984; 259(15):9783-9.

241. Senior, R. M., G. L. Griffin, C. J. Fliszar, S. D. Shapiro, G. I. Goldberg, and H. G. Welgus. Human 92- and 72-kilodalton type IV collagenases are elastases. *J Biol Chem* 1991; 266(12):7870-5.

242. Mazzieri, R., L. Masiero, L. Zanetta, S. Monea, M. Onisto, S. Garbisa, and P. Mignatti. Control of type IV collagenase activity by components of the urokinase-plasmin system: a regulatory mechanism with cell-bound reactants. *Embo J* 1997; 16(9):2319-32.

243. Delclaux, C., C. Delacourt, M. P. D'Ortho, V. Boyer, C. Lafuma, and A. Harf. Role of gelatinase B and elastase in human polymorphonuclear neutrophil migration across basement membrane. *Am J Respir Cell Mol Biol* 1996; 14(3):288-95.

244. Zuo, F., N. Kaminski, E. Eugui, J. Allard, Z. Yakhini, A. Ben-Dor, L. Lollini, D. Morris, Y. Kim, B. DeLustro, D. Sheppard, A. Pardo, M. Selman, and R. A. Heller. Gene expression analysis reveals matrilysin as a key regulator of pulmonary fibrosis in mice and humans. *Proc Natl Acad Sci U S A* 2002; 99(9):6292-7.

245. Houde, M., P. Tremblay, S. Masure, G. Opdenakker, D. Oth, and R. Mandeville. Synergistic and selective stimulation of gelatinase B production in macrophages by lipopolysaccharide, trans-retinoic acid and CGP 41251, a protein kinase C regulator. *Biochim Biophys Acta* 1996; 1310(2):193-200.

246. Montgomery, A. M., H. Sabzevari, and R. A. Reisfeld. Production and regulation of gelatinase B by human T-cells. *Biochim Biophys Acta* 1993; 1176(3):265-8.

247. Miyagi, E., H. Yasumitsu, F. Hirahara, Y. Nagashima, H. Minaguchi, K. Miyazaki, and M. Umeda. Marked induction of gelatinases, especially type B, in host fibroblasts by human ovarian cancer cells in athymic mice. *Clin Exp Metastasis* 1995; 13(2):89-96.

248. Yao, P. M., H. Lemjabbar, M. P. D'Ortho, B. Maitre, P. Gossett, B. Wallaert, and C. Lafuma. Balance between MMP-9 and TIMP-1 expressed by human bronchial epithelial cells: relevance to asthma. *Ann N Y Acad Sci* 1999; 878:512-4.

249. Pardo, A., R. Barrios, V. Maldonado, J. Melendez, J. Perez, V. Ruiz, L. Segura-Valdez, J. I. Sznajder, and M. Selman. Gelatinases A and B are up-regulated in rat lungs by subacute hyperoxia: pathogenetic implications. *Am J Pathol* 1998; 153(3):833-44.

250. Wilhelm, S. M., I. E. Collier, B. L. Marmer, A. Z. Eisen, G. A. Grant, and G. I. Goldberg. SV40-transformed human lung fibroblasts secrete a 92-kDa type IV collagenase which is identical to that secreted by normal human macrophages. *J Biol Chem* 1989; 264(29):17213-21.

251. Strongin, A. Y., I. E. Collier, P. A. Krasnov, L. T. Genrich, B. L. Marmer, and G. I. Goldberg. Human 92 kDa type IV collagenase: functional analysis of fibronectin and carboxyl-end domains. *Kidney Int* 1993; 43(1):158-62.

252. Okada, Y., Y. Gonoji, K. Naka, K. Tomita, I. Nakanishi, K. Iwata, K. Yamashita, and T. Hayakawa. Matrix metalloproteinase 9 (92-kDa gelatinase/type IV collagenase) from HT 1080

human fibrosarcoma cells. Purification and activation of the precursor and enzymic properties. *J Biol Chem* 1992; 267(30):21712-9.

253. Yu, Q., and I. Stamenkovic. Cell surface-localized matrix metalloproteinase-9 proteolytically activates TGF-beta and promotes tumor invasion and angiogenesis. *Genes Dev* 2000; 14(2):163-76.

254. Corbel, M., C. Belleguic, E. Boichot, and V. Lagente. Involvement of gelatinases (MMP-2 and MMP-9) in the development of airway inflammation and pulmonary fibrosis. *Cell Biol Toxicol* 2002; 18(1):51-61.

255. Fukuda, Y., V. J. Ferrans, C. I. Schoenberger, S. I. Rennard, and R. G. Crystal. Patterns of pulmonary structural remodeling after experimental paraquat toxicity. The morphogenesis of intraalveolar fibrosis. *Am J Pathol* 1985; 118(3):452-75.

256. Atkinson, J. J., and R. M. Senior. Matrix metalloproteinase-9 in lung remodeling. *Am J Respir Cell Mol Biol* 2003; 28(1):12-24.

257. Suga, M., K. Iyonaga, T. Okamoto, Y. Gushima, H. Miyakawa, T. Akaike, and M. Ando. Characteristic elevation of matrix metalloproteinase activity in idiopathic interstitial pneumonias. *Am J Respir Crit Care Med* 2000; 162(5):1949-56.

258. Overall, C. M., E. Tam, G. A. McQuibban, C. Morrison, U. M. Wallon, H. F. Bigg, A. E. King, and C. R. Roberts. Domain interactions in the gelatinase A.TIMP-2.MT1-MMP activation complex. The ectodomain of the 44-kDa form of membrane type-1 matrix metalloproteinase does not modulate gelatinase A activation. *J Biol Chem* 2000; 275(50):39497-506.

259. Hedenborg, M., T. Sorsa, A. Lauhio, and M. Klockars. Asbestos fibers induce release of collagenase by human polymorphonuclear leukocytes. *Immunol Lett* 1990; 26(1):25-9.

260. Morimoto, Y., T. Tsuda, H. Nakamura, H. Hori, H. Yamato, N. Nagata, T. Higashi, M. Kido, and I. I. Tanaka. Expression of Matrix Metalloproteinases, Tissue Inhibitors of Metalloproteinases, and Extracellular Matrix mRNA Following Exposure to Mineral Fibers and Cigarette Smoke in Vivo. *Environ Health Perspect* 1997; 105S(Suppl 5):1247-51.

261. Perez-Ramos, J., M. de Lourdes Segura-Valdez, B. Vanda, M. Selman, and A. Pardo. Matrix metalloproteinases 2, 9, and 13, and tissue inhibitors of metalloproteinases 1 and 2 in experimental lung silicosis. *Am J Respir Crit Care Med* 1999; 160(4):1274-82.

262. Yatera, K., Y. Morimoto, H. N. Kim, H. Yamato, I. Tanaka, and M. Kido. Increased expression of matrix metalloproteinase in Clara cell-ablated mice inhaling crystalline silica. *Environ Health Perspect* 2001; 109(8):795-9.

263. Corbel, M., N. Theret, S. Caulet-Maugendre, N. Germain, V. Lagente, B. Clement, and E. Boichot. Repeated endotoxin exposure induces interstitial fibrosis associated with enhanced gelatinase (MMP-2 and MMP-9) activity. *Inflamm Res* 2001; 50(3):129-35.

264. Ruiz, V., R. M. Ordonez, J. Berumen, R. Ramirez, B. Uhal, C. Becerril, A. Pardo, and M. Selman. Unbalanced collagenases/TIMP-1 expression and epithelial apoptosis in experimental lung fibrosis. *Am J Physiol Lung Cell Mol Physiol* 2003; 285(5):L1026-36.

265. Pardo, A., M. Selman, K. Ridge, R. Barrios, and J. I. Sznajder. Increased expression of gelatinases and collagenase in rat lungs exposed to 100% oxygen. *Am J Respir Crit Care Med* 1996; 154(4 Pt 1):1067-75.

266. Swiderski, R. E., J. E. Dencoff, C. S. Floerchinger, S. D. Shapiro, and G. W. Hunninghake. Differential expression of extracellular matrix remodeling genes in a murine model of bleomycin-induced pulmonary fibrosis. *Am J Pathol* 1998; 152(3):821-8.

267. Betsuyaku, T., J. M. Shipley, Z. Liu, and R. M. Senior. Neutrophil emigration in the lungs, peritoneum, and skin does not require gelatinase B. *Am J Respir Cell Mol Biol* 1999; 20(6):1303-9.

268. Lopez-Boado, Y. S., C. L. Wilson, L. V. Hooper, J. I. Gordon, S. J. Hultgren, and W. C. Parks. Bacterial exposure induces and activates matrilysin in mucosal epithelial cells. *J Cell Biol* 2000; 148(6):1305-15.

269. Ohta, S., K. Imai, K. Yamashita, T. Matsumoto, I. Azumano, and Y. Okada. Expression of matrix metalloproteinase 7 (matrilysin) in human osteoarthritic cartilage. *Lab Invest* 1998; 78(1):79-87.

270. Stratton, M. S., H. Sirvent, T. S. Udayakumar, R. B. Nagle, and G. T. Bowden. Expression of the matrix metalloproteinase promatrilysin in coculture of prostate carcinoma cell lines. *Prostate* 2001; 48(3):206-9.

271. Busiek, D. F., V. Baragi, L. C. Nehring, W. C. Parks, and H. G. Welgus. Matrilysin expression by human mononuclear phagocytes and its regulation by cytokines and hormones. *J Immunol* 1995; 154(12):6484-91.

272. Zhang, J. W., and P. E. Gottschall. Zymographic measurement of gelatinase activity in brain tissue after detergent extraction and affinity-support purification. *J Neurosci Methods* 1997; 76(1):15-20.

273. Brown, R. F., R. B. Drawbaugh, and T. C. Marrs. An investigation of possible models for the production of progressive pulmonary fibrosis in the rat. The effects of repeated intratracheal instillation of bleomycin. *Toxicology* 1988; 51(1):101-10.

274. Chakrabarti, S., and K. D. Patel. Regulation of matrix metalloproteinase-9 release from IL-8-stimulated human neutrophils. *J Leukoc Biol* 2005; 78(1):279-88.

275. Fattman, C. L., J. J. Enghild, J. D. Crapo, L. M. Schaefer, Z. Valnickova, and T. D. Oury. Purification and characterization of extracellular superoxide dismutase in mouse lung. *Biochem Biophys Res Commun* 2000; 275(2):542-8.

276. Saari, H., T. Sorsa, O. Lindy, K. Suomalainen, S. Halinen, and Y. T. Konttinen. Reactive oxygen species as regulators of human neutrophil and fibroblast interstitial collagenases. *Int J Tissue React* 1992; 14(3):113-20.

277. Uchida, K., Y. Kato, and S. Kawakishi. A novel mechanism for oxidative cleavage of prolyl peptides induced by the hydroxyl radical. *Biochem Biophys Res Commun* 1990; 169(1):265-71.

278. Desrochers, P. E., K. Mookhtiar, H. E. Van Wart, K. A. Hasty, and S. J. Weiss. Proteolytic inactivation of alpha 1-proteinase inhibitor and alpha 1-antichymotrypsin by oxidatively activated human neutrophil metalloproteinases. *J Biol Chem* 1992; 267(7):5005-12.

279. Parks, W. C., and S. D. Shapiro. Matrix metalloproteinases in lung biology. *Respir Res* 2001; 2(1):10-9.

280. Peterson, M. W., and J. Kirschbaum. Asbestos-induced lung epithelial permeability: potential role of nonoxidant pathways. *Am J Physiol* 1998; 275(2 Pt 1):L262-8.

281. Kleiner, D. E., and W. G. Stetler-Stevenson. Quantitative zymography: detection of picogram quantities of gelatinases. *Anal Biochem* 1994; 218(2):325-9.

282. Corry, D. B., K. Rishi, J. Kanellis, A. Kiss, L. Z. Song Lz, J. Xu, L. Feng, Z. Werb, and F. Kheradmand. Decreased allergic lung inflammatory cell egression and increased susceptibility to asphyxiation in MMP2-deficiency. *Nat Immunol* 2002; 3(4):347-53.

283. Choe, K. H., L. Taraseviciene-Stewart, R. Scerbavicius, L. Gera, R. M. Tuder, and N. F. Voelkel. Methylprednisolone causes matrix metalloproteinase-dependent emphysema in adult rats. *Am J Respir Crit Care Med* 2003; 167(11):1516-21.

284. Selman, M., V. Ruiz, S. Cabrera, L. Segura, R. Ramirez, R. Barrios, and A. Pardo. TIMP-1, -2, -3, and -4 in idiopathic pulmonary fibrosis. A prevailing nondegradative lung microenvironment? *Am J Physiol Lung Cell Mol Physiol* 2000; 279(3):L562-74.

285. Saari, H., K. Suomalainen, O. Lindy, Y. T. Konttinen, and T. Sorsa. Activation of latent human neutrophil collagenase by reactive oxygen species and serine proteases. *Biochem Biophys Res Commun* 1990; 171(3):979-87.

286. Bowler, R. P., J. Arcaroli, J. D. Crapo, A. Ross, J. W. Slot, and E. Abraham. Extracellular superoxide dismutase attenuates lung injury after hemorrhage. *Am J Respir Crit Care Med* 2001; 164(2):290-4.

287. Karlsson, K., J. Sandstrom, A. Edlund, and S. L. Marklund. Turnover of extracellular-superoxide dismutase in tissues. *Lab Invest* 1994; 70(5):705-10.

288. Yoshimura, T., W. Matsuyama, and H. Kamohara. Discoidin domain receptor 1: a new class of receptor regulating leukocyte-collagen interaction. *Immunol Res* 2005; 31(3):219-30.

289. Ridger, V. C., B. E. Wagner, W. A. Wallace, and P. G. Hellewell. Differential effects of CD18, CD29, and CD49 integrin subunit inhibition on neutrophil migration in pulmonary inflammation. *J Immunol* 2001; 166(5):3484-90.

290. Beck-Schimmer, B., R. Schwendener, T. Pasch, L. Reyes, C. Booy, and R. C. Schimmer. Alveolar macrophages regulate neutrophil recruitment in endotoxin-induced lung injury. *Respir Res* 2005; 6(1):61.